

Geochemistry, Geophysics, Geosystems®





RESEARCH ARTICLE

10.1029/2021GC009948

Seismic Volcanostratigraphy: The Key to Resolving the Jan Mayen Microcontinent and Iceland Plateau Rift Evolution

Key Points:

- Structural inheritance, oblique rift-transform, and tectonics characterize continental breakup and seafloor spreading in the NE Atlantic
- Asymmetric rift propagation and hotspot-ridge interaction from breakup to present-day Iceland
- Four rift stages within the Iceland Plateau conditioned the breakup of the Jan Mayen microcontinent from Greenland

Anett Blischke^{1,2} , Bryndís Brandsdóttir¹ , Martyn S. Stoker³ , Carmen Gaina^{4,5} , Ögmundur Erlendsson⁶ , Christian Tegner⁷ , Sæmundur A. Halldórsson¹ , Helga M. Helgadóttir⁶ , Bjarni Gautason² , Sverre Planke^{4,8} , Anthony A. P. Koppers⁹ , and John R. Hopper¹⁰ 

¹Institute of Earth Sciences, Science Institute, University of Iceland – Askja, Reykjavík, Iceland, ²Iceland GeoSurvey, Akureyri, Iceland, ³Australian School of Petroleum and Energy Resources, University of Adelaide, Adelaide, SA, Australia, ⁴Centre for Earth Evolution and Dynamics (CEED), University of Oslo, Oslo, Norway, ⁵School of Earth and Atmospheric Sciences, Queensland University of Technology, Brisbane, QLD, Australia, ⁶Iceland GeoSurvey, Reykjavík, Iceland, ⁷Department of Geoscience—Earth System Petrology, Aarhus University, Aarhus C, Denmark, ⁸Volcanic Basin Petroleum Research AS, Oslo, Norway, ⁹College of Earth, Ocean and Atmospheric Sciences, Oregon State University, Corvallis, OR, USA, ¹⁰Geological Survey of Denmark and Greenland (GEUS), Copenhagen, Denmark

Supporting Information:

Supporting Information may be found in the online version of this article.

Correspondence to:

A. Blischke,
anb@isor.is

Citation:

Blischke, A., Brandsdóttir, B., Stoker, M. S., Gaina, C., Erlendsson, Ö., Tegner, C., et al. (2022). Seismic volcanostratigraphy: The key to resolving the Jan Mayen microcontinent and Iceland Plateau Rift evolution. *Geochemistry, Geophysics, Geosystems*, 23, e2021GC009948. <https://doi.org/10.1029/2021GC009948>

Received 7 JUN 2021
Accepted 11 MAR 2022

Author Contributions:

Conceptualization: Anett Blischke, Bryndís Brandsdóttir, Bjarni Gautason, John R. Hopper
Data curation: Anett Blischke, Ögmundur Erlendsson, Christian Tegner, Sæmundur A. Halldórsson
Formal analysis: Anett Blischke, Ögmundur Erlendsson, Christian Tegner, Sæmundur A. Halldórsson, Helga M. Helgadóttir, Anthony A. P. Koppers
Funding acquisition: Anett Blischke, Bryndís Brandsdóttir
Investigation: Anett Blischke

Abstract Volcanostratigraphic and igneous province mapping of the Jan Mayen microcontinent (JMMC) and Iceland Plateau Rift (IPR) region have provided new insight into the development of rift systems during breakup processes. The microcontinent's formation involved two breakup events associated with seven distinct tectono-magmatic phases (~63–21 Ma), resulting in a fan-shaped JMMC-IPR igneous domain. Primary structural trends and anomalous magmatic activity guided initial opening (~63–56 Ma) along a SE-NW trend from the European margin and along a WNW-ESE trend from East Greenland. The eastern margin of the microcontinent formed during the first breakup (~55–53 Ma), with voluminous subaerial volcanism and emplacement of multiple sets of SSW–NNE-aligned seaward-dipping reflector sequences. The more gradual, second breakup (~52–23 Ma) consisted of four northwestward migrating IPR (I–IV) rift zones along the microcontinent's southern and western margins. IPR I and II (~52–36 Ma) migrated obliquely into East Greenland, interlinked via segments of the Iceland-Faroe Fracture Zone, in overlapping sub-aerial and sub-surface igneous formations. IPR III and IV (~35–23 Ma) formed a wide igneous domain south and west of the microcontinent, accompanied by uplift, regional tilting, and erosion as the area moved closer to the Iceland hotspot. The proto-Kolbeinsey Ridge formed at ~22–21 Ma and connected to the Reykjanes Ridge via the Northwest Iceland Rift Zone, near the center of the hotspot. Eastward rift transfers, toward the proto-Iceland hotspot, commenced at ~15 Ma, marking the initiation of segmented rift zones comparable to present-day Iceland.

Plain Language Summary The Jan Mayen microcontinent within the central NE-Atlantic formed during two breakup processes that involved seven distinct magmatic and tectonic phases over a period of ~40 million years (~63–21 Ma). Compilation of geophysical, geological, and geochemical data has illuminated details of rifting processes during the two breakup events. The first breakup event separated the eastern margin of the Jan Mayen microcontinent (JMMC) from the Norwegian margin, at the opening of the NE-Atlantic by rifting along the now extinct Aegir Ridge. The second breakup, separation of the western margin from E-Greenland, was encompassed four IPR (I-IV) rift zones migrating north-westward into the microcontinent's southern and western margins. The IPR rift zones, interlinked via fracture zone segments, produced overlapping sub-aerial and sub-surface igneous sequences, and anomalously thick igneous crust. The separation of the JMMC-IPR area from East Greenland (~35–23 Ma) was accompanied by uplift, regional tilting, and erosion under the influence of the Iceland hotspot. The proto-Kolbeinsey Ridge formed during the next rift event (~22–21 Ma) connecting to the Reykjanes Ridge, via the Iceland region. Rift transfer towards the centre of the hotspot beneath proto-Iceland (~15 Ma) shifted the plate boundary eastward, similar to the layout of present-day Iceland.

© 2022. The Authors.

This is an open access article under the terms of the [Creative Commons Attribution License](https://creativecommons.org/licenses/by/4.0/), which permits use, distribution and reproduction in any medium, provided the original work is properly cited.

Methodology: Anett Blischke, Martyn S. Stoker, Carmen Gaina, Ögmundur Erlendsson, Christian Tegner, Sæmundur A. Halldórsson, Bjarni Gautason, John R. Hopper

Project Administration: Anett Blischke, Bjarni Gautason

Resources: Ögmundur Erlendsson, Christian Tegner, Helga M. Helgadóttir, Bjarni Gautason, Anthony A. P. Koppers
Software: Anett Blischke, Carmen Gaina, Ögmundur Erlendsson, Bjarni Gautason
Supervision: Bryndís Brandsdóttir, Martyn S. Stoker, Carmen Gaina, Bjarni Gautason, John R. Hopper

Validation: Anett Blischke

Visualization: Anett Blischke, Sæmundur A. Halldórsson

Writing – original draft: Anett Blischke

Writing – review & editing: Bryndís Brandsdóttir, Martyn S. Stoker, Carmen Gaina, Ögmundur Erlendsson, Christian Tegner, Sæmundur A. Halldórsson, Bjarni Gautason, John R. Hopper

1. Introduction

The origin and evolution of the Jan Mayen microcontinent (JMMC) have been debated, especially with regard to its southern continuation into the Iceland Plateau (Figure 1) (e.g., Brandsdóttir et al., 2015; Breivik et al., 2012; Gairaud et al., 1978; Grønlie et al., 1979; Talwani & Udintsev, 1976; Torsvik et al., 2015; or Gaina, Nasuti, et al., 2017). Whether the separation of the JMMC from northeastern Greenland and the initiation of the Kolbeinsey Ridge occurred as a single event, or in multiple phases has remained unresolved (e.g., Blischke, Gaina, et al., 2017; Gaina et al., 2009; Gernigon et al., 2019; Peron-Pinvidic et al., 2012a, 2012b).

Regional scale reconstructions of the central northeast Atlantic conjugate margins (73°N–60°N and 5°E–35°W), including the Norwegian Møre and Vøring margins and the East Greenland margin, have all shown that the tectonic evolution north of Iceland is highly complex compared to regional spreading processes south of Iceland (e.g., Bott et al., 1971; Eggen, 1984; Eldholm et al., 1990; Eldholm & Windisch, 1974; Gairaud et al., 1978; Grønlie et al., 1979; Hopper et al., 2003; Johnson & Heezen, 1967; Johnson & Tanner, 1971; Kharin et al., 1976; Kodaira et al., 1998a; Larsen & Jakobsdóttir, 1988; Larsen et al., 1989, 2014; Meyer et al., 1972; Myhre et al., 1984; Pitman & Talwani, 1972; Skogseid & Eldholm, 1987; Srivastava & Tapscott, 1986; Talwani & Eldholm, 1977; Talwani & Udintsev, 1976; Tegner et al., 2008; Vogt & Avery, 1974; Vogt et al., 1980; Weigel et al., 1995). Various kinematic models of the northeast Atlantic have been primarily based on magnetic and gravity data, describing the dual-breakup process of East Greenland-JMMC-Norway Basin oceanic domain. Model interpretations vary from a ridge-jump scenario driven by plume-ridge interactions (e.g., Gaina, 2014; Gaina et al., 2009; Gaina, Blischke, et al., 2017; Gaina, Nasuti, et al., 2017) to a strictly tectonically driven mid-oceanic ridge formation with ridge jumps being caused by horizontal plate tectonic forces exploiting the underlying inherited structural framework (e.g., Gernigon et al., 2012, 2015, 2019). Seismic reflection data from the Jan Mayen Ridge and the Iceland Plateau have facilitated several detailed stratigraphic analyses that have resulted in the definition of six main depositional phases during the Cenozoic separated by regional unconformities (e.g., Åkermoen, 1989; Blischke, Gaina, et al., 2017; Blischke et al., 2019; Erlendsson, 2010; Gudlaugsson et al., 1988, 1989; Peron-Pinvidic et al., 2012a, 2012b). However, the chronostratigraphic context of the accompanying volcanism within the northeast Atlantic has not been fully considered in any comparable or coherent manner.

To address the complex tectono-magmatic evolution of the JMMC and the Iceland Plateau Rift (IPR) region, we reviewed and interpreted seismic reflection and refraction data combined with gravity and magnetic anomaly data, multibeam bathymetric data, as well as stratigraphic, age and petrochemical data from borehole and seafloor samples. Of particular note in this review is the inclusion of expanded spread profiles (ESP) to better constrain the regional velocity interpretation. Our volcanostratigraphic model was constructed by comparison with igneous formations of the Mid-Norwegian margin (Vøring and Møre), the Faroe Islands, the Greenland-Iceland-Faroe Ridge Complex (GIFRC), and the north-eastern margin of the Blosseville Kyst of central East Greenland (Figures 1–3). Our model portrays igneous processes associated with the opening of the central Northeast Atlantic throughout the Cenozoic and complements previous palaeoenvironmental reconstructions by Blischke, Gaina, et al. (2017), Blischke et al. (2019).

Previous seismic refraction data from ocean-bottom seismometer (OBS) surveys have documented areas of variable crustal thickness, resulting in different interpretations of the Iceland Plateau as continental, oceanic or thick oceanic-type (Icelandic) crust (e.g., Brandsdóttir et al., 2015; Breivik & Mjelde, 2003; Breivik et al., 2008; Eldholm et al., 1990; Kandilarov et al., 2012; Kuvaas & Kodaira, 1997; Scott et al., 2005) (Figure 1b). The crustal domain interpretation of the JMMC by Blischke, Gaina, et al. (2017), Blischke et al. (2019) was based on sonobuoy data (Olafsson & Gunnarsson, 1989) and identified the following domains: (a) continental crustal domain, divided into continental-volcanic (i.e., densely intruded and rifted blocks of the microcontinent) and continental-intra basalt (i.e., densely intruded and interlayered with flood basalt in the Jan Mayen Basin); and (b) oceanic crustal domains east and west of the JMMC associated with the Ægir and Kolbeinsey ridges. The ESP data of this study support the interpretation of the volcanostratigraphic framework as derived from seismic reflection, borehole data, seafloor samples, and potential field data (Figures 1–3).

The primary objective of this study is to describe volcanostratigraphy in context to the tectono-magmatic processes associated with the dual-breakup and formation of the JMMC in correlation to the comprehensive geological and geophysical data record. High-resolution kinematic reconstructions of the JMMC-IPR domain will provide new constraints on the gradual rift-transfer processes that separated the JMMC from East Greenland. We

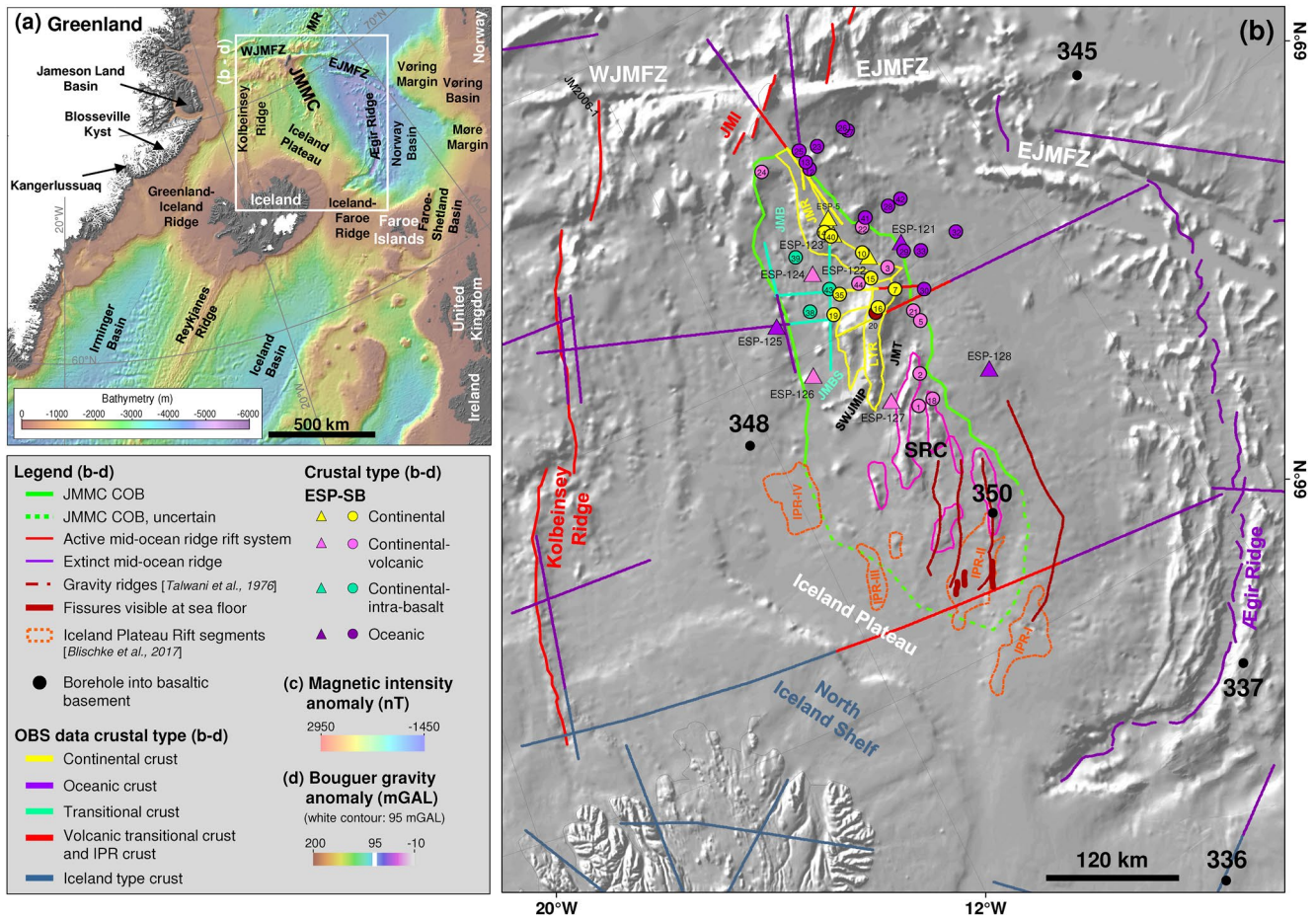


Figure 1. Overview of structural and crustal domains for the Jan Mayen microcontinent, Iceland Plateau and surrounding areas within the North Atlantic. The white frame delineates the study region with detailed (b) bathymetric, (c) magnetic and (d) gravity maps. Crustal type interpretations are based on (e.g., Blischke, Gaina et al., 2017; Blischke et al., 2018; Funck et al., 2014; Funck, Erlendsson, et al., 2017; Funck, Geissler, et al., 2017; Tan et al., 2017), sonobuoy interpretations (Blischke, Gaina et al., 2017; Johansen et al., 1988; Olafsson & Gunnarsson 1989) and expanding spread profiles (ESP), reinterpreted during this study. Seismic refraction profiles include wide-angle data (OBS) from JMKR95 (Kodaira et al., 1998a, 1998b), OBS2003 (Mjelde et al., 2008), JM2006 (Kandilarov et al., 2012), and KRISÉ (Brandsdóttir et al., 2015). Mapped fracture zones and lineaments were compiled from Gernigon et al. (2015) and Blischke, Gaina, et al. (2017), Blischke et al. (2019). DSDP Leg 38 borehole locations drilled into the igneous basement are shown on inserts (b) to (d). Shaded bathymetry data from IBCAO 3.0 (Jakobsson et al., 2012). Background shaded bathymetry data displays for potential field data (c) are from Nasuti and Olesen (2014) and (d) Bouguer gravity anomaly from Haase and Ebbing (2014) and Haase et al. (2017). Gravity ridges were defined by Talwani and Udintsev (1976). Abbreviations: CJMBFZ—Central Jan Mayen Basin Fracture Zone; CNBFZ—Central Norway Basin Fracture Zone; EJMFBZ—East Jan Mayen Fracture Zone segments; IFFZ—Iceland-Faroe Fracture Zone; IPR—Iceland Plateau Rift (segments I-IV); JMB—Jan Mayen Basin; JMBS—Jan Mayen Basin south; JMI—Jan Mayen Island igneous complex; JMR—Jan Mayen Ridge; JMT—Jan Mayen Trough; LYR—Lyngvi Ridge; NVZ—Northern Volcanic Zone; SPFZ—Spa Fracture Zone; SRC—Jan Mayen Southern Ridge Complex; SRCFZ—Southern Ridge Complex Fracture Zone; SWJMBFZ—Southwest Jan Mayen Basin Fracture Zone; SWJMIP—Southwest Jan Mayen igneous province; TFZ—Tjörnes Fracture Zone; WJMFZ—Western Jan Mayen Fracture Zone.

also address how pre-existing structural complexities and/or rift-hotspot/plume processes might have affected spreading obliquity and changes in rift transfer within the JMMC-IPR and GIFRC domains, thus contributing to the ongoing discussion on microcontinent formation (e.g., Gaina et al., 2003; Gaina & Whittaker, 2020; Müller et al., 2001; Nemčok et al., 2016).

2. Geological Setting

The JMMC is a 400–450 km long and 100–310 km wide continental region sandwiched between oceanic domains bounded by the extinct Ægir Ridge to the east and the Kolbeinsey Ridge to the west (Figure 1). Bathymetrically, the JMMC comprises a series of ridges with water depth ranging between 200 and 2,500 m (e.g., Talwani, Udintsev, & Shirshov, 1976; Vogt et al., 1970), subdivided into the Jan Mayen Ridge, the Lyngvi Ridge, the Jan

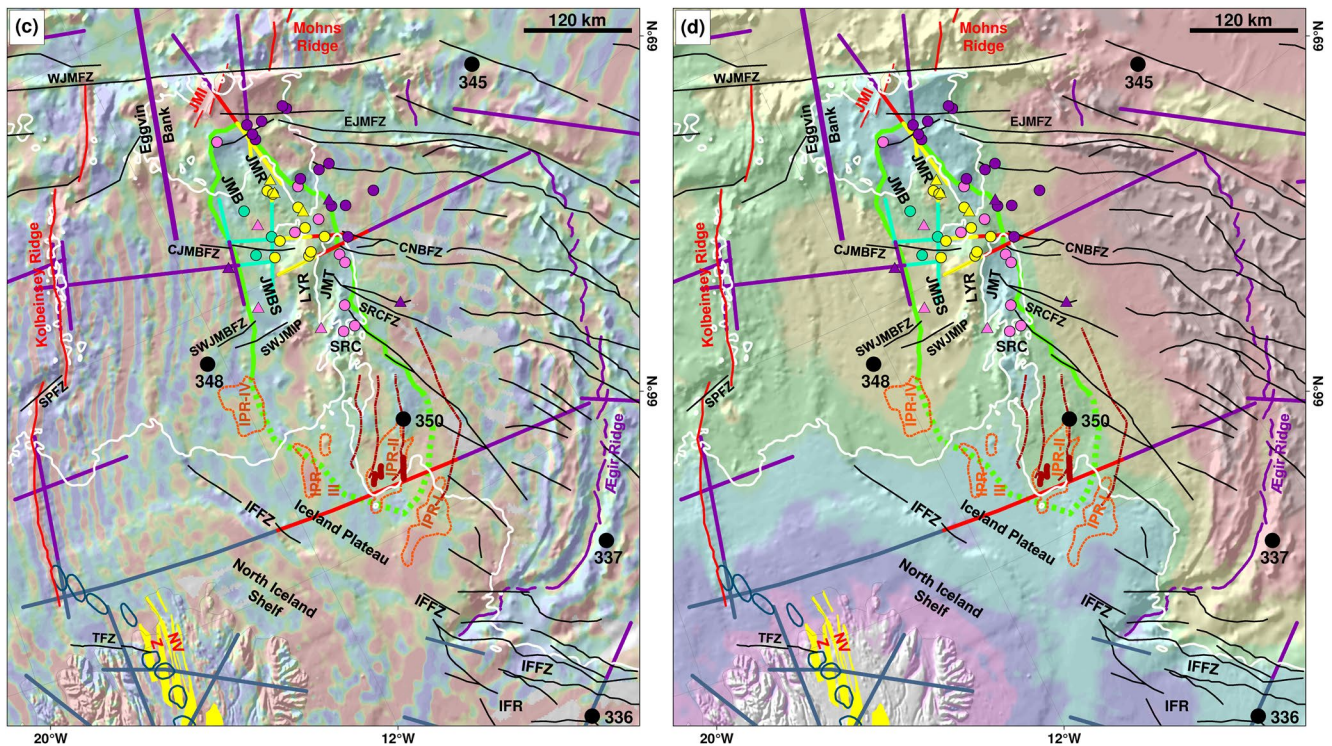


Figure 1. (Continued)

Mayen Basin, the Jan Mayen Trough, and the Jan Mayen Southern Ridge Complex (Figure 1). The Jan Mayen Ridge is a well-defined, continuous, 70–80 km wide, flat-topped structural block, and bathymetric high. The highly eroded Lyngvi Ridge narrows southwards to ~10 km width, where it is abruptly truncated. The Jan Mayen Basin is divided into a northern segment, west of the Jan Mayen Ridge, and a southern segment, west of the Lyngvi Ridge. The NNE–SSW-oriented Jan Mayen Trough widens toward the south-southwest and separates the Lyngvi Ridge from the Jan Mayen Southern Ridge Complex. The latter is composed of several ridges which locally protrude northwards into the Jan Mayen Trough but become indistinct to the south. The northern edge of the JMMC is bordered by the Jan Mayen Island volcanic complex, between the eastern and western segments of the Jan Mayen Fracture Zone (Svellingén & Pedersen, 2003). The eastern margin of the JMMC, which originally developed as the outermost part of the continental shelf of central East Greenland (73°N–68°N), is characterized by eastward-thickening Paleogene strata and basaltic lava flows that dip steeply toward the Norway Basin (e.g., Åkermoen, 1989; Blischke et al., 2019; Erlendsson, 2010; Gairaud et al., 1978; Gunnarsson et al., 1989; Peron-Pinvidic et al., 2012a, 2012b; Skogseid & Eldholm, 1987). The western margin of the JMMC developed by rifting within the Greenland continental shelf, in association with the Paleogene igneous province of the Blosseville Kyst and the Paleozoic-Mesozoic Jameson Land Basin (e.g., Blischke & Erlendsson, 2018; Larsen & Jakobsdóttir, 1988; Larsen et al., 1989, 1999, 2013).

The initiation of the broad fracture zone along the northern margin of the JMMC has been interpreted to have been active since ~55 Ma, based on kinematic modeling using regional potential field and seismic datasets (e.g., Gaina et al., 2009). The broad eastern volcanic margin of the JMMC, adjoining the Norway Basin, developed during the early to mid-Eocene (Ypresian–Lutetian) and is characterized by volcanic escarpments, sills, large-scale intrusive complexes, and early Eocene seaward dipping reflector sequences (SDR; polarity chron C24n2r 53.36 Ma), formed at the initiation of the Aegir Ridge (e.g. Blischke, Gaina, et al., 2017; Blischke et al., 2019; Gaina et al., 2009; Gernigon et al., 2015; Peron-Pinvidic et al., 2012a, 2012b; Skogseid & Eldholm, 1987). The western margin of the JMMC is characterized by tilted extensional fault blocks that form mainly half-graben structures together with a complex of sills and/or lava flows that cover the Jan Mayen Basin, west of the Jan Mayen Ridge (e.g., Blischke & Erlendsson, 2018; Blischke et al., 2018; Hopper et al., 2014; Larsen et al., 2013).

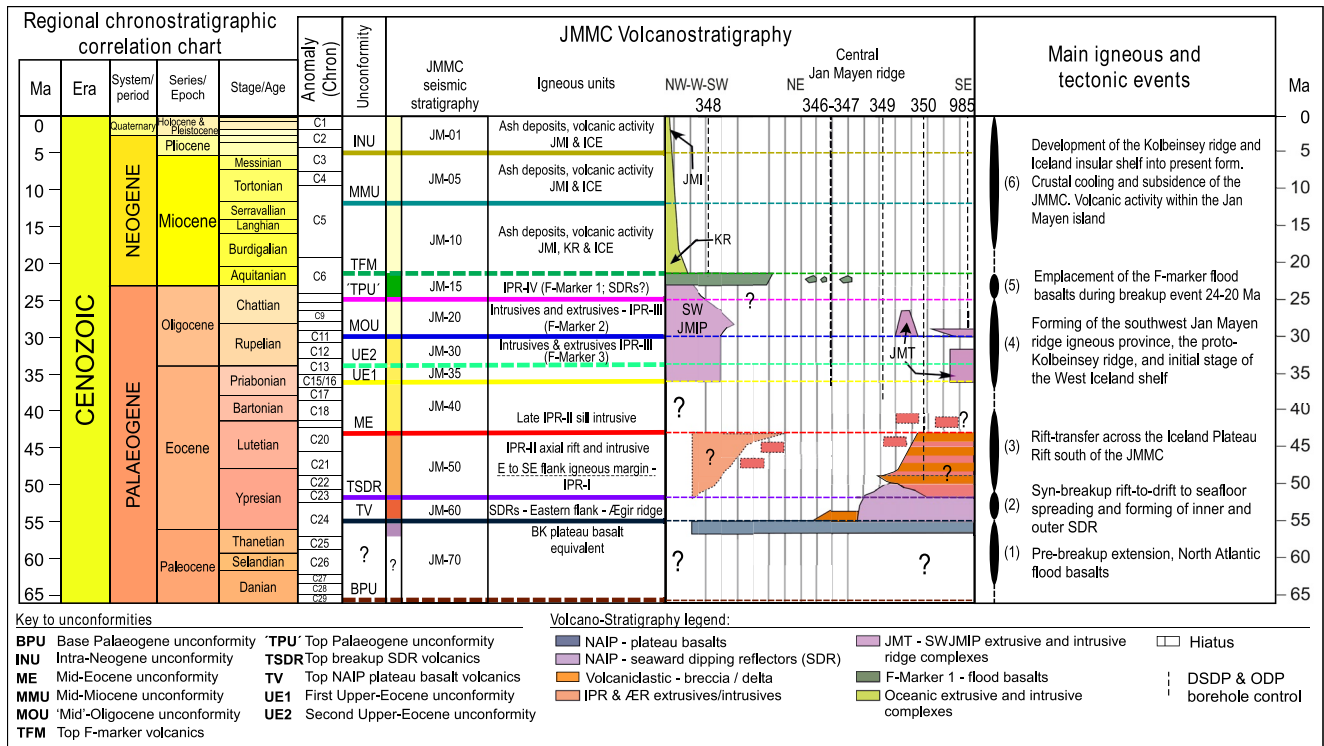


Figure 2. Volcanochronostratigraphic chart of the JMMC modified after Blischke, Gaina, et al. (2017), Blischke et al. (2019) constrained by DSDP Leg 38 sites 346–350 and ODP Leg 162 site 985 boreholes and 2D seismic reflection and refraction data (Butt et al., 2001; Channell, Amigo, et al., 1999; Channell, Smelror, et al., 1999; Jansen et al., 1996; Manum, Raschka, Eckhardt, Schrader, et al., 1976; Manum, Raschka, & Eckhardt, 1976; Manum & Schrader, 1976; Nilsen et al., 1978; Raschka et al., 1976; Talwani, Udintsev, & White, 1976; Talwani, Udintsev, & Shirshov, 1976; Thiede, Firth, et al., 1995; Thiede, Myhre, & Firth, 1995). The time scale is based on Gradstein et al. (2012) and Cohen et al. (2013; updated). Abbreviations: ÆR—Ægir Ridge; BK—Blosseville Kyst; DSDP—Deep Sea Drilling Program; ICE—Iceland; IPR—Iceland Plateau Rift (segments I-IV); JMI—Jan Mayen Island igneous complex; JMT—Jan Mayen Trough; KR—Kolbeinsey Ridge; NAIP—Northeast Atlantic igneous province; ODP—Ocean Drilling Program; SDR—Seaward dipping reflector sequences; SWJMIP—Southwest Jan Mayen igneous province.

The southern part of the microcontinent is generally described as a complex structural and volcanic domain with numerous extrusive and intrusive formations that obscure seismic reflection imaging of underlying structures, specifically within the Jan Mayen Trough (e.g., Blischke, Gaina, et al., 2017; Gaina et al., 2009; Gernigon et al., 2012, 2015; Peron-Pinvidic et al., 2012a, 2012b; Scott et al., 2005; Talwani, Udintsev, & Shirshov, 1976). The southernmost edge of the microcontinent is poorly constrained as it is buried beneath upper Paleogene and Neogene igneous and sedimentary rocks of the Iceland Plateau (Blischke, Gaina, et al., 2017; Blischke et al., 2019; Brandsdóttir et al., 2015). The Iceland Plateau area forms an anomalous region within the Northeast Atlantic with regard to half-spreading rate, crustal thickness variations, and reconstruction models, just as the Iceland-Faroe Ridge or Iceland itself (Gaina et al., 2009; Gaina, Nasuti, et al., 2017; Hopper et al., 2014). The Iceland Plateau south of the Jan Mayen Southern Ridge Complex is considered to be a distinct igneous and oceanic province (Talwani & Eldholm, 1977), with crustal thickness variations of 7–14 km, based on seismic refraction and gravity data (Brandsdóttir et al., 2015; Haase & Ebbing, 2014; Haase et al., 2017) (Figure 1b). Adding such an oceanic province into reconstruction models could explain the half-spreading rate anomaly south of JMMC. The oceanic and highly igneous province interpretations contrast the hyper-stretched continental domain and rift transfer interpretation that was associated with the cessation of spreading along the Ægir Ridge and rift jump to form the Kolbeinsey Ridge (e.g., Blischke, Gaina et al., 2017; Gaina et al., 2009; Gernigon et al., 2015, 2019; Peron-Pinvidic et al., 2012a). Furthermore, Kodaira et al. (1998a) describe magmatic starved breakup margins along the Jan Mayen Basin and Jan Mayen Southern Ridge Complex, which are in stark contrast to the widespread igneous activity that appeared to have affected the western and southwestern margins of the JMMC and within the southern segment of the Jan Mayen Basin, specifically from Oligocene (Rupelian; C13 ~33 Ma) that formed the Southwest Jan Mayen igneous province (SWJMIP) to early Miocene (Aquitainian-Burdigalian; C6 ~18.8–21.6 Ma) to form the Kolbeinsey Ridge (Blischke, Gaina, et al., 2017; Blischke et al., 2019; Gaina et al., 2009; Kharin et al., 1976; Figure 2).

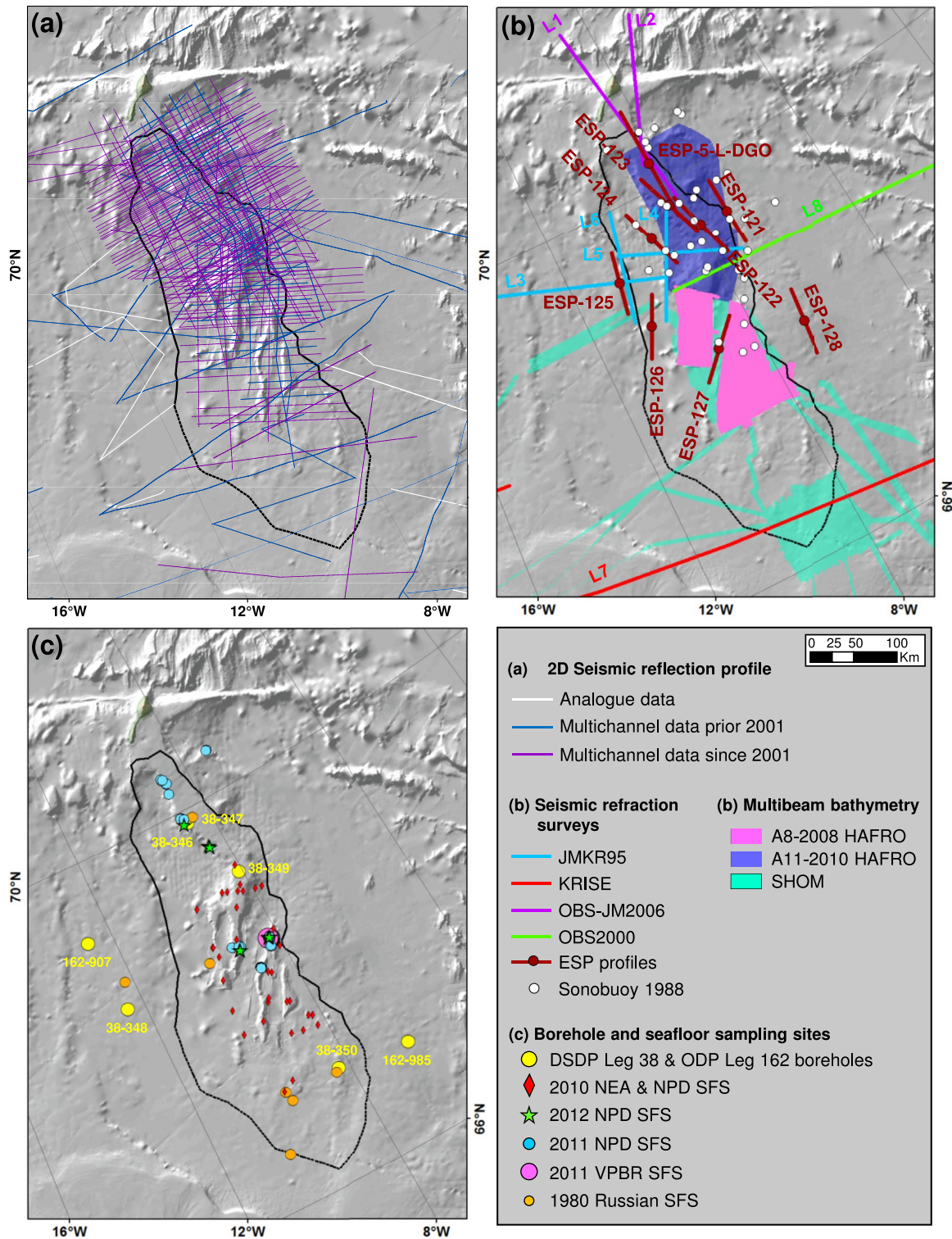


Figure 3. Location of project data for the Jan Mayen region on a hill shaded bathymetry map (Jakobsson et al., 2012): (a) 2D seismic reflection line data; (b) seismic refraction data: OBS (ocean bottom seismic), sonobuoy locations, and expanding spread profiles (ESP) and multibeam bathymetric maps (HAFRO—The Icelandic Marine and Fresh Water Research Institute [MFRI]; National Energy Authority of Iceland [NEA]; Norwegian Petroleum Directorate [NPD]; Spectrum ASA; TGS; Service Hydrographique et Océanographique de la Marine [SHOM]); (c) borehole and seafloor sample data (SFS) (Russian Science Academy; NEA; NPD; Volcanic Basin Petroleum Research AS [VPBR]).

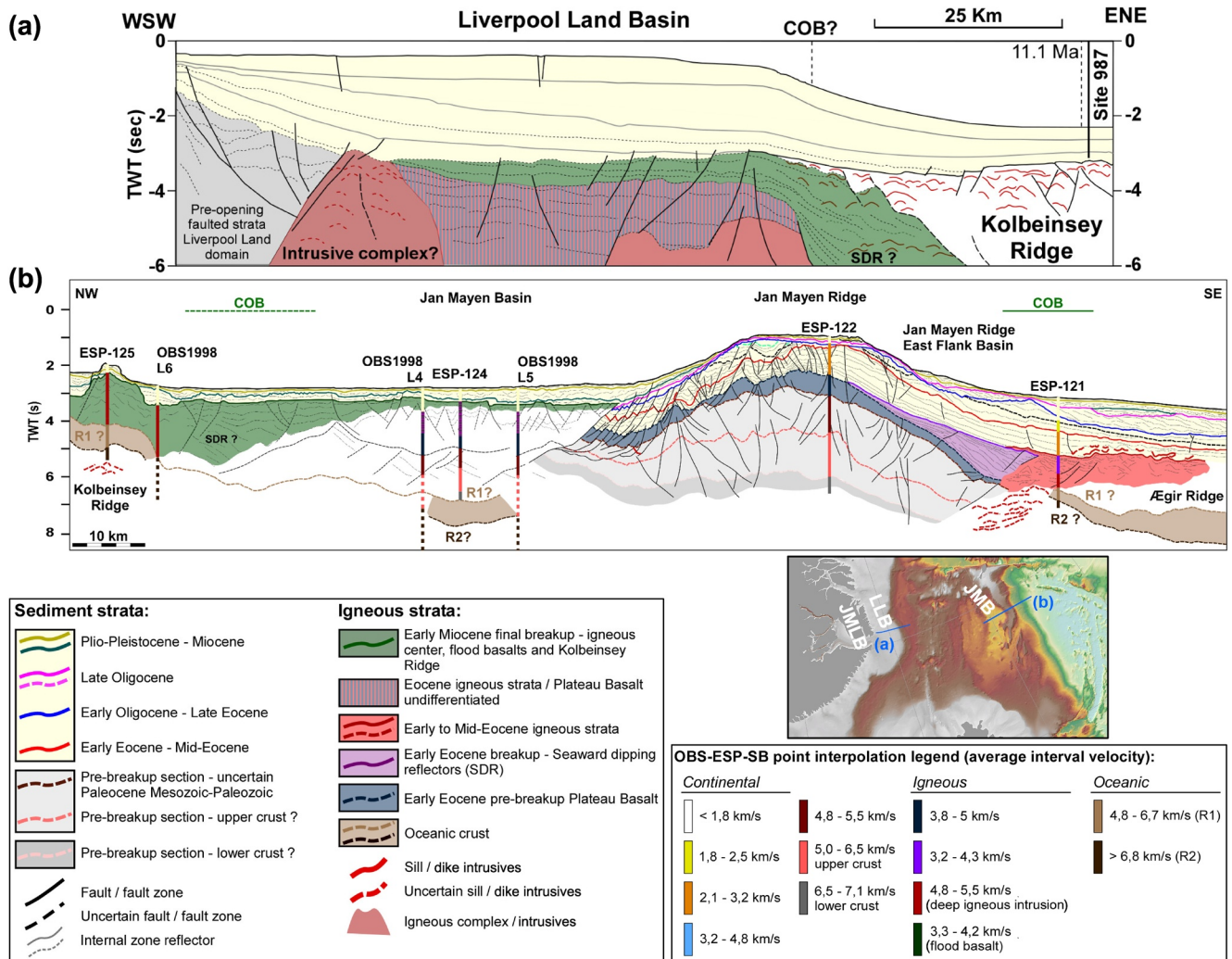


Figure 4. Tectonostratigraphic transects across the Liverpool Land Basin (LLB) (a) and the conjugate Jan Mayen microcontinent margin (b). The tectonostratigraphic type sections are based on 2D multichannel seismic data tied to ESP velocity profiles, sonobuoy and available ODP Leg 162 site 987 borehole data. The pre-breakup section is inferred to contain Paleocene, Mesozoic, and Paleozoic strata by direct comparison with the Jameson Land Basin (JMLB) and the Liverpool Land Basin areas (Blischke & Erlendsson 2018; Blischke, Gaina, et al., 2017, 2019; Hopper et al., 2014; L. M. Larsen et al., 1989). Abbreviations: COB—Continent Ocean Boundary; ESP—Expanding spread profiles; JMB—Jan Mayen Basin; OBS—Ocean bottom seismic; SDR—Seaward dipping reflector sequences; SB—Sonobuoy; TWT—Two-way travel time.

The differing and contradicting interpretations prompt the need for a complete volcanostratigraphic framework and igneous provinces mapping of the JMMC—Iceland Plateau region, to place the area into its chronological order and regional context to infill the apparent gaps from initial breakup within the Norway Basin to the final rift transfer to form the Kolbeinsey Ridge.

3. Data and Methods

For this study we compiled seismic reflection and refraction profiles, gravity and magnetic anomaly data, multi-beam bathymetric imagery, borehole, and seafloor sample analyses as well as thorough reviews of published data presented in Vogt et al. (1970), Vogt (1986), Talwani and Eldholm (1977), Åkermoen (1989), Doré et al. (1999), Lundin and Doré (2005), Rey et al. (2003), Gaina et al. (2009), Gernigon et al. (2012), Hopper et al. (2014), Haase and Ebbing (2014), Nasuti and Olesen (2014), Funck et al. (2014), Funck, Erlendsson, et al. (2017), Funck, Geissler, et al. (2017), and Blischke, Gaina, et al. (2017), Blischke, Erlendsson, et al. (2017) (Figures 3 and 4; Supplements 1–7 in Supporting Information S1).

3.1. Seismic Data

The seismic reflection and refraction database (Figure 3; Supplement 1 in Supporting Information S1) includes both vintage data (1975–2002) and data from more recent surveys: JM-85 and JM-88 (re-processed in 2009), IS-JMR-01 (2001), ICE-02 (2002), WI-JMR-08 (2008), NPD-11 (2011), and NPD-12 (2012). The boundary between the continental JMMC and oceanic domain has been based on older regional 2D data (BGR-75, BGR-76 [Hinz & Schlüter, 1978]), and 1978 Conrad-RC2114 reflection profiles (<https://www.marine-geo.org/index.php>; Talwani et al., 1981). More recent reflection surveys have provided a much denser data coverage of the JMMC area, in particular the 2011–2012 surveys, with considerably higher data quality and improved resolution of the deeper crust and post-igneous strata (Blischke et al., 2019). However, the higher resolution datasets did not improve sub-basalt imaging for the youngest (late Oligocene–early Miocene) flood basalt domain on the western and southern flanks of the JMMC.

Volcanostratigraphic sections of the JMMC were compiled using seismic refraction and reflection data (Brandsdóttir et al., 2015; Breivik et al., 2012; Johansen et al., 1988; Kandilarov et al., 2012; Kodaira et al., 1998a, 1998b; Mjelde et al., 2002, 2007; Olafsson & Gunnarsson, 1989) and shallow offshore boreholes, as well as information derived from previous analysis of the stratigraphic framework (Blischke, Gaina, et al., 2017; Blischke et al., 2019; Peron-Pinvidic et al., 2012a). In addition, ESP data from the ESP-5-L-DGO survey by Eldholm and Grue (1994) and IFP86 (ESP-121 to 128 on Figure 3) were analyzed using the travel-time-to-offset-ratio (e.g., Childs & Cooper, 1978) and the Vp velocity estimation methods of Diebold and Stoffa (1981). The resulting average ESP velocity values were correlated with the velocity facies domains of the JMMC to separate older Jan Mayen Ridge domains from igneous domains along the eastern breakup margin, within the Jan Mayen Basin, the Jan Mayen Trough, and the Jan Mayen Southern Ridge Complex (Figures 1, 3 and 4; Supplements 2, 6b in Supporting Information S1). Volcanostratigraphic interval velocity domains were defined for each velocity profile and tied to the interpretation of nearby seismic reflection profiles, providing a more robust definition of the structural setting, since velocity alone is not necessarily a definitive indication of the crustal type (Figure 4).

3.1.1. Seismic Volcanostratigraphy

The existing Cenozoic stratigraphic framework for the JMMC area (e.g., Blischke et al., 2019; Gunnarsson et al., 1989) was expanded by detailed chronostratigraphic appraisal of the igneous succession, based on seismic reflection, refraction, and potential field data interpretations. Our volcanostratigraphic characterization is based on methods developed by Hinz (1981), Symonds et al. (1998), Planke et al. (2000, 2015), and Bischoff et al. (2019) with facies types and units identified by their shape, reflection patterns, and boundary reflection characteristics, within a chronological context. This approach facilitated mapping and identification of volcanic units, such as subaerial lava flow, SDR sequences, inner and outer SDR subsets, igneous centers, sill and dike complexes, volcanic vents, and axial rift zone structures (Figures 4–6; Supplement 2, 6, 7 in Supporting Information S1).

3.2. Bathymetry

Our study included bathymetric data from two high-resolution multi-beam echo-sounder surveys conducted across the Jan Mayen Ridge and Jan Mayen Southern Ridge Complex in 2008 and 2010. Surveys A8-2008 and A11-2010 were acquired by the National Energy Authority of Iceland (Orkustofnun), the Norwegian Petroleum Directorate (NPD), and the Marine Research Institute of Iceland (HAFRO). In total, 10,500 km² of 50 × 50 m gridded bathymetric data was acquired with a depth range of 790–2,210 m (Blischke, Gaina, et al., 2017; Blischke et al., 2019; Helgadóttir, 2008; Helgadóttir & Reynisson, 2010). Data collected by the French Hydrographic and Oceanographic Office (SHOM) cruise NARVAL-2016 onboard *R/V Beautemps-Beaupré* in 2016 across the Jan Mayen Trough, Jan Mayen Southern Ridge Complex, and the Iceland Plateau Rift was also included (Figure 3; Supplement 1). The NARVAL survey acquired 35,000 km² of 50 × 50 m gridded bathymetric data, sub-bottom profiles, and magnetic data (Dupuy & Sogorb, 2017), providing important constraints on shallow structural trends and volcanic rift segments (Figure 1).

High-resolution multi-beam and ship-track bathymetry data were combined with satellite data and the international bathymetric chart of the Arctic Ocean (IBCAO) Version 3.0 with a 500 × 500 m resolution (Jakobsson et al., 2012). Bathymetry data were converted to two-way-travel time depth for comparison with seafloor depths obtained from seismic reflection lines (Figure 3). The compiled bathymetry data was used to delineate visible structural trends and igneous features at the seafloor.

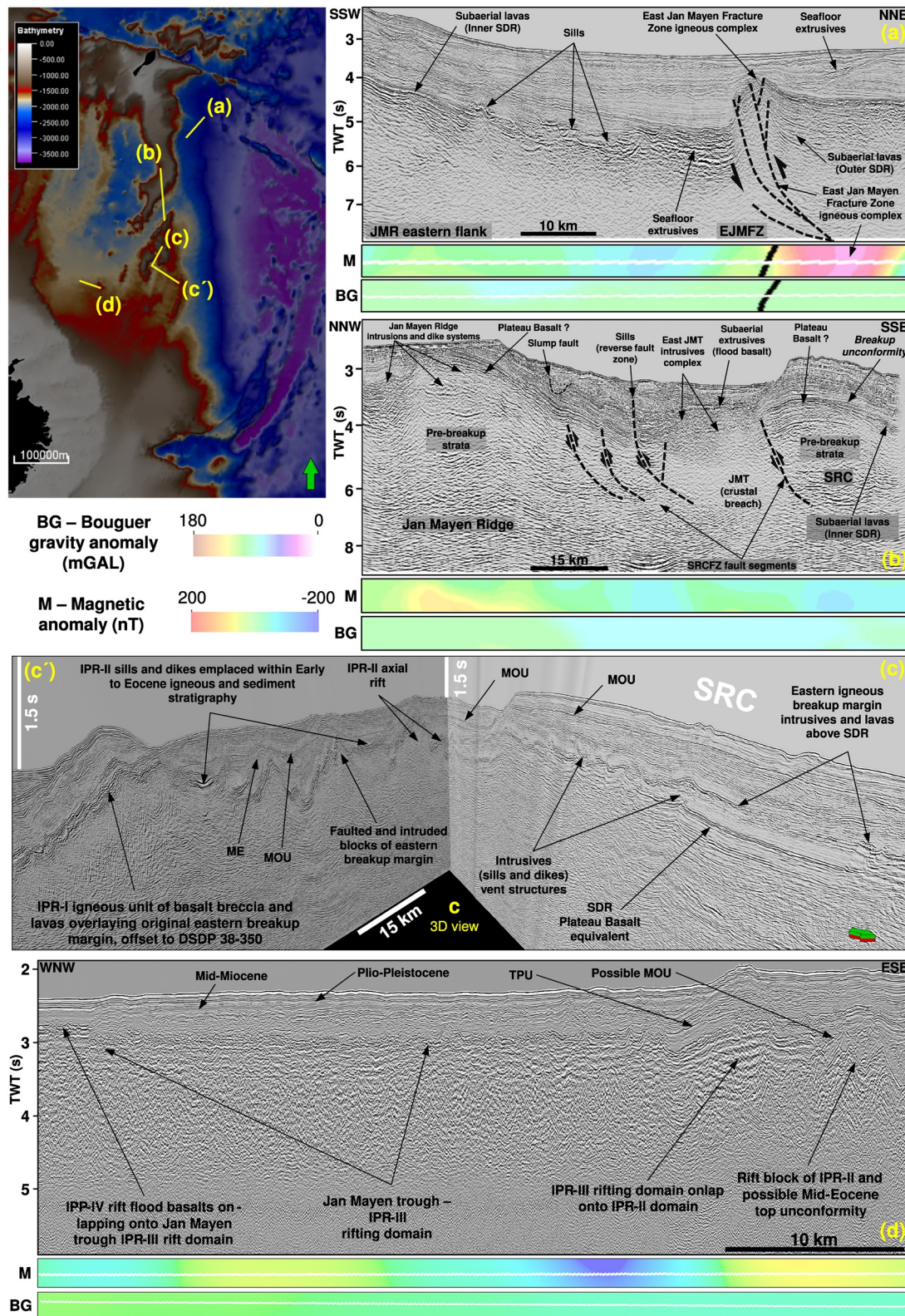


Figure 5.

3.3. Petrology

Borehole and seafloor samples within the northeast Atlantic region are sparse, except for active mid-ocean ridges (Figures 1 and 3; Supplements 1–5 in Supporting Information S1). The Deep-Sea Drilling Program (DSDP) Leg 38 sites 336, 337, 342, 343, 345, 346, 347, 348, 349 and 350 (Talwani, Udintsev, & White, 1976; Talwani, Udintsev, & Shirshov, 1976; Talwani et al., 1976a, 1976b, 1976c, 1976d, 1976e, 1976f, 1976g, 1976h), and the Ocean Drilling Program (ODP) Leg 104 site 642 (Eldholm et al., 1987a, 1987b) and Leg 162 sites 907 and 985 (Jansen et al., 1996) were used as control sites for the overlying Cenozoic sediment cover, with mapped unconformities and horizons tied into the stratigraphic framework of Blischke et al. (2019) (Supplements 2–5 in Supporting Information S1). The stratigraphic framework also includes interpretations based on seafloor sampling campaigns by Geodekyan et al. (1980), Sandstå et al. (2012, 2013), and Polteau et al. (2012, 2018).

To further constrain volcanostratigraphic provinces, we compiled analyses of borehole and seafloor samples from geochemistry databases and other published sources, including PETDB (Lamont Doherty Earth Observatory, Columbia University, New York, <https://www.earthchem.org/petdb>); GEOROC (Max Planck Institute for Chemistry, Mainz, <https://georo~mpch-mainz.gwdg.de/georoc/>); Haase et al. (1996); Kharin et al. (1976); Kokfelt et al. (2006); the Northern Volcanic Zone, Iceland (Grönvold & Mäkipää, 1978); and Tjörnes Fracture Zone offshore northern Iceland (Devey et al., 1994) (Supplements 3 and 5 in Supporting Information S1; see full reference list under Geochemistry data references).

3.3.1. New Petrology Data and Analysis

A total of 19 samples from DSDP sites 348 and 350 were analyzed at the universities of Iceland and Aarhus to better constrain interpretations of petrological composition for comparison to seismic reflection volcanic facies types (Supplement 5 in Supporting Information S1). At the University of Iceland, seven samples were analyzed for their major element compositions SiO_2 , Al_2O_3 , FeO , MnO , MgO , CaO , Na_2O , K_2O , TiO_2 , and P_2O_5 using inductively coupled plasma-optical emission spectroscopy (ICP-OES; SPECTRO CIROS) and methodologies similar to that described by Govindaraju and Mevelle (1987) and Halldórsson et al. (2008). The remaining 12 samples were powdered at Aarhus University (steel press and corundum mortar) and the compositions of whole-rock compositions were measured at Bureau Veritas Commodities Canada Ltd. by X-ray fluorescence (major elements) and by inductively coupled plasma-mass spectrometry (trace elements) as described by Tegner et al. (2019).

3.4. Chronology

Published geochronology data from offshore boreholes (DSDP Leg 38 sites 336, 337, 345, 348 and 350) and onshore data (e.g., Ganerød et al., 2014; Kharin et al., 1976; L. M. Larsen et al., 2013, 2014; Talwani, Udintsev, & White, 1976; Talwani, Udintsev, & Shirshov, 1976; Talwani et al., 1976a, 1976b, 1976c, 1976d, 1976e, 1976f, 1976g, 1976h; Tegner et al., 2008) were reviewed. Large error margins and age ranges in K/Ar dating from DSDP Leg 38 boreholes 348 and 350 (Kharin et al., 1976) prompted resampling of these cores for Ar-Ar dating and geochemical analyses to constrain the timing of the ridge transition along the southern edge of the JMMC and the Iceland Plateau Rift. Middle Eocene basalts were sampled from core 350 located at the southeasternmost extent of the Jan Mayen Southern Ridge Complex, and lower Miocene basalts were sampled from core 348 located along the western igneous margin of the microcontinent (Figure 3; Supplements 2–5 and 6b in Supporting Information S1). Eight igneous rock samples were selected and described at the IODP core lab in Bremen (Germany), and thin sections were analyzed at the Iceland GeoSurvey's petrology lab. The whole-rock basalt samples were dated at the Oregon State University Argon Geochronology Laboratory (Supplement 3 in Supporting Information S1) through incremental heating in the $^{40}\text{Ar}/^{39}\text{Ar}$ Heine resistance furnace connected to the mass analyzer products (MAP) model 215-50 mass spectrometer.

Figure 5. 2D seismic reflection profiles tied with magnetic (M) and Bouguer gravity (BG) data outlining structural and igneous domains, such as major fault and fracture zones, plateau basalt, intrusions, and extrusive units. Abbreviations: EJMfZ—Eastern Jan Mayen Fracture Zone; IPR—Iceland Plateau Rift (segments I-IV); JMR—Jan Mayen Ridge; JMT—Jan Mayen Trough; ME—Mid-Eocene unconformity; MOU—Mid-Oligocene unconformity; SDR—Seaward dipping reflector sequences; SRC—Jan Mayen Southern Ridge Complex; SRCfZ—Jan Mayen Southern Ridge Complex Fracture Zone; TPU—Top Paleogene unconformity; TWT—Two-way travel time.

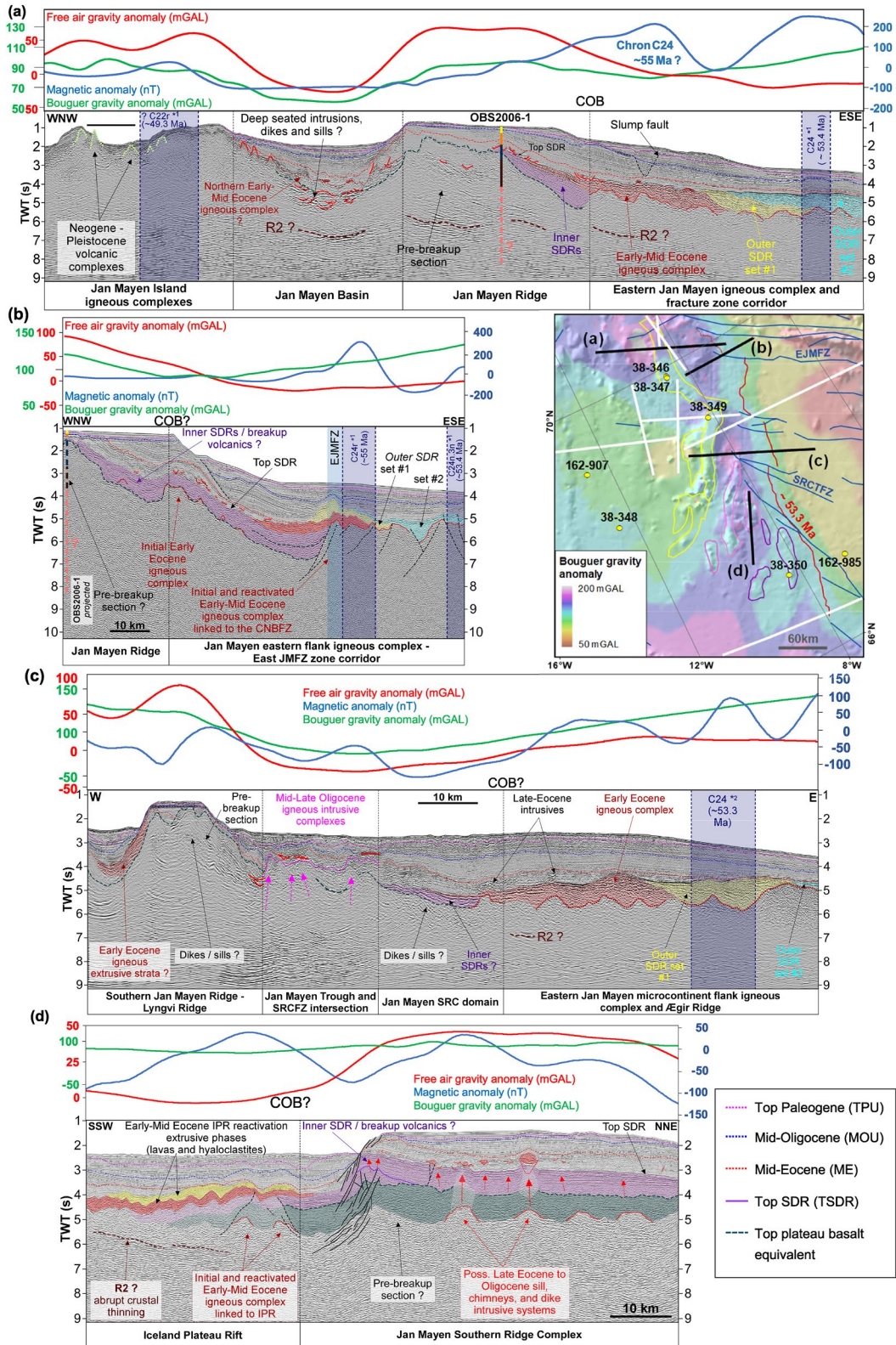


Figure 6.

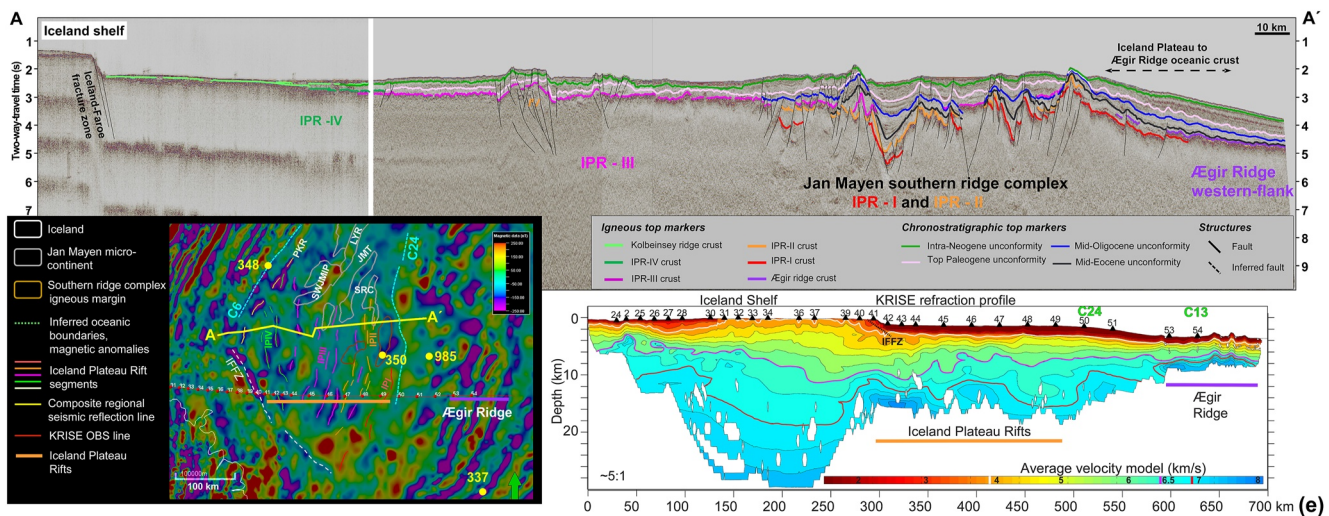


Figure 6. (Continued)

3.5. Kinematic Modeling

Plate-tectonic reconstructions for the relative motion of JMMC with respect to its conjugate margins were obtained using the interactive fitting method of GPlates (<https://www.gplates.org>; see also Gaina, Nasuti, et al., 2017) and GIS visualization for each reconstruction stage (~56–55 Ma; ~55–49 Ma; and 33–21 Ma). To derive the relative motion of the JMMC tectonic block, the larger-scale kinematic reconstruction of Greenland, Eurasia, and the JMMC of Gaina, Nasuti et al. (2017) was used as a starting point, and local adjustments were derived by fitting the data on a GIS platform. The opening of the Norway Basin and the evolution of the Ægir Ridge system were based on the high-resolution magnetic data interpretation by Gernigon et al. (2015). Detailed kinematic reconstructions for the separate JMMC tectonic blocks were tied to the chronostratigraphic succession and best fit of the fault and block topography in chronologic order based on Blischke, Gaina, et al. (2017), Blischke et al. (2019).

4. The JMMC Seismic Volcanostratigraphy

Volcanostratigraphic units were defined on their chronological context, shape, and seismic reflection patterns, in line with methods developed by Larsen and Jakobsdóttir (1988); Symonds et al. (1998), and Planke et al. (2000) for the NE-Atlantic region.

Figure 6. Key seismic reflection cross-sections of the JMMC igneous domains: (a) E-W profile from the Jan Mayen Island igneous complex (JMI), across the northern Jan Mayen Ridge (JMR) and into the East Jan Mayen Fracture Zone (EJMFZ); (b) ENE-WSW profile across the eastern flank of the Jan Mayen Ridge, the East Jan Mayen Fracture Zone and Eocene volcanic complex; (c) E-W profile from the southern Jan Mayen Ridge across the northern Jan Mayen Trough (JMT) and the Jan Mayen Southern Ridge Complex (SRC); and (d) N-S profile from the southern termination of Jan Mayen Southern Ridge Complex into the Iceland Plateau Rift (IPR) system. Bold red lines represent sill or dike intrusions, OBS seismic refraction profile legend as in Figures 1 and 3. (e) E-W seismic reflection profile (A–A') across the Iceland Plateau Rifts, between the Ægir Ridge and proto-Kolbeinsey Ridge (PKR). Major sediment unconformities are delineated. The IPR-I and IPR-II rifts represent structurally segmented initial stages of the Ægir-Kolbeinsey rift transition, mostly intrusives within nascent axial rift segments, whereas IPR-III and IPR-IV represent more typical oceanic rift domains. Lower left: Magnetic intensity anomaly map from Nasuti and Olesen (2014) showing profile A–A' in yellow and the KRISSE reflection-refraction profile in red. Lower right: The KRISSE crustal velocity structure (Brandsdóttir et al., 2015). Sediment-basement boundary (iso-velocity contour 4 km/s), upper-lower crustal boundary (iso-velocity contour 6.5 km/s), and iso-velocity contour 7 km/s are indicated with white, purple, and red lines, respectively. The IPR rifts are underlain by high-velocity lower crustal domes (275–425 km along profile). A marked increase in sediment and lower crustal thickness between OBS48 and OBS50 is attributed to the oldest part of the profile (i.e., west of magnetic anomaly C24). The 2D multi-channel seismic reflection data is based on the NPD 2011 survey, ICE02, 2009 reprocessed data set of the JM-85, and WI-JMR-08 surveys. Base map: Bouguer gravity (Haase & Ebbing, 2014), magnetic polarity chrons *1 Gaina, Nasuti, et al. (2017) for C24 (~55 Ma) and C24n3n (53.4 Ma), and *2 Gernigon et al. (2015) for C24n2r (53.3 Ma). Borehole control is shown refer to DSDP Leg 38 sites 337, 346–350 and ODP Leg 162 sites 907 and 985. Remaining abbreviations: COB—Continent Ocean boundary; JMT—Jan Mayen Trough; LYR—Lyngvi Ridge; SRC—Jan Mayen Southern Ridge Complex; SRCFZ—Jan Mayen Southern Ridge Complex Fracture Zone; SWJMIP—Southwest Jan Mayen igneous province; TWT—Two-way travel time.

4.1. Seismic Characteristics of Volcanic Units

Our classification of five different seismic units representing landward flows—flood basalts, seaward dipping reflector sequences, igneous and volcanic complexes, intrusions, and volcanic vent and ridge structures (Figure 5), is based on seismic characteristics as defined by L. M. Larsen et al. (2013), Hopper et al. (2014), Horni et al. (2017), Gaina, Blischke et al. (2017), Geissler et al. (2017), and Hjartarson et al. (2017).

4.1.1. Landward Flows—Flood Basalts

Uniformly layered flow sections within the seismic records that underlie the inner SDR wedges or occur as a landward continuation from the SDR wedges onto the Jan Mayen Ridge segments are interpreted as early Eocene plateau basalts (Figures 5b and 5c; Supplement 2.5c in Supporting Information S1). These flow units display sheet-like and relatively smooth seismic reflections with high amplitudes that are assigned to subaerial and shallow marine inner flows as described by Abdelmalak et al. (2015) for the Vøring margin. These flood basalt reflections vary locally but are generally sub-parallel. Prograding seismic reflections, observed toward the north-east flank and eastern margin of the Jan Mayen Ridge, reflect lava and/or deltaic seismic units (Figures 6a–6c). Younger, late Oligocene to early Miocene flood basalt units form flat-lying marker horizon within the Jan Mayen Basin, Jan Mayen Trough, and south of the JMMC (Figure 5d; Supplements 2b, 2c, and 6e in Supporting Information S1). The flood basalts within the southern Jan Mayen Basin overlap older rift segments (Figure 5d), Oligocene sediments, and volcanic strata (Supplements 2c, 6e in Supporting Information S1).

4.1.2. Seaward Dipping Reflector Sequences

SDR sequences are subaerial flood basalt units characterized by strong acoustic impedance contrasts. They form distinct seaward-dipping wedges, often with concave-downward shapes (Figures 5a, 6a, and 6b; Supplement 2, 6 in Supporting Information S1). Inner SDR wedges are commonly associated with continental breakup (Hinz, 1981; Larsen & Jakobsson, 1988). The formation of igneous centers along the continent-ocean boundary (COB; Figures 6a–6c), referred to as outer highs (see below), have been interpreted as subaqueous extrusions indicating submergence of a nascent spreading center (Hopper et al., 2003; Planke et al., 2000).

4.1.3. Igneous and Volcanic Complexes

The outer high igneous centers are characterized by chaotic internal seismic reflection patterns and a strong top reflection. They appear as mounded or sloping shapes and can form circular features on magnetic and gravity datasets, especially along the north-eastern flank of the Jan Mayen Ridge (Figures 6a and 6b; Supplement 6a in Supporting Information S1) where an igneous center appears to have been active over a long-time-interval, apparently linked to a segment of the East Jan Mayen Fracture Zone (Figures 5a and 6b). This igneous complex is aligned with magnetic anomaly C24r (~55 Ma) (Gaina, Nasuti, et al., 2017).

The Jan Mayen Island igneous complex is also characterized by homogenous and chaotic seismic reflection patterns, apparent deep-seated high-amplitude reflections, and young volcanic complexes that pierced through older igneous sequences (Figure 6a; Supplement 2 in Supporting Information S1). A younger volcanic center along the western boundary of the JMMC is clearly observed on seismic reflection and refraction data and possibly relates to the early Miocene proto-Kolbeinsey Ridge breakup margin (Figure 4b; Supplement 2 in Supporting Information S1). Other Neogene to Pleistocene volcanic centers along the northwestern margin intruded into an interpreted Eocene igneous section and form near-surface volcanic cone structures (Figure 6a).

4.1.4. Intrusives

Smaller-scale igneous intrusions, related to dikes and sills, are typically observed as local, often isolated, low frequency, high amplitude reflections that terminate abruptly, and are commonly connected to vent structures (Figures 5 and 6; Supplement 6 in Supporting Information S1). Their structural disposition ranges from semi-parallel to stratigraphic layering or along fault planes to discordant and crosscutting the strata as “smiley” shaped features, specifically along the JMMC eastern flank, the Jan Mayen Southern Ridge Complex (Figures 5a, 5b and 6), the Jan Mayen Trough, and within the Jan Mayen Basin.

4.1.5. Volcanic Ridges—Axial Rift Zones

Volcanic ridges and axial rift zones characterize the Jan Mayen Southern Ridge Complex and Jan Mayen Trough regions, where they form up-doming structures of volcanic material close to fault or fracture zones. They are

located mostly in the southern area of the Jan Mayen Southern Ridge Complex and along the northern end of the Jan Mayen Trough and are visible on seismic reflection and bathymetry data (Figures 1, 5b, 5c and 6b–6d). They appear both as centralized structures within the Jan Mayen Trough and along large fault zones that serve as conduits of rising magma, causing deformation and uplift of the overburden. A higher density of smaller-scale intrusions within nearby sedimentary strata appears to be associated with these conduits.

4.2. Igneous Sites South and West of the JMMC

To further constrain the igneous framework and provinces, petrophysical and age parameters of igneous samples from DSDP Leg 38 sites 348 and 350 were correlated with conjugate igneous outcrops, specifically along the Blossville Kyst (Figures 7 and 8; Supplements 3–5 in Supporting Information S1). These outcrops provide a potential stratigraphic analog for the deeper Cenozoic and pre-breakup strata, for example, the lower Paleogene plateau basalt succession (e.g., Blischke, Gaina, et al., 2017; Blischke et al., 2019; L. M. Larsen et al., 2013, 2014; M. Larsen et al., 2002, 2005; Pedersen et al., 1997). Geochronological data from conjugate areas provided by Storey et al. (2007), Hald and Tegner (2000), Tegner et al. (2008), or Ganerød et al. (2014) were also implemented within the geodynamic model of the JMMC-IPR.

4.2.1. DSDP Leg 38 Site 348

DSDP Leg 38 site 348 is located within the oldest oceanic crust of the Kolbeinsey Ridge and serves as a control site west of the JMMC (Figure 1; Supplement 3a in Supporting Information S1). At site 348, 17.4 m of fractured but homogenous basalt section was penetrated at 526.6 m below the seafloor. Geochemical analysis by Kharin et al. (1976), Ridley et al. (1976), and Mohr (1976) revealed abyssal tholeiites and dike or sill complexes.

Core resampling and thin-section analyses (Supplement 3a in Supporting Information S1) also showed finely crystalline olivine-tholeiite with volcanic glass (now replaced by smectite) close to the basalt/sediment contact, indicating that the intrusions penetrated the overlying sediments. The basalt is slightly porphyritic, with micro-phenocrysts of plagioclase and olivine, the latter now pseudomorphed and altered to iddingsite. Many plagioclase crystals exhibit skeletal growth and a "swallow-tail" morphology. Combined with the apparent glass content, this suggests that the basalt cooled rapidly (e.g., Lofgren, 1974). Clinopyroxene and opaque minerals are unaltered but exhibit dendritic or feather-like morphology deeper in the cored section, which is common for ocean floor basalts (e.g., Lofgren, 1983). The lowermost section consisted of fine- to medium-grained crystalline, aphyric olivine-tholeiite with large vesicles, possibly indicating rapid surface ascent as sills or dikes; a conclusion also reached by Kharin et al. (1976) and White and Schilling (1978), who argued that the absence of lava-flow characteristics, including pillow structures and glassy rims, did not support a submarine extrusion.

The K_2O and Na_2O content of DSDP site 348 basalts fall within the Mid-Ocean Ridge Basalt (MORB) field on the total-alkali-silica (TAS) classification diagram (Le Bas et al., 1989) (Figure 7a), along with samples from the Ægir-, Kolbeinsey- and Mohns ridges, as well as the Tjörnes Fracture Zone (TFZ; purple field in Figure 7a). TiO_2 ranges from 1.29 to 1.65 wt%, K_2O from 0.02 to 0.08 wt%, and MgO between 6.02 and 8.25 wt%; values considerably lower than samples from the Jan Mayen Fracture Zone, Vesteris Seamount, and Vøring Plateau. Basalts from the Iceland Plateau Rift (DSDP site 350) and northern volcanic zone of Iceland are considerably higher in K_2O and slightly higher in TiO_2 than site 348.

Previous K-Ar radiometric dating of samples from this site ranged between 19.4 ± 2.2 Ma and 18.2 ± 2.4 Ma (Kharin et al., 1976). Our new $^{40}Ar/^{39}Ar$ dating of three core samples (Figure 8; Supplements 3a and 4 in Supporting Information S1) provided an age range between 22.15 ± 0.26 Ma to 23.19 ± 0.61 Ma, corresponding to magnetic polarity chron C6b to C6c (Gradstein et al., 2012).

4.2.2. DSDP Leg 38 Site 350

The basalt section sampled at DSDP Leg 38 site 350, at the southern tip of the easternmost Jan Mayen Southern Ridge Complex (Figures 1, 7 and 8; Supplements 3b; 4 and 5 in Supporting Information S1), was recovered from an acoustically opaque layer between 362 and 388 m below the seafloor. The 26-m-thick section was initially described as a thick layer of highly altered tuff breccia with chlorite, zeolites, calcite, and doleritic basalt at its base (Kharin et al., 1976; Raschka et al., 1976; Ridley et al., 1976). The uppermost section consists of 95% basalt breccia with angular fragments of altered and aphyric hyalobasalt (partly altered to palagonite) with plagioclase, pyroxene, and altered olivine crystals (Raschka et al., 1976). The deeper section at site 350 consists of very fresh,

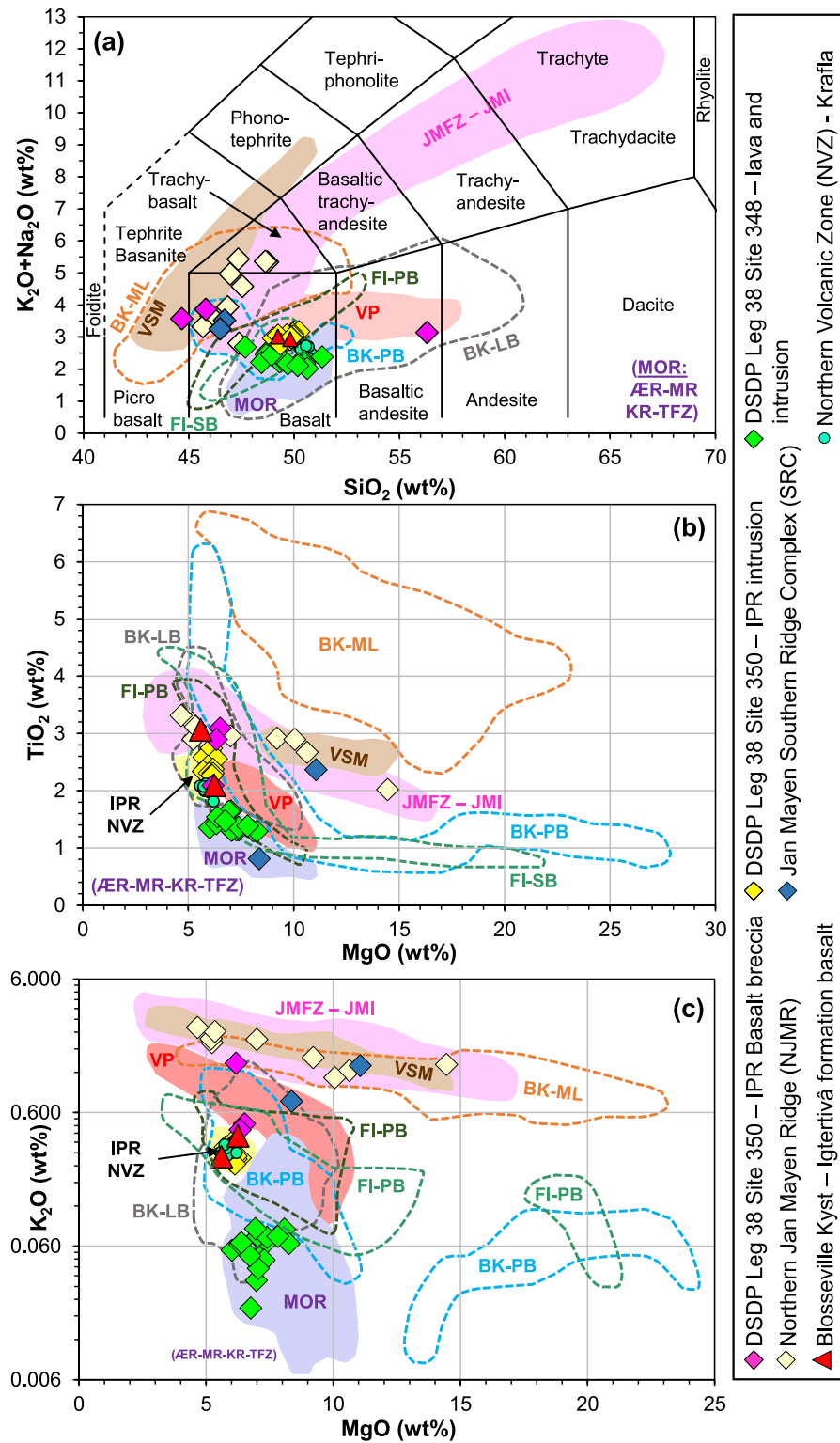


Figure 7.

holocrystalline, fine- to medium-grained basalt, with rare plagioclase and pyroxene phenocrysts (2–5 mm), thin chlorite-calcite veins, and slickensides. The basalt has a homogenous appearance with various textures including micro-porphyritic, sub-ophitic, and trachytoid (Raschka et al., 1976).

Core resampling and thin-section analyses (Supplement 3b in Supporting Information S1) showed that the basalt fragments have a thin chlorite-calcite-zeolite-smectite edging coated evenly on all sides. The breccia is cut by white-yellowish layered calcite veins with occasional pyrite occurrences. Geochemical analyses show elevated TiO_2 (2.09–3.09 wt%), K_2O (0.45–1.41 wt%), and slightly lower MgO (6.17–6.51 wt%) relative to the samples of site 348 and typical MORBB rocks (Figures 7b and 7c). Interestingly, the altered samples from site 350 have compositions similar to geochemical trends for the Jan Mayen Fracture Zone, Jan Mayen Island igneous complex, northern Jan Mayen Ridge, and Vesteris seamount.

Reexamination of the deeper basalt section revealed a doleritic basalt intrusion with a distinct chilled margin against the basalt breccia, confirming the hypotheses of a younger intrusion, as observed in the seismic reflection data (Supplement 6b in Supporting Information S1). The stratigraphic unit that overlies the basalt breccia unit consists of turbiditic sedimentary rocks that are hydrothermally altered and lithified, indicative of contact-metamorphism by igneous activity after the emplacement of the turbidite section.

Analyses of the basalt intrusive samples show TiO_2 content between 2.34 and 2.75 wt%, a K_2O of 0.27–0.37 wt%, and MgO between 5.75 and 6.34 wt% (Figures 7b and 7c). The site 350 basalt intrusion is richer in plagioclase than typical MORB rocks of site 348 (Figure 7a), reflected by higher K_2O and Na_2O content on the total-alkali-silica (TAS) classification diagram. The samples fall within the same range as the Blosseville Kyst plateau basalts and overlap partly the Vøring margin ranges (Figure 7a; Supplements 3b in Supporting Information S1). With a higher concentration of titanium and potassium than typical MORB rocks, the intrusive section is geochemically analogous to present-day basalts from the Northern Volcanic Zone (NVZ) of Iceland and from the Vøring Plateau.

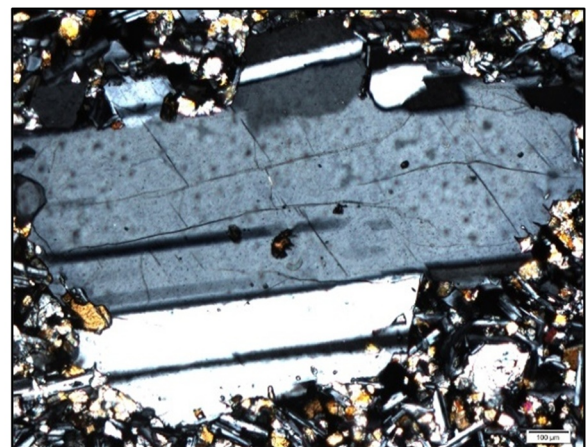
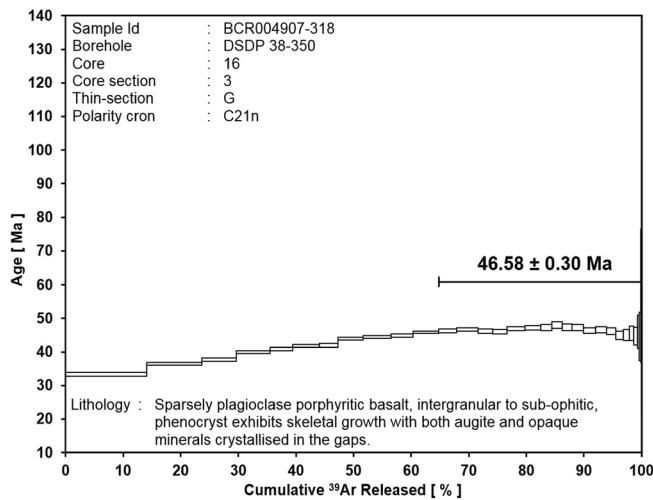
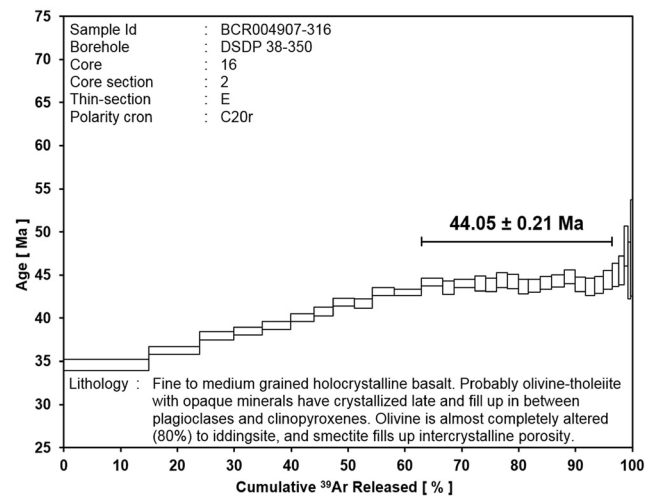
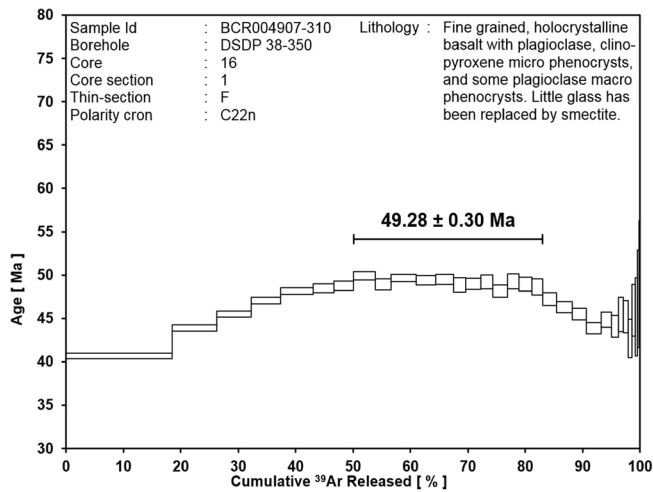
Previous K/Ar age determinations provided an age range between 33.5 Ma \pm 2.8 Ma and 50.5 Ma \pm 5.5 Ma for the doleritic intrusion (Kharin et al., 1976) (Figure 8a; Supplements 3b, 4 in Supporting Information S1). The doleritic intrusion was resampled and analyzed by ^{40}Ar - ^{39}Ar dating which provided an age ranging from \sim 49.28 \pm 0.3 Ma to 44.05 \pm 0.21 Ma, corresponding to polarity chrons C22n to C20r (Gradstein et al., 2012) (Figure 8a; Supplement 4 in Supporting Information S1).

4.2.3. Dredged Seafloor Samples

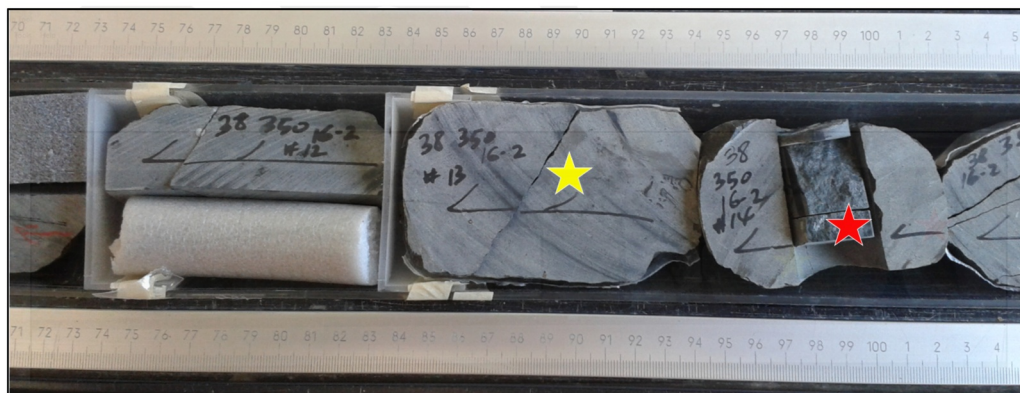
Samples obtained during a dredging and gravity coring survey by Polteau et al. (2018) on the Jan Mayen Southern Ridge Complex were described as freshly broken, subaerially erupted, vesicular, and altered basalts, or brecciated volcanoclastic and dolerite basalt fragments. Two of the less altered samples are MgO-rich (8.36–11.06 wt%) basalts based on the TAS classification (Le Bas et al., 1989) (Figure 7a, blue diamonds). However, they have different compositions based on their titanium and potassium content, one being closer to the MORB type, and the other to the Blosseville Kyst-Milne Land and Faroe Island Plateau basalt domains and syn-rift series (Figures 7b and 7c).

Age determination of basaltic material dredged from the escarpment along the eastern flank of the Lyngvi Ridge and the northwesternmost flank of the Jan Mayen Southern Ridge Complex has been problematic due to the altered state of the samples. They consist of partially unaltered vesicular basalt, volcanoclastic breccias, and dolerite fragments. A varying degree of alteration was observed for the primary micro-crystalline basalt with mineralized vesicles (Polteau et al., 2012, 2018; Sandstå et al., 2012, 2013). Polteau et al. (2018) infer an age range of basalt emplacement between \sim 59 and 47 Ma (late Paleocene to early Eocene) (Figure 2; Supplement 5a in Supporting Information S1). The age is based on sediment dredge samples below and above the basaltic dredge section and regional reference. Uncertainty remains regarding the in-situ nature of these samples, and an allochthonous origin cannot be discounted.

Figure 7. Geochemical composition diagrams (a) TAS classification diagram (Le Bas et al., 1989); (b) (TiO_2 vs. MgO) and (c) (K_2O vs. MgO) from DSDP Leg 38 sites 348 and 350 core samples in comparison with data from DSDP Leg 38 and ODP Leg 162 boreholes within the JMFZ, the SRC dredge samples (Polteau et al., 2018), Vøring and Blosseville Kyst igneous margins; Ægir-, Mohns- and Kolbeinsey ridges; Iceland (TFZ and NVZ) (Figure 1; Supplements 3–5); and regional igneous provinces, based on data from PETDB (Lamont Doherty Earth Observatory, Columbia University, New York, <http://www.earthchem.org/petdb>); GEOROC (Max Planck Institute for Chemistry, Mainz, <https://georo-mpch-mainz.gwdg.de/georoc/>; Grönvold & Mäkipää, 1978; Kharin et al., 1976). Abbreviations: ÆR—Ægir Ridge; BK-ML—Blosseville Kyst Milne Land formation; BK-PB—Blosseville Kyst main Plateau Basalt; BK-LB—Blosseville Kyst—lower basalt series; FI-PB—Faroe Islands pre-breakup series; FI-SB—Faroe Island syn-breakup series; IPR—Iceland Plateau Rift; JMFZ—Jan Mayen Fracture Zone; JMI—Jan Mayen Island; KR—Kolbeinsey Ridge; MOR—mid-oceanic ridge; MR—Mohns Ridge; NJMR—northern Jan Mayen Ridge; NVZ—Northern Volcanic Zone; SRC—Jan Mayen Southern Ridge Complex; TFZ—Tjörnes Fracture Zone; VP—Vøring igneous margin; VSM—Vesteris Seamount.



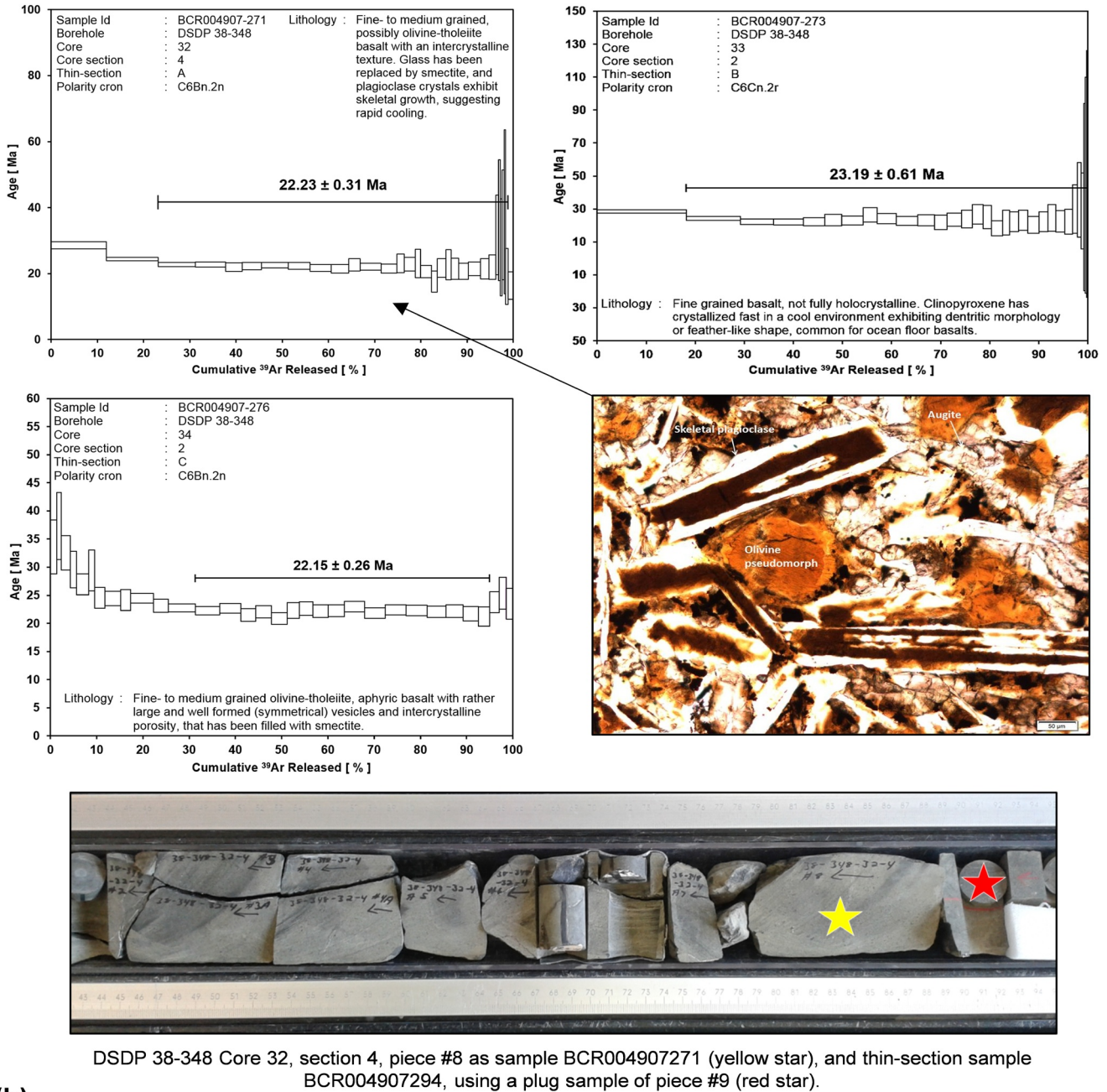
Plagioclase phenocryst around 1 mm in length.



DSDP 38-350 Core 16, section 2, piece #13 as sample BCR004907316 (yellow star), and thin-section sample BCR004907320, using a plug sample of piece #14 (red star).

(a)

Figure 8. ⁴⁰Ar/³⁹Ar radiometric age determinations of samples from boreholes DSDP Leg 38 sites 350 and 348, (a) radiometric diagram and description of samples from core 16 of DSDP Leg 38 site 350, and (b) radiometric diagram and description of samples from core 32 of DSDP Leg 38 site 348. Abbreviations: DSDP, Deep Sea Drilling Program.



(b)

Figure 8. (Continued)

5. The Formation of the JMMC Igneous Provinces

Based on seismic-stratigraphic mapping, magnetic and gravity data, as well as geochemical analyses, seven distinct igneous phases have been identified within the JMMC region: pre-breakup and syn-breakup, followed by four Eocene-early Miocene rift propagation phases within the Iceland Plateau, a post-breakup phase, here referred to us a proto-Kolbeiney Ridge phase, and finally the initiation of spreading along the Kolbeinsey Ridge, as detailed below.

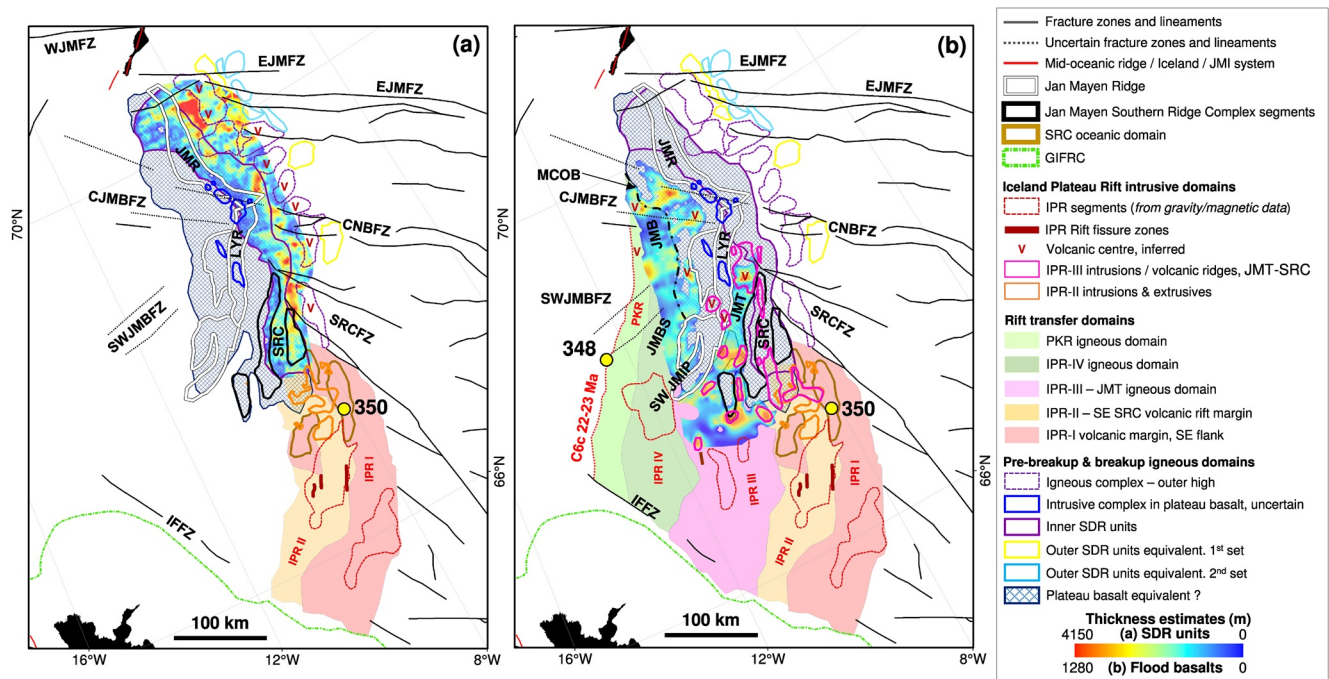


Figure 9. Maps showing JMMC volcanic provinces and stratigraphic thickness estimates for the SDR sequences and flood basalts along the eastern flank and within the Jan Mayen Trough and Basin. (a) Early Eocene breakup volcanism along the eastern margin of the JMMC. Note increase in SDR thickness near igneous (v) centers. (b) Thickness estimate of Eocene to early Miocene flood basalts within the F-Marker region. Fracture zones modified from Gernigon et al. (2015) and Blischke, Gaina, et al. (2017), Blischke et al. (2019). Boreholes from DSDP Leg 38. Abbreviations: CJMBFZ—Central Jan Mayen Basin Fracture Zone; CNBFZ—Central Norway Basin Fracture Zone; EJMfZ—East Jan Mayen Fracture Zone segments; GIFRC—Greenland-Iceland-Faroe Ridge Complex; IFFZ—Iceland-Faroe Fracture Zone; IPR—Iceland Plateau Rift (segments I-IV); JMB—Jan Mayen Basin; JMBS—Jan Mayen Basin south; JMI—Jan Mayen Island igneous complex; JMR—Jan Mayen Ridge; JMT—Jan Mayen Trough; MCOB—inferred western microcontinent ocean boundary; PKR—proto-Kolbeinsey Ridge; LYR—Lyngvi Ridge; SDR—Seaward dipping reflector sequences; SRC—Jan Mayen Southern Ridge Complex; SRCFZ—Southern Ridge Complex Fracture Zone; SWJMIP—Southwest Jan Mayen igneous province; SWJMBFZ—Southwestern Jan Mayen Basin Fracture Zone; WJMfZ—West Jan Mayen Fracture Zone.

5.1. The Jan Mayen Ridge—Pre-Breakup Phase

The oldest igneous section of the Jan Mayen Ridge (stratigraphic unit JM-70, Figure 2) has been associated with pre-breakup volcanic activity during the late Paleocene and early Eocene (Blischke et al., 2019). Unit JM-70 underlies the inner SDR units along the eastern flank of the JMMC and onlaps the Jan Mayen igneous complex to the north (Figures 4 and 6; Supplement 2 in Supporting Information S1). On seismic reflection data, JM-70 is characterized by a laterally continuous succession of parallel-bedded seismic reflections, interpreted as stacked plateau-basaltic flows (Blischke et al., 2019). The parallel-bedded seismic reflections have been mapped across the Jan Mayen Ridge, Lyngvi Ridge, Jan Mayen Southern Ridge Complex, and partially along the eastern edge of the Jan Mayen Basin (Figures 9 and 10). The uppermost 0.5–1.0-s-thick section of the sub-parallel, stratified lower Eocene pre-breakup basalts has a *P*-wave velocity between 3.8 km/s and 5.0 km/s based on seismic refraction data, similar to the flood basalts from ODP borehole 917A of Leg 152 from Southeast Greenland, where a *P*-wave velocity range between 2.5 and 5.5 km/s was recorded for brecciated and vesicular flow tops and 5–7 km/s for the central and lower part of the lavas (Planke & Cambray, 1998). Based on these values, the stratigraphic thickness of the lower Eocene basalt succession is about 1 km across the central Jan Mayen Ridge, increasing southward to approximately 3 km on the southernmost Lyngvi Ridge (dark gray layer in Figures 4b and 10b; Supplement 2a in Supporting Information S1). As the JMMC has subsequently been affected by major erosive events, the original stratigraphic thickness of this layer cannot be determined. The basalt succession is comparable in stratigraphic architecture to rocks exposed on the conjugate central East Greenland coast and imaged on offshore seismic reflection lines along the East Greenland continental margin (Blischke & Erlendsson, 2018; Blischke et al., 2020) (Figure 2a).

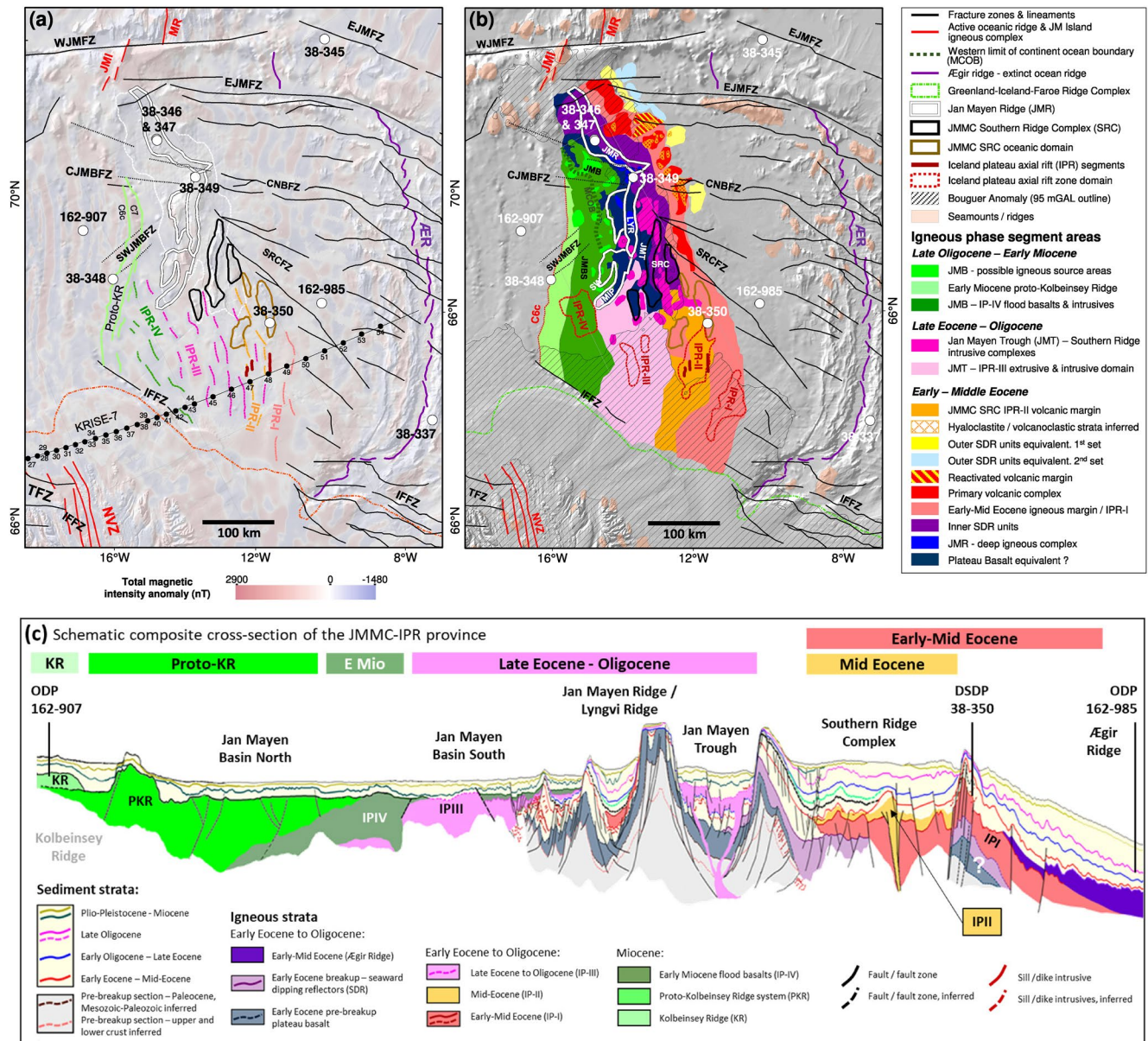


Figure 10. Overview of the JMMC volcanic domains and IPR segments: (a) in reference to magnetic anomaly data (Haase & Ebbing, 2014), the KRISE Line 7 seismic refraction data (Brandsdóttir et al., 2015), and boundary magnetic anomalies C24b (Gernigon et al., 2015) and C6c this study; and (b) the volcanic facies and provinces maps in order of emplacement: Early-Middle Eocene, Late Eocene-Oligocene, and Late Oligocene-Early Miocene igneous facies types and units, including intrusive and extrusive strata, plateau basalt equivalent, igneous centers, SDR, hyaloclastite volcanic strata, flood basalts. Abbreviations: ÆR—Ægir Ridge; CJMBfZ—Central Jan Mayen Basin Fracture Zone; CNBfZ—Central Norway Basin Fracture Zone; COB—Continent ocean boundary; EJMfZ—East Jan Mayen Fracture Zone segments; IFFZ—Iceland-Faroe Fracture Zone; IPR—Iceland Plateau Rift (segments I-IV); JMI—Jan Mayen Island complex; JMB—Jan Mayen Basin; JMS—Jan Mayen Basin south; MCOB—Western margin continent-ocean boundary; JMR—Jan Mayen Ridge; JMT—Jan Mayen Trough; LYR—Lyngvi Ridge; MR—Mohns Ridge; SDR—Seaward dipping reflector sequences; SRCfZ—Jan Mayen Southern Ridge Complex Fracture Zone; SRC—Jan Mayen Southern Ridge Complex; SWJMBfZ—Southwest Jan Mayen Basin Fracture Zone; SWJMIP—Southwest Jan Mayen igneous province; TFZ—Tjörnes Fracture Zone; and WJMFZ—Western Jan Mayen Fracture Zone.

Locally disrupted zones with chaotic seismic reflection patterns most likely represent smaller intrusive centers. These are embedded within the plateau basalt strata on the Lyngvi Ridge and on the northernmost segment of the Jan Mayen Southern Ridge Complex (Figures 6a–6c, 9, 10b; Supplement 2a, 2c in Supporting Information S1). These intrusions appear to be focused within the Jan Mayen and Lyngvi Ridge segments and do not deform the post-breakup formations and, thus, could be related to the pre-breakup volcanism as well.

5.2. The JMMC Eastern Margin Igneous Domain—Syn-Breakup Phase

This syn-breakup igneous phase, stratigraphic unit JM-60, includes SDR units along the eastern flank of the JMMC, which discordantly overlies the plateau basalts of unit JM-70 (Blischke, Gaina, et al., 2017; Blischke et al., 2019) (Figures 2, 4–6, 9a, 10b; Supplements 2, 6, 7 in Supporting Information S1). The top surface of the unit (TSDR on Figure 2) is marked by high amplitude, continuous seismic reflections, providing a reliable correlation horizon across faults or graben structures that offset the SDR unit. Skogseid and Eldholm (1987) described a wide volcanic breakup margin that linked the JMMC across the eastern Jan Mayen Fracture Zone to the Vøring margin with distinct sets of SDR wedges forming along both margins during the breakup. Based on the dense grid of seismic reflection data, three sets of SDR units can be delineated along the northeastern margin of the JMMC close to the eastern Jan Mayen Fracture Zone. An igneous complex separates the innermost set from the two outer sets of SDR units (Figures 6a–6c, 9a, 10b) representing the outer highs of the volcanic breakup margin, as defined by Planke et al. (2000). This igneous complex is interpreted as a conjugate feature to the Vøring margin (e.g., Hinz, 1981; Mutter et al., 1982; Skogseid & Eldholm, 1987; Planke et al., 2000) across the eastern Jan Mayen Fracture Zone as indicated by plate tectonic reconstructions (Figures 11a and 12).

The inner (and older) SDR units onlap westward onto the Jan Mayen Ridge and Jan Mayen Southern Ridge Complex, where they unconformably pinch out onto the plateau basalts of unit JM-70 (Figures 2, 6, 9a). The inner SDR units exhibit a parallel bedded, eastward prograding seismic reflection pattern, with localized hummocky to lenticular patterns that tend to be thinner (<1.5 km). The inner SDR are up to 4 km in stratigraphic thickness and are related to the landward, subaerial lava flows (Figures 6a, 9a and 10b; Supplements 2 and 6 in Supporting Information S1) (see e.g., comparison in Hinz, 1981; Mutter et al., 1982; Planke et al., 2000). The transition between the inner SDR wedge and the outer high is commonly parallel to the interpreted continent-ocean boundary zone and limits the eastward extent of the Jan Mayen Ridge and Jan Mayen Southern Ridge Complex domains (e.g., Figures 6a–6c; Supplement 2 in Supporting Information S1).

Previously, the eastern Jan Mayen Ridge volcanic margin has been mapped as a continuous feature (e.g., Gaina et al., 2009, Skogseid & Eldholm, 1987, or Peron-Pinvidic et al., 2012a). The data presented here, however, suggests that the margin is segmented and made up of distinct igneous complexes that are related to the inner SDR set, outer high complexes, and one or two outer SDR sets (Figures 9a, 10b and 11a). The igneous complexes along the eastern margin are characterized by chaotic seismic reflection patterns that probably represent shallow sill and dike systems (Figures 6, 9a, 10b, 11; Supplement 6 in Supporting Information S1). A faulted igneous complex is tied to a segment of the eastern Jan Mayen Fracture Zone (Figure 6b), where deposits from several volcanic episodes are stacked vertically rather than in a typical seaward progression as in Figures 6a and 6c. Some of these complexes appear semi-circular and have possibly formed volcanic cone structures in a shallow marine environment, as they are covered by prograding seismic reflection units possibly related to hyaloclastite and volcanoclastic depositional patterns (Figure 10b; Supplement 6 in Supporting Information S1).

The outer highs of the primary volcanic margin have been correlated with the early Eocene polarity chron C24 magnetic anomaly (Figures 6a, 6b and 10a), previously defined as polarity chron C24B (56–53 Ma) by (Skogseid & Eldholm, 1987); or C24r (~55 Ma) by Gaina et al. (2009) and Gernigon et al. (2015). The oldest continuous magnetic anomaly in this region is C24n3n (~53.4 Ma) (Gaina et al., 2009; Gernigon et al., 2015) (Figures 6a–6c). Anomalies C24 and C24n3n lie parallel to the two outer SDR units (Figures 6a–6c), which represent younger events since they onlap onto the inner SDR units. The eastward prograding outer SDR units appear to stack on top of each other, within a distinct and longer-lived volcanic system that developed at the termination of one of the eastern Jan Mayen Fracture Zone segments (Figures 6b, 9a and 10b). SDR wedges disappear south of the central Norway Basin Fracture Zone (CNBFZ) and are recognizable only across the northernmost two ridges of the Jan Mayen Southern Ridge Complex (Figures 6c, 9a and 10b).

The outer SDR units and oldest oceanic basement of the eastern JMMC volcanic margin have a P-wave velocity range from 4.8 to 5.5 km/s, whereas the inner SDR units have a slightly lower range of 3.2–4.3 km/s, similar to the Vøring and Møre margins (Blischke et al., 2019). A subseafloor layer in between the seismic horizons R1 and R2, has irregular seismic reflection characteristics (Figures 4b and 6; Supplement 2 in Supporting Information S1) with P-wave velocities of 4.8–6.8 km/s, which corresponds to the outer SDR units and oldest oceanic basement as part of the eastern JMMC volcanic margin. Similarly, wide volcanic breakup margins have been observed along the East Greenland, Møre, and Vøring margins (e.g., Breivik & Mjelde, 2003; Breivik et al., 2008, 2012; Faleide

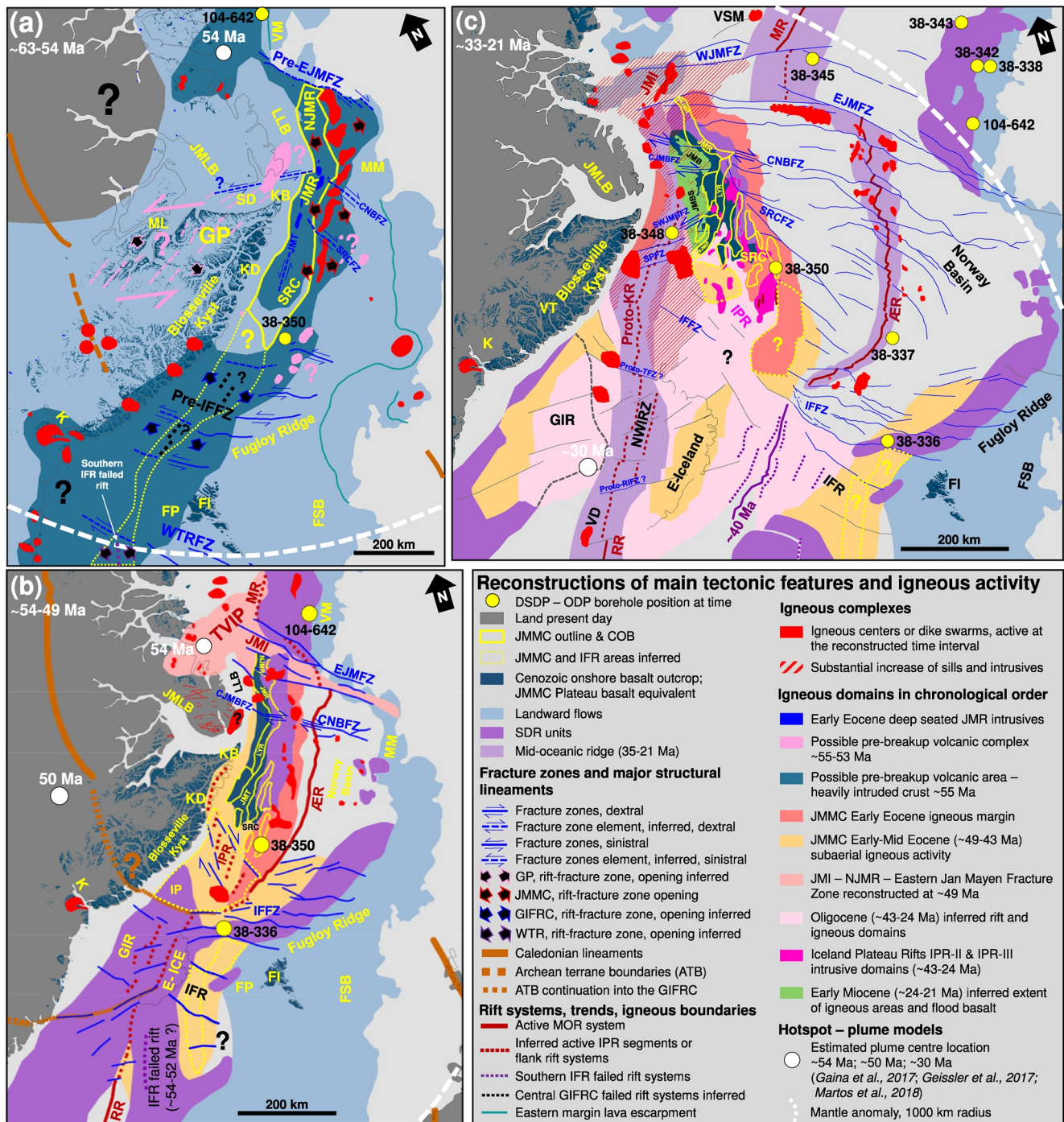


Figure 11.

et al., 2010; Gernigon et al., 2015, 2021; Mjelde et al., 2016; Weigel et al., 1995; Theissen-Krah et al., 2017; or Zastrozhnov et al., 2018).

Seafloor samples from the northern Jan Mayen Ridge have not been dated, but appear to be related to younger volcanic activity, based on comparison to basalts from the Jan Mayen Fracture Zone, Vesteris seamount, and the early Eocene Prinsen af Wales Bjerger Formation on the Blossesville Kyst (Debaille et al., 2009; Haase et al., 1996) (Figure 7). Their compositions are basaltic to trachybasaltic (SiO_2 45–49 wt%), correlating well with syn-breakup

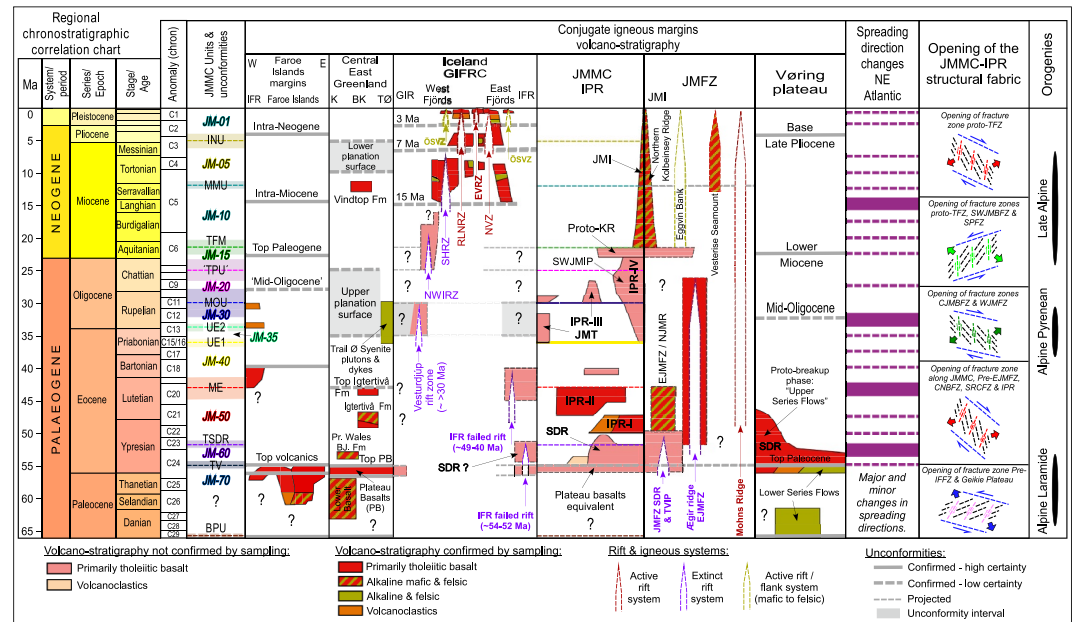


Figure 12. Regional chronostratigraphic summary chart of the JMMC volcanostratigraphy in relation to its conjugate igneous margins. Changes in spreading direction are those modeled by Gaina, Blischke, et al. (2017), Gaina, Nasuti, et al. (2017); information on the main igneous provinces and rift relocations is derived from Sæmundsson (1979), Harðarson et al. (1997, 2008), Saunders et al. (2013), Brandsdóttir et al. (2015), Blischke, Gaina, et al. (2017), Blischke et al. (2019), Geissler et al. (2017), Parsons et al. (2017), and Hjartarson et al. (2017); information on mid-oceanic ridge systems and orogeneses is modified after Lundin and Doré (2002). Time scale from Gradstein et al. (2012). For unconformity and JMMC abbreviations, see Figure 2; abbreviations for conjugate igneous margins, provinces, and rift relocations are: BK—Blosseville Kyst; CJMBFZ—Central Jan Mayen Basin Fracture Zone; CNBFZ—Central Norway Basin Fracture Zone; EJMFZ—Eastern Jan Mayen Fracture Zone; EVRZ—Eastern Volcanic Zone; Fm—Formation; GIFRC—Greenland-Iceland-Faroe Ridge complex; GIR—Greenland-Iceland Ridge; IFFZ—Iceland-Faroe Fracture Zone; IFR—Iceland-Faroe Ridge; IPR—Iceland Plateau Rift; JMFZ—Jan Mayen Fracture Zone; JMI—Jan Mayen Island igneous province; JMMC—Jan Mayen microcontinent; JMR—Jan Mayen Ridge; K—Kangerlussuaq; KR—Kolbeinsey Ridge; NAIP—North Atlantic igneous province; NJMR—Northern Jan Mayen Ridge; NVZ—Northern Volcanic Zone; NWIRZ—Northwest Iceland Rift Zone; PB—Plateau Basalt; RLNZR—Reykjanes-Langjökull-North Iceland Rift Zone; Pr. Wales B.J. formation—Prinsen af Wales Bjerge formation; proto-RIFZ—inferred proto-Reykjanes-Iceland Fracture Zone; SDR—Seaward dipping reflector sequences; SHRZ—Snæfellsnes-Húnaflói Rift Zone; SRCFZ—Jan Mayen Southern Ridge Complex Fracture Zone; SPFZ—Spa Fracture Zone; SWJMBFZ—Southwest Jan Mayen Basin Fracture Zone; SWJMIP—Southwest Jan Mayen igneous province; proto-TFZ—inferred proto-Tjörnes Fracture Zone; TØ—East Greenland Traill Ø margin; TVIP—Trail Ø-Vøring igneous complex; ÖSVZ—Öræfi Intraplate Volcanic Zone, and WJMFZ—Western Jan Mayen Fracture Zone.

Figure 11. Reconstructions of igneous provinces in the Northeast Atlantic. East Greenland and main tectonic blocks of JMMC shown in an absolute position (relative to the mantle) according to kinematic parameters that were computed by carrying out visual fits (in GPlates 2.0.0; <https://www.gplates.org>) for the (a) pre-breakup to synbreakup (~63–54 Ma); (b) syn-breakup to drift phase (~54–49 Ma); and (c) final breakup phase along the western JMMC margin (~33–21 Ma) and the full formation of the Kolbeinsey Ridge. Features displayed are modified from data and interpretations by L. M. Larsen et al. (1989, 1999); Pedersen et al. (1997); Hald and Tegner (2000); Planke et al. (2000); Henriksen (2008); Funck et al. (2014); Hopper et al. (2014); Gernigon et al. (2015); Blischke et al. (2016); Gaina (2014); Gaina et al. (2009); Blischke, Gaina, et al. (2017); Gaina, Nasuti, et al. (2017); Geissler et al. (2017); Hjartarson et al. (2017); Horni et al. (2017); Martos et al. (2018). Boreholes from reconstructed time for DSDP Leg 38 and ODP Leg 104. Abbreviations: ÆR—Ægir Ridge; CJMBFZ—Central Jan Mayen Basin Fracture Zone; CNBFZ—Central Norway Basin Fracture Zone; COB—Continent ocean boundary; DSDP—Deep Sea Drilling Program; E-ICE—East Iceland; EJMFZ—East Jan Mayen Fracture Zone segments; FI—Faroe Islands; FSB—Faroe-Shetland Basin; FP—Faroe Plateau; GIFRC—Greenland-Iceland-Faroe Ridge Complex; GIR—Greenland-Iceland Ridge; GP—Geikie Plateau; IFFZ—Iceland-Faroe Fracture Zone; IFR—Iceland-Faroe Ridge; IP—Iceland Plateau; JMB—Jan Mayen Basin; JMBS—Jan Mayen Basin south; JMI—Jan Mayen island igneous complex; JMLB—Jameson Land Basin; JMMC—Jan Mayen microcontinent; JMR—Jan Mayen Ridge; JMT—Jan Mayen Trough; IPR—Iceland Plateau Rift; K—Kangerlussuaq; KB—Kap Brewster; KD—Kap Dalton; KR—Kolbeinsey Ridge; LLB—Liverpool Land Basin; ML—Milne Land; MM—Møre margin; MR—Mohns Ridge; NJMR—Northern Jan Mayen Ridge; NWIRZ—Northwest Iceland Rift Zone; ODP—Ocean Drilling Program; proto-RIFZ—inferred proto-Reykjanes-Iceland Fracture Zone; RR—Reykjanes Ridge; SD—Scoresby Sund; SDR—Seaward dipping reflector sequences; SRC—Jan Mayen Southern Ridge Complex; SRCFZ—Jan Mayen Southern Ridge Complex Fracture Zone; SPFZ—Spa Fracture Zone; SWJMBFZ—Southwest Jan Mayen Basin Fracture Zone; proto-TFZ—inferred proto-Tjörnes Fracture Zone; TVIP—Trail Ø-Vøring igneous complex; VD—Vesturdjúp Rift Zone; VSM—Vesteris Seamount; VM—Vøring margin; VT—Vindtoppen formation; WJMFZ—Western Jan Mayen Fracture Zone; WTR—Wyville-Thomson Ridge; and WTRFZ—Wyville-Thomson Ridge Fracture Zone.

volcanism during the formation of the early Eocene volcanic margin along the northern Jan Mayen Ridge domain, and intrusive complexes within the Jan Mayen Basin (Figure 6a).

The seafloor samples recovered from the Jan Mayen Southern Ridge Complex were placed in a stratigraphically consistent order along the available dredge profile. These samples have an estimated age range between 59 and 47 Ma (Polteau et al., 2012, 2018), which correlates to the plateau and SDR basalts (see Jan Mayen Trough flanks on Figure 6c). Their geochemical composition is, however, different from the main SDR's lower series basalts on the Vøring margin, as well as the lower basalt and plateau basalt series on the Blosseville Kyst (Figure 7a). The Jan Mayen Southern Ridge Complex samples are located within the uppermost part of the plateau and SDR basalts series and are best placed within the syn-breakup igneous strata, where we tentatively assign an age range estimate of ~55–52 Ma (early Eocene) within the SDR sequence JM-60. This later-stage early Eocene volcanism was coincident with the formation of the JMMC eastern flank volcanic margin and SDR units, possibly correlating with the Prinsen of Wales Bjerger formation (54–53 Ma) of the Blosseville Kyst (L. M. Larsen & Watt, 1985; L. M. Larsen et al., 1989, 2013) and the intrusive phase (56–54 Ma) described by Tegner et al. (2008) just south of the Kangerlussuaq Fjord and southwest of the JMMC. Based on this correlation, it appears probable that the SDR formations originally reached across the southern extent of the JMMC domain toward central East Greenland, which has since been subjected to several magmatic and erosive events resulting in the removal of approximately 2–3 km volcanic section (Blischke et al., 2019; Japsen et al., 2014; Mathiesen et al., 2000) (Figures 4, 11a, and 12).

5.3. Eocene Rift Propagation, the Iceland Plateau Rift I—IPR-I

A second phase of breakup igneous activity occurred coevally with seismic unit JM-50; early to mid-Eocene igneous rocks are preserved overlying the outer high igneous complexes of the primary eastern JMMC volcanic margin and the inner SDR units of stratigraphic unit JM-60 (Figures 2, 5c, 6, 9a, and 10). This phase of igneous activity appears to represent a period of enhanced volcanism with post-SDR lava flows, volcanoclastic extrusions, sill and dike intrusion along the entire JMMC eastern flank, around the Jan Mayen Southern Ridge Complex ridges, and the southeastern JMMC margin, forming the Iceland Plateau Rift I (IPR-I) domain (Figure 10).

The IPR-I rift extrusives overlay the Jan Mayen Southern Ridge Complex blocks and are best observed within the southernmost two ridges, along a volcanic margin that is estimated to have been active during the early Eocene from 52 to ~50 Ma (lower JM-50 unit; Figures 2, 6d, 9a, and 10). The IPR-I igneous phase included dike and sill intrusions associated with small-scale faulting within the blocks of the Jan Mayen Ridge and Jan Mayen Southern Ridge Complex as well as the extrusion of lava flows, possibly interlayered with volcanoclastic flows (e.g., Figures 5c, 6b, and 6d; Supplement 6a-iii & 6a-iv, 6b in Supporting Information S1). The IPR-I domain (Figure 9) is characterized by high-amplitude irregular seismic reflection patterns that dip toward the Ægir Ridge domain with an increase in seismic velocities from 4.8 to 5.5 km/s in the basaltic strata (Figures 5c and 6d; Supplement 6a-ii, 6b in Supporting Information S1). This succession of the Jan Mayen Southern Ridge Complex volcanic margin overlies the JM-60 SDR unit and the JM-70 plateau basalts. Moreover, the original eastern breakup margin is buried and obscured by the IPR-I volcanic units (Figures 6d, 9a and 10; Supplement 6b in Supporting Information S1). The IPR-I volcanic rocks may be the source of the magnetic anomalies that closely align with the very southeastern edge of the JMMC-IPR domains that are parallel to the initial Ægir Ridge axis (Figure 10a). Geochemically the basalt breccia of IPR-I in site 350 shows similar MgO versus TiO₂ (wt%) and MgO versus K₂O (wt%) trends to samples from the Jan Mayen Fracture Zone and Jan Mayen igneous complex (Figure 7).

5.4. The Iceland Plateau Rift II (IPR-II)

The Iceland Plateau Rift II (IPR-II) igneous phase along the eastern volcanic margin of the Jan Mayen Southern Ridge Complex, coeval with seismic units JM-50 to JM-40 during the early-middle Eocene (~49–40 Ma), is represented primarily by the intrusion of sills and dikes that developed northwestward along faults or weak crustal zones, and volcanoclastic extrusive units (Figures 2, 5c, 6, 9a, and 10). DSDP Leg 38 site 350 encountered an IPR-II- intrusion that was emplaced into an apparently older and heavily altered basalt-breccia unit stratigraphically assigned to IPR-I (Figures 7 and 8; Supplements 3–5; 6b in Supporting Information S1). The IPR-II volcanism occurred coevally with the production and accumulation of ash deposits preserved in the sediment

record of the nearby DSDP drill sites (Talwani, Udintsev, & White, 1976; Talwani, Udintsev, & Shirshov, 1976; Talwani et al., 1976a, 1976b, 1976c).

The IPR-II rift was accompanied by normal and transpressional faulting by oblique extension and by widespread dike and sill emplacements, parallel to small-scale lava flows in the adjacent graben areas (Figures 5c, 6d, 6e, 9a, 10b). West of site 350, a segment of the IPR-II rift is visible in gravity and magnetic data which show structural trends aligned with the faulted graben structure, fault-parallel dikes, and shallow sills (Figures 5c and 10; Supplements 6b & 6e, 7 in Supporting Information S1).

The mid-Eocene unconformity is dated to $\sim 43 \pm 3$ Ma based on seafloor samples recovered from the northwestern Jan Mayen Ridge (Sandstå et al., 2012), the Jan Mayen Southern Ridge Complex (Polteau et al., 2018; Talwani et al., 1976b), and seismic chronostratigraphic mapping (Blischke et al., 2019). Sills and small intrusions observed on seismic reflection data have deformed or uplifted sediments around the unconformity (ME on Figures 2 and 6d). The IPR-II volcanism was originally considered to have an age range between 50 and 33 Ma (mid- to late Eocene) based on K-Ar dating of samples from site 350 (Kharin et al., 1976). However, based on the paleontological record of the overlying sediments, Raschka et al. (1976) proposed that the basalts were most likely emplaced no later than 40–44 Ma. New ^{40}Ar - ^{39}Ar dates range from 49.28 ± 0.3 Ma to 44.05 ± 0.21 Ma consistent with this latter interpretation, suggesting that the volcanic activity is chronologically similar in age to the intrusions described by Tegner et al. (2008) for the Kangerlussuaq Fjord area (50–47 Ma) and coincident with the emplacement of the Igtertivå Formation at Kap Dalton (~ 49 –43 Ma) (L. M. Larsen et al., 2013). All three areas were thus volcanically active during the early to mid-Eocene (Figure 11b).

The intrusive section of IPR-II is geochemically similar to MORB and the Blosseville Kyst plateau basalts (Figure 6a). The MgO versus TiO_2 (wt%) and MgO versus K_2O (wt%) of the sill intrusion shows a good correlation with the Igtertivå formation of the Blosseville Kyst, as well as recent volcanic rocks within the Northern Volcanic Zone of Iceland and the Faroe Island syn-breakup series compositions (Figures 6b and 6c).

5.5. Rift Transfer and the Magmatic Incursion of the Iceland Plateau Rift III (IPR-III)

A gradual westward rift transfer within the Iceland plateau occurred between the late Eocene and late Oligocene, forming the Iceland Plateau Rift III (IPR-III), which is coeval with seismic units JM-35 to JM-20 (Figures 1, 2, 5b, 5d, 6c, 6e, 9b; Supplements 2, 6a & c in Supporting Information S1). The IPR-III phase strongly affected the Jan Mayen Trough and the southwestern Jan Mayen igneous province (Figure 9b) with increased faulting and igneous activity.

The IPR-III phase affected a much wider area than IPR-II, with substantial sill and dike emplacements and the formation of volcanic ridges within the Jan Mayen Trough extending into the late Oligocene (Figures 5b–5d and 6c, and 9b). The volcanic ridges within the Jan Mayen Trough and between the Jan Mayen Southern Ridge Complex blocks are oriented in an N–S direction, parallel to Bouguer gravity and magnetic lineaments and appear to coincide with the formation of fault-bounded pre-IPR-III fault blocks (Figures 9b and 10; Supplement 7b in Supporting Information S1). This implies extensive igneous activity extending from the Iceland-Faroe Ridge into the Jan Mayen Southern Ridge Complex, the Jan Mayen Trough, and into the southernmost extent of the Lyngvi Ridge region that is associated with the rift relocation along the southern margin of the JMMC (Figures 5b, 6c, 6e, 9b, and 10; Supplement 6a–viii in Supporting Information S1). The record of this activity is clearly observed at the intersection of the Jan Mayen Trough and the Jan Mayen Southern Ridge Complex fracture zone (SRCFZ) on Figures 1, 5b, and 6c) as a northward rift propagation.

5.5.1. Correlating Key Unconformities and Igneous Features

Both the mid-Oligocene and top Paleogene unconformities (Figures 2, 5b, 5d, and 6c; Supplements 2, 6b, 6c in Supporting Information S1) are characterized by distinctive flat-topped topography across the main Jan Mayen Ridge as well as the highest parts of the Jan Mayen Southern Ridge Complex. The mid-Oligocene unconformity has been deformed by subsequent faulting and intrusive activity. It is overlain by extrusive volcanics located below the top Paleogene unconformity. The Jan Mayen Trough and the southern end of the Lyngvi Ridge show an increased prevalence of intrusive complexes that appear to expand into the JMMC domain, separating the Jan Mayen Southern Ridge Complex from the main ridge and thus forming the Jan Mayen Trough and southwestern Jan Mayen igneous province (Figures 8c, 9b and 10).

Volcanic ash layers present within late Eocene to late Oligocene ($\sim 43\text{--}30\text{ Ma} \pm 4\text{ Ma}$) sediments at DSDP Leg 38 sites 346, 347, and 349 signal volcanic and phreatic activity affecting the entire area. In contrast, ash layers are absent in the Oligocene sediments of site 350 (Sylvester, 1975, 1978; Talwani, Udintsev, & White, 1976; Talwani, Udintsev, & Shirshov, 1976; Talwani et al., 1976a, 1976b, 1976e, 1978). This suggests that site 350 was further away from later Oligocene volcanic and phreatic activity and coincided with igneous activity south of the Kangerlussuaq Fjord at 37–35 Ma southwest of the JMMC-IPR area (Tegner et al., 2008). An east-to-west shift of igneous activity across the JMMC-IPR area can be observed by tracing the seismic horizons related to extrusive and intrusive areas that appear connected to flood basalt events. The oldest flood basalt marker horizon “F-Marker 3” (Figure 2) and “IPR-II intrusions & extrusives” (Figure 9) lie within the late Eocene to the mid-Oligocene interval. A further subsequent flood basalt event, referred to as “F-Marker 2,” occurs within the mid- to late Oligocene stratigraphic succession (Figure 2) and forms the Jan Mayen Trough–IPR-III rift domain (Figure 9b; Supplement 6d–viii, 6c in Supporting Information S1).

5.5.1.1. F-Marker 3 - IPR-II Intrusions & Extrusives

Horizon “F-Marker 3” is observed over approximately 1250 km² and appears related to the mid-Oligocene unconformity within the Jan Mayen Southern Ridge Complex region, overlying the early-mid Eocene strata within the Jan Mayen Southern Ridge Complex, IPR-I, and IPR-II domains (Figures 2 and 9b). On seismic profiles, F-Marker 3 is characterized by a relatively flat-lying hummocky to irregular seismic reflection that locally infills smaller graben areas that are connected to a series of small intrusive features. These grabens contain up to 2.5 km of stratigraphic infill material, including igneous rocks (Figure 5c). Late Eocene to mid-Oligocene faulting, smaller-scale intrusions, and vents are observed within the faulted, southernmost Jan Mayen Southern Ridge Complex, IPR-I, and IPR-II domains.

5.5.2. F-Marker 2—Jan Mayen Trough—IPR-III Rift Domain

The mid- to late Oligocene sub-aerial extrusive and intrusive features of the horizon “F-Marker-2” (Figures 2, 5b, and 9b; Supplement 6a–viii in Supporting Information S1) are manifested as strong seismic reflections covering an area of approximately 8,100 km² and are well defined within the Jan Mayen Trough. Thus, a variable stratigraphic thickness estimate of up to 990 m for the IPR-III flood basalts is postulated within the Jan Mayen Trough domain (Figure 9b). The flood basalts of the Jan Mayen Trough—IPR-III rifting domain terminate against the rotated fault blocks and structural highs of the Lyngvi Ridge, the Jan Mayen Southern Ridge Complex western margin, and faulted blocks within the Jan Mayen Trough (Figures 5b and 5d). Little seismic energy appears to penetrate this horizon and deeper structures and strata are not well imaged. The partly irregular and hummocky structure of F-Marker 2 is possibly related to extrusions emplaced sub-aqueously, or perhaps into thin, unconsolidated wet sediments.

5.6. The Western Igneous Margin, and IPR-IV to the Kolbeinsey Ridge Transition (Proto-KR)

The last rift-transfer phase is associated with the Iceland Plateau Rift system IV (IPR-IV) at the southwestern limit of the visible Jan Mayen Ridge segments. The formation of this igneous domain represents the last rift transfer phase between central East Greenland and the JMMC during the late Oligocene and early Miocene (Figure 2), forming the western margin of the microcontinent. Its western boundary is marked by the first clear magnetic polarity chron C6c (23.3–22.5 Ma), which is tied to DSDP Leg 38 site 348 (Figures 6e, 9b and 11c). The IPR-IV domain is characterized by dike and sill emplacements, igneous complexes, and regionally extensive flood basalts identifiable on seismic reflection data (Figures 4b and 5d; Supplements 6a–vii, 6b in Supporting Information S1). The IPR-IV domain represents the direct conjugate to the central East Greenland margin along the Blossville Kyst shelf. Rifting leading to breakup is estimated to have been active from ~ 25 to 24 Ma (e.g., Blischke, Gaina, et al., 2017; Blischke et al., 2018; Talwani & Eldholm, 1977) (Figures 1, 4, 9b, and 11c; Supplement 7 in Supporting Information S1). The flood basalts associated with this phase of volcanism are marked by a distinct seismic horizon, “F-Marker 1” (Figure 2), that corresponds to seismic unit JM-15 and onlaps onto the JMMC structures and older igneous domains (Figures 4b and 5d; Supplement 2b, 2c in Supporting Information S1).

5.6.1. Tectonic Evolution of the Jan Mayen Basin

The northern and southern segments of the Jan Mayen Basin that form part of the JMMC's western breakup margin are different in structure, crustal thickness, and igneous character. The entire western flank of the JMMC

is strongly faulted into several westward-rotated fault blocks along segments that have partly slid into the basin, forming half-graben and small graben structures. Most of the faults and tilted features are overprinted by intrusive rocks (Blischke, Gaina, et al., 2017; Blischke et al., 2019). The basin is bounded to the south by the SW-NE aligned southwestern Jan Mayen Basin Fracture Zone, which has the same orientation as the younger Spar Fracture Zone on the Kolbeinsey Ridge (Figures 1b, 1c, 10b, and 11c). The southwestern edge of the Jan Mayen Basin is reconfigurable to a large igneous center located offshore the central Blossesville Kyst, active ~33–22 Ma (Figure 11c).

The deep Jan Mayen Basin appears to have formed gradually along the WNW-ESE-striking central Jan Mayen Basin Fracture Zone from the mid-Eocene to the early Miocene, and along the NW-SE-striking normal fault system of the Jan Mayen Ridge margin (Figures 9b, 10b, 11c, and 12), that is, opposite the N-S- to NE-SW-striking normal fault systems south of the central Jan Mayen Basin Fracture Zone. Seismic refraction data indicate that crustal thickness varies from 6 to 12 km within the basin (Blischke, Gaina, et al., 2017; Blischke et al., 2019; Kodaira et al., 1998a; Olafsson & Gunnarsson, 1989) (Figure 1; Supplements 6b, 7 in Supporting Information S1). Thinned crust with seismic velocities >6.8 km/s (Figures 1 and 4b; Supplement 2b-c), reflect crustal extension and subsidence. In addition, the southern Jan Mayen Basin segment is characterized by different Bouguer gravity anomaly values (>150 mGAL) than the northern segment (<150 mGAL). The proto-Kolbeinsey Ridge is oriented parallel to magnetic anomaly C6c within the southern Jan Mayen Basin segment (Figures 1b and 10a; Supplement 2b, 2c in Supporting Information S1).

The F-Marker 1 horizon is interpreted as an early Miocene flood basalt marking the top of seismic-stratigraphic unit JM-15 (Figures 2, 5d, and 9b; Supplements 6a-vii, 6b in Supporting Information S1). It is characterized by a flat-lying high-amplitude reflection in seismic data with an aerial extent of approximately 9,400 km² within the low areas of the Jan Mayen Basin. Subsequent faulting in response to continued extension later offsets what is interpreted as an initially continuous set of lava flows. The basalt layer is approximately 300–500 m thick based on refraction data (Supplement 6b in Supporting Information S1). Thickness estimates increase up to ~1.2 km near inferred igneous centers, which are likely source areas for the flood basalts, as fissure or axial rift segments are not observed in this region (Figures 4b and 9b).

5.6.2. The Initiation of the Kolbeinsey Ridge (Proto-KR)

Initial igneous complexes of the Kolbeinsey Ridge appear to be associated with wedge-shaped sections of SDR sequences along the western edge of the Jan Mayen Basin, and a conjugate sequence along the eastern edge of the Liverpool Land Basin (Figure 4). The seismic reflection data imply an overlap of highly thinned JMMC crust within the Jan Mayen Basin, onto Late Oligocene to Early Miocene SDR sequences from the initial volcanic complexes within the proto-Kolbeinsey domain (Figures 4 and 10). Based on the higher-resolution post-2011 seismic reflection data the SDR units appear to be consistent across the central Jan Mayen Basin, just south of the central Jan Mayen Basin Fracture Zone (Figures 9b and 10). The SDR units form a relatively wide zone (40–50 km) adjacent to the first clear magnetic spreading anomaly, C6c. Combined with the conjugate central East Greenland margin, a wide and complex volcanic transition zone formed along the Eocene-Miocene breakup margin, prior to full seafloor spreading along the Kolbeinsey Ridge.

5.7. The Post-Breakup Neogene-Quaternary Phase

After the Kolbeinsey Ridge was established, an oceanic domain formed west of the JMMC and igneous activity decreased significantly within the microcontinent (Figures 10 and 11c), except around the Jan Mayen igneous complex and western Jan Mayen Fracture Zone northwest of the JMMC. The record of Neogene volcanic activity is observed in DSDP and ODP cores within the JMMC as interbedded volcanic ash and tuff layers within the deep-marine sediments (Blischke, Gaina et al., 2017; Sandstå et al., 2012, 2013; Talwani, Udintsev, & White, 1976; Talwani, Udintsev, & Shirshov, 1976; Talwani et al., 1976a, 1976b, 1976e, 1978). Seafloor basalt samples of the northern Jan Mayen Ridge show similar geochemical trends as the Jan Mayen Fracture Zone and Jan Mayen igneous complex (Figure 8), though no age data are available. However, samples from the northwesternmost breakup margin have an age range from 13.2 to 0.1 Ma (e.g., Campsie et al., 1990; Davis & McIntosh, 1996; Fitch, 1964; Mertz et al., 2004).

5.8. JMMC Igneous Provinces—Summary

The reconstructed tectonic evolution of the JMMC-IPR domain consists of seven distinct local to regional tectono-magmatic phases (Figures 11 and 12) that can be summarized as follows:

1. An initial breakup phase characterized by anomalous magmatic activity that followed an SW-NE opening trend along WNW-ESE-striking pre-existing fracture zones south and west of the JMMC, here inferred as an oblique opening of the Geikie Plateau into the central Jan Mayen Ridge domain (~63–56 Ma);
2. Formation of multiple SDR sets along the JMMC eastern igneous margin during syn-breakup in the early Eocene. Segments of SSW-NNE-striking SDR units propagated northwards as a precursor to the formation of the Ægir Ridge spreading system, which opened along the NW-SE-striking eastern Jan Mayen Fracture Zone, central Norway Basin Fracture Zone, and Jan Mayen Southern Ridge Fracture Zone segments (~55–53 Ma).
3. Activation of the Iceland Plateau Rift (IPR-I) along the eastern JMMC breakup margin, and the southernmost part of the Ægir Ridge system (~52–50 Ma) represented by flood basalts, intrusive complexes, volcanic breccia, and volanoclastic sequences.
4. Activation of the IPR-II segment in association with an SW-NE-aligned magmatic event between the GIFRC and the JMMC. The IPR-II rift intersected the IPR-I segment and the southernmost Jan Mayen Southern Ridge Complex contemporaneously with the Ægir Ridge. Volcanism within these axial rift segments by intrusions and flood basalts (~49–36 Ma).
5. Activation of the IPR-III rift domain, during an SW-to-NE magmatic incursion into the southern margin of the JMMC, severing the Jan Mayen Southern Ridge Complex from the main Jan Mayen Ridge (Lyngvi Ridge) forming the Jan Mayen Trough and volcanic ridges within the Jan Mayen Southern Ridge Complex domain (~35–24 Ma).
6. The final breakup of the JMMC, along the IPR-IV segment and formation of the western JMMC igneous margin (~24–23 Ma).
7. Initiation of the Kolbeinsey Ridge along the proto-KR segment and the western Jan Mayen Fracture Zone segments (~22–21 Ma).

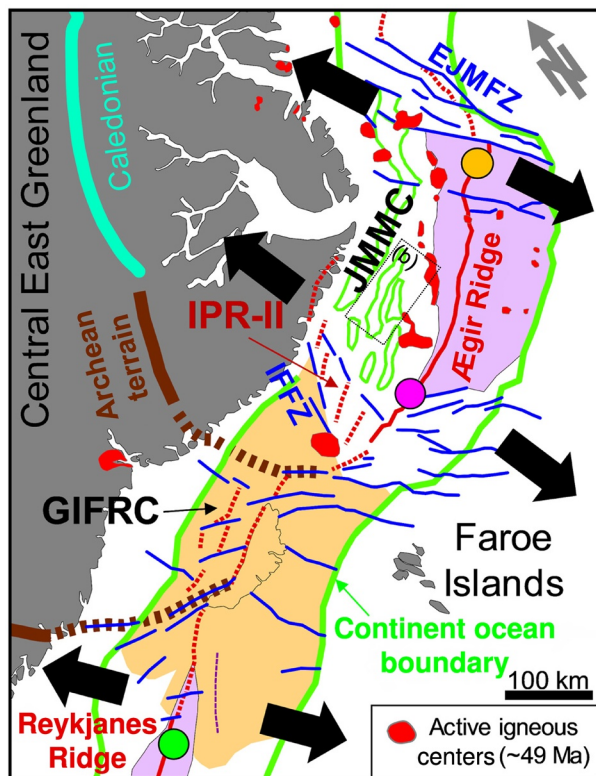
6. Geodynamic Evolution of the JMMC-IPR Region

Seismic volcanostratigraphy combined with tectonic and paleogeographic reconstructions of the JMMC highlight the complex igneous history of parallel rift systems within the Iceland Plateau and the early stage of the development of the Kolbeinsey Ridge. Interpretations of the JMMC domains (Figure 10) which rely on reconstructed regional igneous province maps (Figure 11) and the stratigraphic correlation chart (Figure 12) have improved our understanding of breakup-related tectonic and magmatic processes along both flanks of the JMMC, between ~55 and ~21 Ma (Figures 13 and 14). Mapped structural trends, fracture zones, rift zones, and igneous complexes are based on present-day potential field data (Hopper et al., 2014), detailed kinematic reconstruction models (Blischke, Gaina et al., 2017), and published work from adjacent margins and Iceland (e.g., Berndt et al., 2001; Blischke et al., 2016; Doubrovine et al., 2012; Einarsson, 2008; Einarsson et al., 2020; Funck et al., 2014; Funck, T., Erlendsson, et al., 2017; Gaina et al., 2009; Gaina, Nasuti, et al., 2017; Geissler et al., 2017; Gernigon et al., 2015, 2019, 2021; Henriksen, 2008; Hjartarson et al., 2017; Horni et al., 2017; Karson et al., 2018, 2019; L. M. Larsen et al., 1989, 1999; Pedersen et al., 1997; Planke et al., 2000; Skogseid et al., 2000).

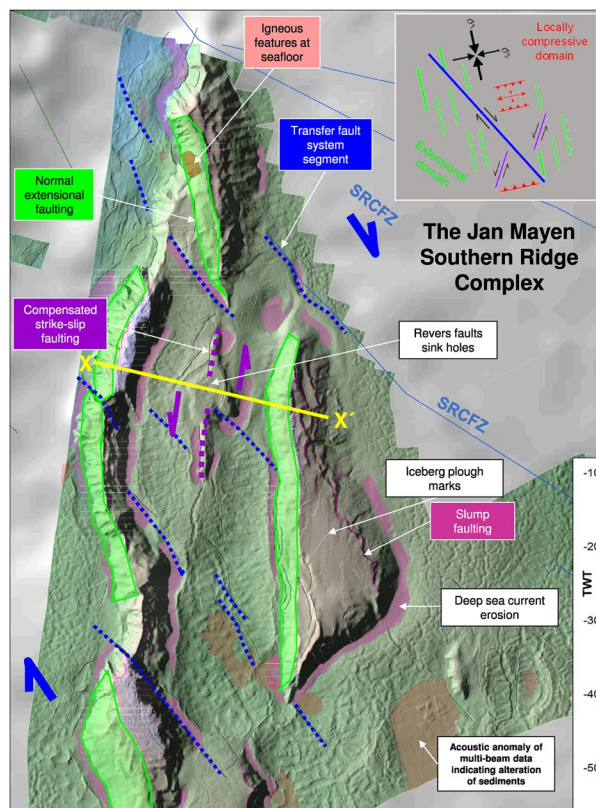
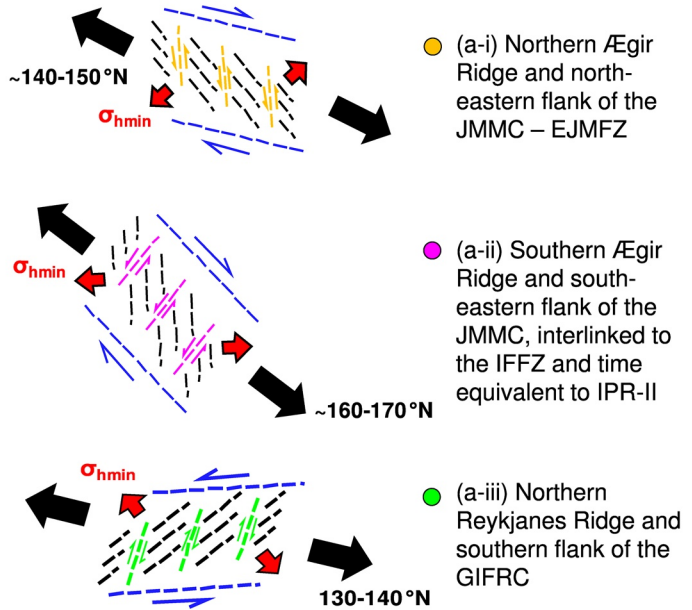
6.1. Igneous Provinces

6.1.1. Pre-Breakup Setting

Pre- and primary breakup igneous units west and southeast of the JMMC-IPR (Figures 11a and 12) are contemporaneous with the lower basalt sections of their conjugate margins. The lower basalt sections along the central East Greenland margin range in age from ~63 Ma to 56 Ma (e.g., L. M. Larsen et al., 1989; Pedersen et al., 1997), whereas the conjugate pre-breakup lower basalts of the Faroe Island Basalt Group (FIBG) range from ~61 to 56 Ma (e.g., Mudge, 2015; Ólavsdóttir et al., 2019). Rocks from these conjugate areas are of alkaline and felsic-to-mafic compositions, suggesting contamination with continental crust (Kokfelt & Ártíng, 2014; L. M. Larsen et al., 1999; Meyer et al., 2009; Parson et al., 1989; Tegner et al., 1998). The seismic reflection characteristics and velocity structure of these lower basalt sections are broadly comparable to the JMMC-IPR region (Figures 4b and 8; Supplements 2, 6a–6i in Supporting Information S1).



(a)
This study: Early Eocene (Ypresian) ~49 Ma reconstruction of the central Northeast Atlantic (Jan Mayen microcontinent (JMMC) – Iceland Plateau Rift (IPR) – Greenland-Iceland-Faroe Ridge Complex (GIFRC))



(b)
Opening and rifting of the Jan Mayen Southern Ridge Complex in comparison to the apparent opening fabric of the EJMfZ and the IPR-II – Iceland-Faroe Fracture Zone system (IFFZ) [modified from Blischke et al., 2021, 2017b]

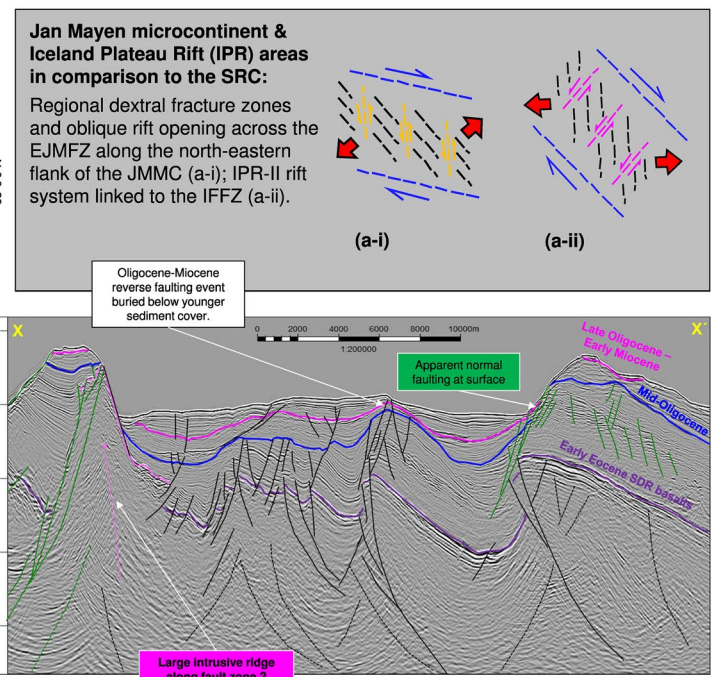


Figure 13.

Prior to breakup, the Faroe Plateau and the Faroe Islands were located south-southwest of the JMMC domain (Figures 11a and 14). The Lopra and Beinisvørð formations, which are part of the Faroe Island Basalt Group, have pre-breakup age ranges from 60.94 ± 2.1 Ma to 55.9 ± 1.1 Ma (e.g., Ártíng et al., 2014; Horni et al., 2017). These formations consist of a mixture of intrusives, lavas, volcanoclastic, and hyaloclastite units. Thick hyaloclastite units have been drilled on the Faroe shelf into the deepest levels of the pre-breakup Faroe Island Basalt Group, but an accurate definition of its base is missing (Ólavsdóttir et al., 2019). The pre-breakup Base Palaeogene unconformity (BPU) is marked as a strong seismic reflection beneath the Jan Mayen and Lyngvi ridges; however, it is marked by an irregular and locally faulted erosion surface across the Jan Mayen Southern Ridge Complex and the Jan Mayen Basin, where truncated Mesozoic strata is inferred to be overlain predominantly by pre-breakup plateau basalts (e.g., Blischke et al., 2019) (Figures 4b and 6; Supplement 2 in Supporting Information S1).

We interpret the JM-70 plateau basalt section to be equivalent to the Blosseville Kyst basalts, as the JMMC-PR area was located ~50 km east of onshore East Greenland (Figure 11a). The plateau basalt section appears to increase in stratigraphic thickness toward the south, including the Jan Mayen Southern Ridge Complex (Figures 6 and 11a). Similarly, Brooks (2011) described a northeast-to-southwest increase in plateau basalt thickness from Jameson Land basin through Scoresby Sund and the Blosseville Kyst toward the Kangerlussuaq basin. The inland and northern areas show regional onlap onto structural highs with subsequent erosion estimated to have removed 2–3 km of basaltic stratigraphy in central East Greenland (L. M. Larsen et al., 1999, 2014; Mathiesen et al., 2000; Passey, 2009; Passey & Hitchen., 2011; Passey & Jolley, 2009). This magnitude of denudation has been related to several phases of uplift and erosion events for the central East Greenland area (Figure 12). In particular, Eocene-Oligocene uplift and erosion resulted in the formation of the Upper Planation Surface that was accompanied by faulting and intrusion of magmatic bodies with extensive mass wasting on the East Greenland shelf (e.g., Bonow & Japsen, 2021; Bonow et al., 2014; Japsen et al., 2014, 2021). The marked north-to-south increase in thickness of the pre-breakup lower series and plateau basalt sections of the Blosseville Kyst, from ‘absent’ to up to 6–7 km suggests a deep-seated source located at the intersection of the Blosseville Kyst and the proto-Iceland-Faroe Fracture Zone (Figure 11a). Furthermore, large deep-seated igneous sources appear to be located close to the Scoresby Sund and Geikie plateau as distinct magnetic anomalies are present adjacent to the southern end of the Jameson Land Basin, and alongside extensive intrusive systems within the sedimentary basins of Jameson Land, Liverpool Land and the continental margin of the Blosseville Kyst (Figure 11a; Supplement 8 in Supporting Information S1) (e.g., Blischke & Erlendsson, 2018; Eide et al., 2021; Franke et al., 2019; Guarnieri et al., 2016).

Kinematic reconstructions show how the JMMC area was conjugated with central East Greenland (Figure 11a). Pre-breakup structural trends in the Jameson Land Basin match those inferred from the JMMC. Several igneous centers along the eastern flank of the JMMC, arranged slightly en-echelon and narrowing southward might have formed along the initial breakup margin prior to the formation of syn-breakup SDR units. This igneous activity is likely to have been contemporaneous with underplating suggested beneath the Jan Mayen igneous complex by Kandilarov et al. (2012) and deep intrusions along major Jan Mayen fault segments (Blischke et al., 2019), as observed on seismic reflection, gravity, and magnetic anomaly data (e.g., Figures 5a and 6b). The higher-velocity lower crust of the eastern JMMC margin is mostly located oceanward, close to the projected microcontinent-ocean boundary, and within an oceanic crust domain (*horizons R1 and R2* on Figures 4b and 6; Supplement 2 in Supporting Information S1). The initial opening was from north to south within a regional NE-SW spreading direction. Two inferred dextral fracture zones (proto CNBFZ and SRCFZ) separated individual spreading segments (Figures 11a and 11b). The dextral proto-Jan Mayen Fracture Zone opened at a ~60° angle to the northeastern margin of the JMMC, lending further support to an overall right-lateral oblique rift opening along the northern boundary of the JMMC during the initial breakup. The JMFZ was the regional transfer element between the Norwegian and East Greenland margins (Figures 10 and 11a). The Norwegian Basin opened south of the NW-SE striking JMFZ, in response to gradual subsidence along the eastern JMMC margin (Figures 11a

Figure 13. Comparison of the mapped oblique rift zones and fracture/transfer zone systems for the greater JMMC–IPR region to present-day: (a) reconstructed early Eocene (~49 Ma) reconstruction along the northern Ægir Ridge and EJMFZ, along the southern Ægir Ridge associated with cessation of spreading and increase in IPR-II rift activity, the IPR-II–IFFZ, and the northernmost extent of the Reykjanes Ridge; (b) Opening and rifting of the Jan Mayen Southern Ridge Complex in comparison to the apparent opening fabric of the EJMFZ and the IPR-II–Iceland-Faroe Fracture Zone system (IFFZ) (modified after Blischke et al., 2021, 2017). Abbreviations: EJMFZ – Eastern Jan Mayen Fracture Zone; GIFRC – Greenland-Iceland-Faroe Ridge complex; IFFZ – Iceland-Faroe Fracture Zone; IPR – Iceland Plateau Rift; JMFZ – Jan Mayen Fracture Zone; JMMC – Jan Mayen microcontinent; SRCFZ – Jan Mayen Southern Ridge Complex Fracture Zone; and TWT – Two-way travel time.

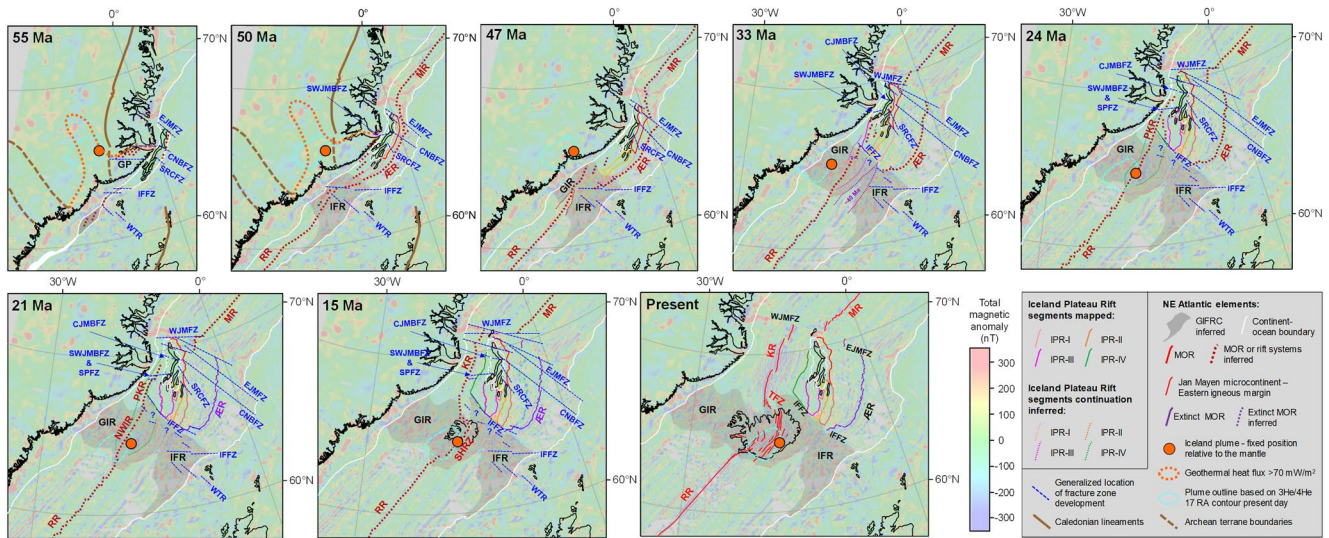


Figure 14. Simplified NE-Atlantic plate-tectonic evolution from pre-breakup (55 Ma) to present, based on magnetic anomalies and geodynamic models modified after (Blischke, 2020; Gaina, Nasuti, et al., 2017). Magnetic anomaly data background from magnetic Nasuti and Olesen (2014). Modeled Iceland plume relative to the mantle after Doubrovine et al. (2012), the Caledonian and Archean structural elements after Henriksen (2008) and Hopper et al. (2014), and the center area of estimated heat flux ($>70 \text{ mW/m}^2$) after Martos et al. (2018). Outline of the Iceland Plateau Rift stages and the thick ($\sim 30 \text{ km}$) crust along the Greenland-Iceland-Faeroe-Ridge with inferred Iceland-Plateau and ridge segment interactions from this study. Note that the modern $^3\text{He}/^4\text{He}$ anomaly (a proxy for underlying mantle anomaly (Harðardóttir et al., 2018) is shown in 0 Ma panel, where the active ridge system is trailing west (behind) the plume center. This was different up to pre-21 Ma when the spreading center was ahead (east) of the plume center. Abbreviations: ÆR—Aegir Ridge; CJMBFZ—Central Jan Mayen Basin Fracture Zone; CNBFZ—Central Norway Basin Fracture Zone; COB—Continent ocean boundary; EJMfZ—Eastern Jan Mayen Fracture Zone; GP—Geikie Plateau; GIFRC—Greenland-Iceland-Faeroe Ridge Complex; GIR—Greenland-Iceland Ridge; IFFZ—Iceland Faroe Fracture Zone; IFR—Iceland Faroe Ridge; IPR—Iceland Plateau Rift; SHRZ—Iceland Snæfellsnes-Húnaflói rift zone; KR—Kolbeinsey Ridge; MOR—Mid-oceanic Ridge; MR—Mohns Ridge; NWIRZ—Northwest Iceland Rift Zone, PKR—Proto Kolbeinsey Ridge; RR—Reykjanes Ridge; SHRZ—Snæfellsnes-Húnaflói Rift Zone; SPFZ—Spa Fracture Zone; SRCFZ—Jan Mayen Southern Ridge Complex Fracture Zone; SWJMBFZ—Southwest Jan Mayen Basin Fracture Zone; TFZ—Tjörnes Fracture Zone; and WJMFZ—Western Jan Mayen Fracture Zone; and WTR—Wyville-Thomson Ridge.

and 11b). In contrast to subsidence within the Norway Basin, the Vøring Plateau and Transform Margin remained bathymetrically elevated during early Eocene. The breakup unconformity of the top volcanic units there has been dated at $\sim 55 \text{ Ma}$ (Figure 12) (e.g., Berndt et al., 2001; Hjelstuen et al., 1997, 1999; Polteau et al., 2020), supporting the existence of a transpressional region north of the Jan Mayen Fracture Zone.

The Traill Ø volcanic igneous province (Figure 11b) and Vøring margin were linked through the Jan Mayen Fracture Zone and northernmost JMMC (Figures 11a and 11b). The SW-NE-striking Geikie Plateau (Figure 11a) appears to align parallel to the magnetic trend observed at the Traill Ø-Vøring igneous complex (Figure 11b) but is offset by the proto-Jan Mayen Fracture Zone. The Vøring margin is interpreted to contain a high-velocity lower crustal body that was generated by magmatic underplating, possibly associated with magma leaking along a large-scale fracture zone (e.g., Abdelmalak, et al., 2016; Gernigon et al., 2019, 2021). Similar observations have been reported for the Jameson Land Basin and Scoresby Sund area by Eide et al. (2021) in East Greenland.

Several NE-SW-striking magnetic lineaments aligned parallel to presumably contemporaneously active onshore igneous centers, southwest of the Blossville Kyst (Figure 11a) may mark the area of the initial breakup between East Greenland and the Faroe Islands, generating the oldest segment of the GIR and the Iceland-Faeroe Fracture Zone. These events would also have affected the southernmost part of the JMMC, an area that is presently unresolved due to sparse seismic data coverage. Our reconstructions leave open the possibility that the southernmost limit of the JMMC may well lie beneath the northeast Iceland shelf or is, in part, embedded into the Iceland-Faeroe Ridge. Based on refraction measurements, the western Iceland-Faeroe Ridge and Eastern Iceland areas comprise up of 30–35 km thick Iceland-type crust (Smallwood et al., 1999; Staples et al., 1997). The reconstructed Iceland-Faeroe Fracture Zone domain aligns with the Kangerlussuaq area, across to the Faroe Islands platform and Fugloy ridge, and into the Møre margin.

6.1.2. Syn-Breakup Setting

The syn-breakup-to-drift phase was dominated by the formation of SDR units and oceanic crust along the Ægir ridge at the initiation of the Norway Basin (Figure 11b). A wide igneous area with thick SDR units lies along the East Greenland Traill Ø margin, north of the Jan Mayen Fracture Zone. The primary breakup margin along the eastern flank of the JMMC is aligned with distinct igneous complexes, represented by onlapping, inner SDR sets within polarity chron C24r (~55 Ma). The oldest magnetic polarity chron within the Norway Basin is C24n.3n (~53.4 Ma, based on the timescale of Gradstein et al. (2012)), associated with the outer SDR units (e.g., Gaina et al., 2009; Gernigon et al., 2015; Skogseid & Eldholm, 1987) (Figures 6a–6c). The outer SDR units can therefore be considered as a direct conjugate to the early Ypresian (55–52 Ma) syn-breakup volcanic rocks that have been sampled along the Vøring margin and have been mapped on seismic reflection data for the East Greenland Traill Ø margin (e.g., Franke et al., 2019; Geissler et al., 2017; Gernigon et al., 2015; Horni et al., 2017; Planke & Eldholm, 1994; Polteau et al., 2020) (Figures 11b and 12).

Thickness variations within the JMMC-SDR units most probably represent fluctuations in the focus of volcanic activity within the central volcanic systems along the eastern JMMC breakup margin, and segmented separation of the microcontinent from the Norway Basin and an apparent decrease of SDR unit widths toward the Southern Ridge Complex (Figures 9a, 10b, 11b, and 12). The southernmost blocks of the Jan Mayen Southern Ridge Complex are overlain by a younger early- to mid-Eocene volcanic margin, which obscures underlying igneous strata (Figures 5c and 6d; Supplement 2c in Supporting Information S1). Seismic reflection data from the underlying lava units exhibit amplitudes and semi-parallel reflection characteristics of classic SDR units and landward flow units. Thus, the early- to mid-Eocene igneous margin of the Jan Mayen Southern Ridge Complex region is synchronous with the formation of the southern Ægir Ridge, conjugate to the southern Møre Basin and the Fugloy Ridge (Figure 11b).

The wide igneous SDR margin between Greenland and the Faroe Island, extends northeast along the Fugloy Ridge and the southern Møre margin (Figure 11b), indicating a clear asymmetry in the early opening of the Norway Basin. Norcliffe et al. (2019) suggest that asymmetric SDR units form preferentially above a waning thermal anomaly in the mantle or due to variations in the pre-rift lithospheric structure. This latter possibility is clearly appropriate for the eastern JMMC, implying that the structural setting that facilitated rift transfer systems was already established prior to rifting. These rifting processes appear to coincide with a change in spreading direction of the Northeast Atlantic system, that is, a regional rather than a localized event (Gaina, Nasuti, et al., 2017) (Figure 12). Anomalously thick SDR sections along the southeasternmost Jan Mayen Southern Ridge Complex region most likely represent overlapping of different axial rift segments similar to those that have been observed south of the Iceland Faroe Ridge (e.g., Blischke et al., 2016; Erlendsson & Blischke, 2013; Hjartarson et al., 2017).

The wider and partially stacked SDR units of the northeast JMMC margin narrow southwards, reflecting opening from north to south within the Norway Basin at the initiation of the Ægir Ridge (Figure 11b). In contrast, SDR units between East Greenland and the Faroe Islands narrow northwards, to the Southern Ridge Complex and the Bosseville Kyst. These opposite rift opening directions during breakup were accommodated by a rift transfer along the southern JMMC and the activation of the Iceland Plateau Rifts, which gradually sheared the microcontinent from the East Greenland margin.

6.1.3. Rift-Transfer Within the Iceland Plateau

The timing of this early to mid-Eocene IPR rift transfer corresponds with an overall change in spreading direction, accompanied by decreased seafloor spreading rates within the NE Atlantic (Gaina, Nasuti, et al., 2017) (Figure 12). As no major tectonic events occurred during this time, this rift re-organization is most likely related to large-scale magmatic processes, which generated a regional uplift and development of the mid-Eocene unconformity (Figure 12) (Blischke et al., 2019). The IPR is petrographically similar to the Igtertvå Formation and appears to be part of the same rift system; its higher-than-typical MORB TiO₂ and K₂O contents may also be indicative of a mantle anomaly influence (Figure 8). The substantially increased magmatic activity in the N-Atlantic region affected the adjacent rift systems, including the Reykjanes Ridge and the asymmetric Ægir Ridge. The IPR rift transfer was contemporaneous with regional volcanism from mid- to late Eocene (approximately 43–40 Ma) along the northern margin of the JMMC, eastern Jan Mayen Fracture Zone, Jan Mayen Island, Traill Ø igneous province, and within the Iceland-Faroe Ridge (e.g., Blischke et al., 2019; Gaina et al., 2009; Geissler

et al., 2017). Individual IPR segments align with the projected orientation of rift segments from the Reykjanes ridge across the GIFRC in an SSW–NNE direction at ~54–49 Ma (Figure 11b), albeit offset by segments of the Iceland-Faroe Fracture Zone. Parallel, subaerial, rift systems formed south of the JMMC, connected by short fracture zone segments, including a failed axial rift system across the Iceland-Faroe Ridge (~49–40 Ma; Figures 11b and 11c).

The two-rift transfer phases (IPR I-II) accommodated the oblique spreading system of the Ægir ridge that intersected the southernmost JMMC domain and the northern IFR (Figures 10, 11b, 11c, 12, and 14). The oldest continuous magnetic anomaly, chron C21 (late Ypresian-early Lutetian, ~48–46 Ma) (Blischke, Gaina, et al., 2017; Ellis & Stoker, 2014; Gaina et al., 2009), formed after the emplacement of IPR-I and overlapped that volcanic succession (~52–50 Ma). In turn, the IPR-I appears to overlap the syn-breakup JMMC and SDR units (Figures 6d and 11b). Segment IPR-II on the other hand intersected IPR-I and the underlying early Eocene margin, most likely between ~49 and 44 Ma. The IPR-II correlates chronologically and geochemically with the Igterivå formation (~49–43 Ma) of Kap Dalton and the central Blosseville Kyst area. Thus, the overall southeast-to-northwest oriented Iceland Plateau Rift system, extending from the northern IFR into the southeastern part of the JMMC, constitutes the tectono-magmatic connection between the Iceland-Faroe Ridge and the Blosseville Kyst areas.

6.1.4. Final Breakup Along the Western JMMC

Breakup along the western margin of the JMMC commenced initially with a westward transfer of IPR-III activity into the central graben of the Jan Mayen Trough during the Oligocene (~35–25 Ma; Figures 1, 5b, 6c, 9b, 11c, and 12), synchronously with decreased spreading rate along the southern Ægir Ridge (Gaina, Nasuti, et al., 2017; Gernigon et al., 2015). The IPR-III period is characterized by massive magmatic intrusions, emplacement of volcanic ridges, dikes, and flood basalts, extending into the IPR-IV phase and the early stages of Kolbeinsey Ridge formation. The intrusions appear related to an S–N-aligned magnetic and Bouguer gravity anomaly trend within the Jan Mayen Trough, the northern Jan Mayen Southern Ridge Complex, and the southwest Jan Mayen igneous complex immediately south of the Lyngvi Ridge. Thus, supporting the interpretation of a rift system that segmented and propagated into the southern extent of the JMMC.

The final JMMC breakup phase (~24–23 Ma) occurred along the southwestern and western flank of the microcontinent, where evidence for increased volcanic activity is preserved, including the emplacement of igneous complexes within the IPR-IV region, increased dike and sill emplacement, extrusive flood basalts, and the western SDR margin (Figures 4b, 9b, 10, and 11c; Supplements 2, 6 in Supporting Information S1). The formation of a distinct igneous margin along the western JMMC instigated full separation from central East Greenland along the proto-Kolbeinsey ridge by magnetic anomaly C6c (23.3–22.5 Ma) that was linked to the Mohns Ridge via the western Jan Mayen Fracture Zone to the east (Figures 1, 6a, 10b, and 11c). To the west, the western Jan Mayen Fracture Zone was partially inverted during the Mid-Oligocene, which was accompanied by the intrusion of a syenite pluton and dikes at around 30 Ma (Blischke et al., 2019; Geissler et al., 2017; Parsons et al., 2017) (Figure 12).

Reconstructed magnetic and gravity anomalies suggest several SW–NE rift systems, offset by WSW–ENE fracture zones during the late Oligocene to earliest Miocene, parallel to JMMC's southwestern and western volcanic margin (Figures 11c and 12) (Blischke, Gaina, et al., 2017; Blischke et al., 2019). SW–NE rift systems are also present in the area west of the NW Iceland Rift Zone (~25 Ma) (Harðarsson et al., 1997, 2008), and the volcanic complex of Vesturdjúp (~30 Ma) on the southern Iceland shelf (Hjartarson et al., 2017) (Figures 11c and 12).

Global plate-motion reorganizations are believed to have triggered changes in spreading rates and directions in the NE Atlantic, around 33 Ma, when the relative motion between Greenland and the Eurasian plates changed from NNW–SSE to a WNW–ESE direction (Gaina et al., 2009). Around 35 Ma, the Western Mediterranean-Alpine area changed from subduction to a collision mode that pushed the Adriatic plate into the European margin (Le Breton et al., 2021), coinciding with a change in plate motion of the Eurasian plate from SSE–NNW to WSW–ENE (~40–33 Ma) (Gaina et al., 2009; Gaina, Nasuti et al., 2017). These events coincided with major erosional events across the central NE Atlantic region as well as to changes in spreading directions associated with the final rift transfer of IPR-III and IPR-IV (Figure 12). Thus, the mid-Alpine Pyrenean orogeny occurred at the same time as this final phase of the Northeast Atlantic opening, placing the NW European plate margin between the active ocean spreading ridges and the orogenic belt (Figures 11c and 12) (e.g., Lundin & Doré, 2002; Ritchie et al., 2008). This process may have enabled a rearrangement of active spreading centers within the

Northeast Atlantic region, which caused reactivation and compression along the southeastern JMMC domain, generating inversion structures within the Jan Mayen Southern Ridge Complex highs and within the Iceland-Faroe Ridge area (Blischke et al., 2019; Gaina et al., 2009). Furthermore, the center of the Iceland plume hotspot track was located offshore Greenland underneath the western segment of the GIFRC, the Greenland-Iceland Ridge, in the proximity of the JMMC around 30 Ma (Figure 11c), indicating that a mantle impingement may have caused the eastward regional tilt of the GIFRC, which corresponds to a collapse of the JMMC's eastern flank that triggered massive slumping (Blischke et al., 2019; Gaina, Nasuti et al., 2017; Stärz et al., 2017) (Supplement 6b, 6c in Supporting Information S1).

6.2. Tectono-Magmatic Evolution of the JMMC

The JMMC displays many of the characteristics of microcontinents as described by Müller et al. (2001), Nemčok et al. (2016), and Gaina and Whittaker (2020), such as inherited lithospheric heterogeneities, wrench tectonics, and oblique rifts. Highly oblique spreading ridges have been recognized globally in relation to slow, intermediate, and super-fast spreading centers. They are assumed to be related to reorganizations of plate boundaries and magmatic overpressure, causing spreading obliquity generally up to $\sim 10^\circ$ and in a few cases even up to 30° – 40° , as can be observed for the Mohn's Ridge just north of the JMMC (e.g., Dauteuil & Brun, 1993; Zhang et al., 2018).

Variable crustal thickness (6–22 km) across the Iceland Plateau and Jan Mayen region reflect substantial variation in extension and magmatism (Kandilarov et al., 2012; Kodaira et al., 1998a, 1998b; Mjelde et al., 2002, 2008), where lower crustal high-velocity domes represent deep crustal intrusives (Figure 6e) (Brandsdóttir et al., 2015). Spreading obliquity associated with deep crustal intrusives was active along the eastern JMMC margin, in the early Eocene, where a wedge-shaped asymmetric SDR complex, narrowing and thinning southwards, formed prior to the V-shaped Ægir Ridge (Figures 9–11).

The IPR spreading centers formed in a southeast-to-northwest direction simultaneously with southward cessation of spreading along the Ægir Ridge. The IPR rifts sheared the JMMC from East Greenland in four stages (IPR-I to IPR-IV; Figures 11 and 12). IPR blocks are separated by graben and half-graben structures and intersecting rift segments. This heterogeneity appears to reach far into the JMMC and is especially apparent within the Jan Mayen Southern Ridge Complex, where IPR-II rifting intersects the IPR-I domain and abrupt thinning is observed (Figures 1, 6, 9 and 10; Supplement 7 in Supporting Information S1).

Overlapping rift systems are also likely to have formed across the GIFRC, specifically in relation to Iceland's pre-Neogene eastern and western domains (20–40 km), that is, adjacent to the Neovolcanic zones, where crustal thickness decreases rapidly (< 20 km) (e.g., Brandsdóttir & Menke, 2008; Holbrook et al., 2001; Menke et al., 1998; Reiche et al., 2011; Richardson et al., 1998; Staples et al., 1997; White et al., 1995). Oblique rift systems characterize present-day Iceland: in the north, the dextral Tjörnes Fracture Zone system connects the Northern Rift Zone with the Kolbeinsey Ridge, whereas in the south, sinistral propagating volcanic systems along the Reykjanes Peninsula connect into the South Iceland Seismic Zone (e.g., Einarsson, 2008; Einarsson & Sæmundsson, 1987; Einarsson et al., 2020; Hreinsdóttir et al., 2001; Karson et al., 2018, 2019; Murton & Parson, 1993; Taylor et al., 1994) (Figures 13b and 14).

The present-day oblique rift systems form microplates affected by strike-slip and crustal deformation processes, as observed in outcrops (e.g., Einarsson, 2008; Einarsson et al., 2020; Karson et al., 2018, 2019). Similar relationships are observed on seismic reflection data within the Jan Mayen Southern Ridge Complex, where the overall right-lateral opening of the Southern Ridge Complex Fracture Zone and Southern Ridge Complex includes left-lateral compensating or block-rotating strike-slip elements (Figure 13b) (Blischke, 2020).

The orientation of rift opening, and therefore the obliquity of a given rift segment changes through time and location along a rift zone, just as for the JMMC–IPR structural fabric (Figures 12 and 13). This can be solved by calculating spreading-time directions from the finite rotation of each tectonic segment within a kinematic reconstruction (e.g., Gaina, 2014; Gaina, Nasuti, et al., 2017). Thus, for each given tectonic block within such a reconstruction, the opening direction could, in turn, reflect a unique stress-field orientation (Figure 13).

The reconstructed time ~ 49 Ma was constrained using the northern Ægir Ridge, the southern Ægir Ridge, and the northernmost tip of the Reykjanes Ridge, to assess if the calculated opening direction and its associated potential

overall horizontal stress-field fits the documented fault and fracture zone patterns (Figure 13). All three locations vary in the opening direction and sense of shear within dextral or sinistral oblique rift segments (Figure 13) and reflect the orientation of normal fault sets, block fault rotation-related strike-slip faulting, or overall fracture zone orientations. These zones represent wide fracture zones that impact entire structural domains. Extinct rift segments are “frozen” in place and are rotated out of their original position by younger rifting episodes.

6.2.1. The Iceland Plume

Large tectonic elements have been suggested as the primary reason for the complex breakup history and rift formation along the GIFRC (e.g., Foulger et al., 2020; Gernigon et al., 2012; Higgins & Leslie, 2008; Ritchie et al., 2011) and as a primary mechanism of magmatically inflated and stretched continental crust forming a hybrid continental-oceanic lithosphere along the GIFRC (Foulger et al., 2020, 2021). Seismic tomography, spectral analysis of magnetic data, Bouguer gravity anomaly, and thermal models have illuminated the hotspot track beneath Greenland, Jan Mayen, and Iceland in higher detail (e.g., Bjarnason, 2008; Martos et al., 2018; Mordret, 2018; Wolfe et al., 1997; or Toyokuni et al., 2020a, 2020b). Modeled hotspot track segments aligned with anomalous areas on Bouguer gravity, magnetic anomaly, and seismic refraction data along the GIFRC (e.g., Mordret, 2018; or Toyokuni et al., 2020a, 2020b), around the Eggvin Bank and the western Jan Mayen Fracture Zone, which have been interpreted as thick heterogeneous crust along the northern JMMC and the Jan Mayen igneous complex (Tan et al., 2017, 2018) (Figures 1, 9b, 10, and 11c). These observations all confirm previous models of a large mantle anomaly with a regional impact in the Blossville Kyst, JMR–SRC, and GIR–IFR areas (Figure 11). An area where underlying structural complexity most certainly existed prior to the breakup, between central East Greenland and the Faroe Plateau (Figure 11a). However, this region may contain thin slivers of highly stretched and intruded continental crust, as observed within the ridge segments of the Jan Mayen Southern Ridge Complex and inferred within the Iceland–Faroe Ridge (Figure 11).

6.2.1.1. Petrologic Provenance

Asymmetric rift development and transfer across Iceland serves as an important example of a hotspot-ridge interaction system for the GIFRC as well, both geodynamical and geochemically. Iceland-type basalts, as in the case of the Northern Volcanic Zone, have a wide variation that could be linked to changes in mantle source composition or variation in mantle melting conditions, such as plume temperature, reflecting heterogeneities in the Icelandic mantle that are described as a large-scale regional magmatic source that produced the Northern Volcanic Zone sub-alkaline tholeiite basalts (e.g., Chauvel & Hémond, 2000; Fitton et al., 1997; Kokfelt et al., 2006; Thirlwall et al., 2004). The early influence of the Iceland plume in the JMMC–IPR domain formation can be inferred by comparing to the geochemical compositions of the Northern Volcanic Zone basalts that are similar to the IPR-II core samples and the Igtertivá Formation for East Greenland in terms of $\text{MgO}/\text{K}_2\text{O}$ (wt%) and MgO/TiO_2 (wt%) contents (Figure 7). However, geochemical composition variations can relate to potential crustal assimilation of slivers of continental crust from the outermost breakup margins not just within the JMMC (Figure 11c). In order to answer the question of which of the two interpretations is more applicable, drill samples for each IPR phase would be required to compare those to the onshore outcrop analogs and spars borehole record in the region, which is targeted for future research (e.g., Larsen, Blischke, Halldórsson, et al., 2021; Larsen, Blischke, Brandsdóttir, et al., 2021). Similarly, seafloor sampling along the eastern scarp of Lyngvi Ridge and the western scarp of the Jan Mayen Southern Ridge Complex has given strong indications that East Greenland continental fragments of Late Permian–Early Triassic to Early Cretaceous ages underlie the JMMC (e.g., Polteau et al., 2018; Sandstå et al., 2012) (Figure 3).

Basalts from both Iceland and the Jan Mayen igneous complex are associated with distinct chemical anomalies (e.g., Kokfelt & Árting, 2014). However, their source in terms of compositions, temperatures, and depth of origin has been long debated (e.g., Breddam, 2002; Chauvel & Hémond, 2000; Fitton et al., 1997; Hanan et al., 2000; Hanan & Schilling, 1997; Kempton et al., 2000; Kokfelt et al., 2006; Mertz et al., 1991; Mertz & Haase, 1997; Parkin & White, 2008; Skovgaard et al., 2001; Stracke et al., 2003; Trønnes et al., 1999). The Jan Mayen igneous complex anomaly is characterized by more enriched and alkaline compositions, like the volcanic flank zones of Iceland (Debaille et al., 2009), the northern Jan Mayen Ridge, the Jan Mayen Fracture Zone, and, in part, the Vesteris Seamount (Figure 8). Different compositions of the Jan Mayen igneous complex are considered to be related either to a mantle plume or to MORB melts that have been contaminated by continental lithosphere (Hanan et al., 2000; Kokfelt & Árting, 2014). Variations along the southernmost part of the Kolbeinsey Ridge

indicate geochemically transitional signatures varying between typical depleted MORB and Icelandic basalts (Hart et al., 1973; Kokfelt & Ártung, 2014; Schilling et al., 1999; Sun et al., 1975; Thirlwall et al., 2004).

6.2.1.2. Mid-Oceanic Ridge Asymmetry

V-shaped ridges flanking the Reykjanes Ridge are commonly attributed to the pulsing of the Iceland mantle plume from around 35 Ma, at a frequency of 3 to 8 m.y. (e.g., Parnell-Turner et al., 2014; White et al., 1995). The initiation of pulsing coincides with the formation of IPR-III and the separation of the JMMC from the central East Greenland margin. Whereas some of the inferred plume-pulsing events south of the GIFRC correlate with changes in spreading directions Gaina, Nasuti, et al. (2017), they are inconsistent with the chronology outlined for rifting events north of the GIFRC. Major unconformities around the JMMC are associated with regional tectonic and magmatic events that do not correlate with the plume-pulsing events along the Reykjanes Ridge. Instead, they are associated with gradual rift transfer of an oceanic spreading system from the Ægir Ridge to the Kolbeinsey Ridge via the four phases of the Iceland Plateau Rift system, which was likely influenced by the Iceland mantle anomaly from IPR-III onwards.

6.2.2. Structural Inheritance Within the North-Atlantic

At the time of the breakup, the Jan Mayen Ridge and Jan Mayen Basin were juxtaposed to the Blossville Kyst and Scoresby Sund areas in East Greenland. Fault trends and the SW-NE-striking magnetic anomaly interpreted across the Geikie plateau appear to terminate against the JMMC (Figures 11a and 14; Supplement 8 in Supporting Information S1). This is interpreted as indirect evidence for intrusive complexes located within pre-breakup sediments just north of Kap Brewster at the mouth of the Scoresby Sund and observed on seismic reflection data throughout the Jameson Land Basin (e.g., Blischke & Erlendsson, 2018; Eide et al., 2021) (Figure 11a). The Geikie plateau structures have distinct magnetic trends associated with pre-breakup and breakup lava flows that cover the area. There is no clear geochemical evidence at the surface to link these lava flows to specific feeder dike systems (e.g., L. M. Larsen et al., 1989; Pedersen et al., 1997). However, the magnetic anomalies across the Geikie plateau might represent deep-seated faults that served as pathways for upwelling magma. These structural features align with the modeled hot-spot track estimates for heat flux >70 mW/m² (Martos et al., 2018) (55–50 Ma on Figure 14). The right-stepping alignment of these magnetic anomalies and potential fracture systems would correspond to a left-lateral opening of that area, as proposed by Guarnieri (2015) for the GIFRC and northward into the Scoresby Sund area, thus linking the tectonic fabric to the magmatic emplacement processes during the initial breakup phase (Figures 12 and 14; Supplement 8 in Supporting Information S1).

Large tectonic elements, such as the main Caledonian thrust belt, the Archean terrane, fracture zones crossing into the Fugloy Ridge, or the Moine Thrust Fault (e.g., Foulger et al., 2020; Gernigon et al., 2012; Higgins & Leslie, 2008; Ritchie et al., 2011) (Figure 14), appear to connect East Greenland with the European margin via a broad sinistral shear zone. Anomalous magnetic anomaly patterns, potential fracture zones, and structural lineaments continue across the GIFRC (Figure 14) indicating pre-rift lithospheric structures that appear to connect to the large tectonic elements. Two primary structural trends formed during the syn-breakup phase: a WNW-to-ESE trend across the main GIFRC, and an NW-to-SE trend forming the Iceland Plateau and the proto-eastern Jan Mayen Fracture Zone, north of the GIFRC. The Iceland Plateau and GIFRC structural trends were reactivated during later rift phases, gradually extending the Iceland-Faroe Fracture Zone along the northern edge of the GIFRC and the JMMC fracture zone systems throughout the formation of the Ægir Ridge and Iceland Plateau rifts (Figures 11b, 11c, 12, 13, and 14). The Iceland-Faroe Fracture Zone linked adjoining rift systems, the Ægir Ridge, and subsequently the IPR from the northeast and the Reykjanes Ridge from the southwest (Figure 14).

The initial settings of the proposed fracture zones (55 Ma on Figure 14) display two primary structural trends that appear to have guided the opening of this area; a SE-NW trend that links the JMMC to the European margin, and a WNW-ESE trend linking the JMMC to East Greenland. The structural setting and overall rift and oblique rift systems appear to guide the breakup (55–47 Ma on Figure 14), with the Ægir and Reykjanes ridges “turning” westward toward East Greenland that might be linked structurally or toward a proposed hot-spot track (Martos et al., 2018). From the Late Eocene and Early Oligocene (~35 Ma on Figure 14), the hot-spot is northwest of the main rift system IPR-III; there was a substantial increase of volcanic intrusives and extrusives in the region; and a west-to-east tilting of the GIFRC. Separating the JMMC–IPR domain from the East Greenland shelf (~24–21 Ma on Figure 14), the IPR-IV rift merged with the proto-Kolbeinsey Ridge in southward continuation with the NW Iceland Rift Zone and Reykjanes Ridge, whilst located just above the hotspot center. By ~15 Ma,

the plate boundary within the Iceland region had shifted eastwards as the hotspot moved east of the rift zone (e.g., Harðarson et al., 1997, 2008) requiring an oblique SE-to-NW rift transition similar to the IPR. Thus, the Snæfellsnes-Húnaflói Rift Zone (~15–7 Ma) was linked to the Kolbeinsey Ridge via a transfer system west of the Iceland-Faroe Fracture Zone (~15 Ma on Figure 14). The interaction of the GIFRC and IPR rift segments with the center of the hotspot, instigated the formation of complex rift, rift-flank, and fracture zone systems (e.g., IPR, Iceland-Faroe Fracture Zone, Snæfellsnes-Húnaflói Rift Zone, and the Tjörnes Fracture Zone on Figure 14) from the second JMMC breakup to present day.

7. Conclusions

Detailed volcanostratigraphic mapping based on geological, geophysical, and petrological data have provided a new kinematic model for the opening of the central NE-Atlantic. The Jan Mayen microcontinent developed through seven tectono-magmatic phases over a period of ~40 million years (~63–21 Ma). The Cenozoic evolution of the NE-Atlantic region is a prolonged history of continental breakup and seafloor spreading, highlighting the complexity of rift evolution interconnected to a hotspot region from breakup to the present.

Initial breakup within the N-Atlantic (~63–56 Ma) was accompanied by enhanced igneous activity that was linked to preexisting structural features. Primary fracture zones accommodated the opening of the JMMC region along a SE-NW trend at the European margin and a WNW-ESE trend in East Greenland. Microcontinent formation was accomplished by oblique opening within two fan-shaped domains: Initial breakup, from NNE-SSW along the segmented northeastern JMMC igneous margin, forming thick, overlapping sets of SSW-NNE-aligned igneous sections (SDR; ~55–53 Ma), prior to the activation of rifting at the Ægir Ridge and opening of the Norway Basin (~55–26 Ma). Second breakup, from SE-NW through rift transfer along the western JMMC igneous margin, within four Iceland Plateau Rift systems (IPR-I to IPR-IV). The overlapping and propagating IPR rift segments, interlinked via fracture zones, gradually separated the JMMC from East Greenland, over a period of ~25 million years (~52–23 Ma).

The Iceland Plateau Rift domain links the Iceland-Faroe Ridge with East Greenland's central Blossville Kyst, through both tectonics and geochemistry. The overlapping IPR rift systems contributed to vertical accretion of lava flows that resulted in an anomalous thick igneous crust in this region. Direct Iceland hotspot-rift interaction most likely coincided with IPR phase III (~35–24 Ma), and substantial increase in intrusives and extrusives in the region, and a west to east tilt of the JMMC, Iceland Plateau Rift, and Greenland-Iceland Ridge domains. Full separation occurred during IPR phase IV (~24–23 Ma), during which the Reykjanes Ridge and the proto-Kolbeinsey Ridge connected via the NW Iceland Rift Zone, near the center of the hotspot (~22–21 Ma).

Oblique rift transitions continued within the proto-Iceland region, as the hotspot migrated eastward. The NW Iceland Rift Zone (~21–15 Ma) and the Snæfellsnes-Húnaflói Rift Zone (~15–7 Ma) are likely to have connected the Reykjanes and Kolbeinsey ridges through fracture zones at this time, progressively generating plate boundary structures observed in Iceland today.

Data Availability Statement

This project's database, including published and confidential data sets, their data portal links, and primary reference information is summarized in supplement 1. Furthermore, previously unpublished data is provided in the supplement sections and the online data repository ZENODO (<https://zenodo.org/record/6346888#.YitQlZX-LeUk>) under DOI: [10.5281/zenodo.6346888](https://doi.org/10.5281/zenodo.6346888). The repository contains all supplement material, specifically new geochronological (supplements 3 and 4) and petrochemical data (supplement 5). For other data access inquiries, contact the corresponding author Anett Blischke (anb@isor.is).

References

- Abdelmalak, M. M., Meyer, R., Planke, S., Faleide, J. I., Gernigon, L., Frieling, J., et al. (2015). Pre-breakup magmatism on the Vøring margin: Insight from new sub-basalt imaging and results from ocean drilling Program Hole 642E. *Tectonophysics*, *675*, 258–274. <https://doi.org/10.1016/j.tecto.2016.02.037>
- Abdelmalak, M. M., Planke, S., Faleide, J. I., Jerram, D. A., Zastrozhnov, D., Eide, S., & Myklebust, R. (2016). The development of volcanic sequences at rifted margins: New insights from the structure and morphology of the Vøring Escarpment, mid-Norwegian Margin. *Journal of Geophysical Research: Solid Earth*, *121*, 5212–5236. <https://doi.org/10.1002/2015JB012788>

Acknowledgments

This research project at the University of Iceland, the Iceland GeoSurvey, and the Centre for Earth Evolution and Dynamics, University of Oslo, was funded by the National Energy Authority of Iceland (Orkustofnun), the Iceland GeoSurvey, and supported by the Norwegian Research Council by Centres of Excellence funding to CEED (project number 223272). Data permissions were provided by the National Energy Authority of Iceland (Orkustofnun), the Norwegian Petroleum Directorate (NPD), Spectrum ASA, TGS; the University of Oslo (UiO), the Bundesanstalt für Geowissenschaften und Rohstoffe (BGR), and Geological Survey of Denmark and Greenland (GEUS). We thank the Marine Research Institute of Iceland (MRI), for making the multibeam and backscatter data available and the Norwegian Petroleum Directorate (NPD) for use of their 2D multichannel reflection data sets from 2011 to 2012, and Prof. emerit. Olav Eldholm for permission to use the unpublished JMMC ESP data set. Seafloor borehole core samples were obtained from the Bremen Core Repository of the International Ocean Discovery Program (IODP). The dating of core samples was carried out at the Oregon State University (OSU) Argon Geochronology Laboratory. Geochemical analyses were conducted at the University of Iceland, and the Aarhus University. Unpublished geochemical analyses of cores 32, 33, and 34 of DSDP Leg 38 site 348, and cores 14 and 15 of DSDP Leg 38 site 350 were kindly made available by Professor Godfrey Fitton at the University of Edinburgh and Prof. Christian Tegner at the Aarhus University. Martyn Stoker gratefully acknowledges the award of Visiting Research Fellow at the Australian School of Petroleum and Energy Resources at the University of Adelaide. Anett Blischke would like to thank Dr. Lotte Melchior Larsen and Dr. Hans Christian Larsen for valuable advice throughout this project. We thank the two anonymous reviewers and J. A. Karson for their insightful advice and constructive reviews.

- Åkermoen, T. (1989). *Jan Mayen-ryggen: et seismisk stratigrafisk og strukturelt studium*. Cand. Scient. Thesis. University of Oslo.
- Árting, U., Kokfelt, T., Hjartarson, Á., Stewart, M., á Horni, J., Geissler, W.H., et al. (2014). Regional volcanism. In J. R. Hopper, T. Funck, M. S. Stoker, U. Árting, G. Peron-Pinvidic, H. Doornenbal, & C. Gaina (Eds.), *Tectonostratigraphic Atlas of the North-East Atlantic region. The Geological Survey of Denmark and Greenland (GEUS)* (1st ed.).
- Berndt, C., Planke, S., Alvestad, E., Tsikalas, F., & Rasmussen, T. (2001). Seismic volcanostratigraphy of the Norwegian margin: Constraints on tectonomagmatic break-up processes. *Journal of the Geological Society*, 158(3), 413–426. <https://doi.org/10.1144/jgs.158.3.413>
- Bischoff, A., Nicol, A., Cole, J., & Gravley, D. (2019). Stratigraphy of architectural elements of a buried monogenetic volcanic system. *Open Geosciences*, 11(1), 581–616. <https://doi.org/10.1515/geo-2019-0048>
- Bjarnason, I. T. (2008). An Iceland hotspot saga. *Jökull Journal*, 58, 3–16.
- Blišchke, A. (2020). *The Jan Mayen microcontinent and Iceland plateau: Tectono-magmatic evolution and rift propagation*, PhD dissertation. Faculty of Earth Sciences, University of Iceland.
- Blišchke, A., & Erlendsson, Ö. (2018). *Central East Greenland—Conjugate margin of the Jan Mayen microcontinent—Database, structural and stratigraphical mapping project*. Iceland GeoSurvey. ÍSOR-2018/024, 1-95, 2 maps, Appendices 1 to 5, Reykjavik, Iceland.
- Blišchke, A., Erlendsson, Ö., Brandsdóttir, B., Hjartardóttir, Á. R., & Gautason, B. (2020). The Iceland Plateau—Jan Mayen volcanic breakup margin: An analogue for axial rift and transfer zone North Iceland. In *Proceedings World Geothermal Congress 2021* (pp. 1–12).
- Blišchke, A., Erlendsson, Ö., Brandsdóttir, B., Hjartardóttir, Á. R., & Gautason, B. (2021). The Iceland Plateau—Jan Mayen volcanic breakup margin: An analogue for axial rift and transfer zone North Iceland. In *Proceedings World Geothermal Congress 2021* (p. 1–12).
- Blišchke, A., Erlendsson, Ö., Einarsson, G. M., Ásgeirsson, V. L., & Árnadóttir, S. (2017). *The Jan Mayen Microcontinent project database and seafloor Mapping of the Dreki area input data, geological and geomorphological Mapping and analysis*. Iceland GeoSurvey. ÍSOR-2017/055.
- Blišchke, A., Erlendsson, Ö., Guarnieri, P., Brandsdóttir, B., & Gaina, C. (2018). *Structural links between the Jan Mayen microcontinent and the central East Greenland coast prior to, during, and after breakup*The 33rd Nordic geological winter meeting 2018. The Geological Society of Denmark.
- Blišchke, A., Gaina, C., Hopper, J. R., Péron-Pinvidic, G., Brandsdóttir, B., Guarnieri, P., et al. (2017). The Jan Mayen microcontinent: An update of its architecture, structural development and role during the transition from the Ægir ridge to the mid-oceanic Kolbeinsey ridge. *Geological Society, London, Special Publications*, 447(1), 299–337. <https://doi.org/10.1144/SP447.5>
- Blišchke, A., Planke, S., Tegner, C., Gaina, C., Brandsdóttir, B., Halldórsson, S. A., et al. (2016). *Seismic volcano-stratigraphic characteristics and igneous province assessment of the Jan Mayen microcontinent, central NE-Atlantic* (pp. T33A–T3008). AGU Fall Meeting.
- Blišchke, A., Stoker, M. S., Brandsdóttir, B., Hopper, J. R., Peron-Pinvidic, G., Ólavsdóttir, J., & Japsen, P. (2019). The Jan Mayen microcontinent's Cenozoic stratigraphic succession and structural evolution within the NE-Atlantic. *Marine and Petroleum Geology*, 103, 702–737. <https://doi.org/10.1016/j.MARPETGEO.2019.02.008>
- Bonow, J. M., & Japsen, P. (2021). Peneplains and tectonics in North-East Greenland after opening of the North-East Atlantic. *GEUS Bulletin*, 45(2), 154–5297. <https://doi.org/10.34194/geusb.v45.5297>
- Bonow, J. M., Japsen, P., & Nielsen, T. F. D. (2014). High-level landscapes along the margin of southern east Greenland: A record of tectonic uplift and incision after breakup in the NE Atlantic. *Global and Planetary Change*, 116, 10–29. <https://doi.org/10.1016/j.gloplacha.2014.01.010>
- Bott, M. H. P., Browitt, C. W. A., & Stacey, A. P. (1971). The deep structure of the Iceland-Faeroe Ridge. *Marine Geophysical Researches*, 1(3), 328–351. <https://doi.org/10.1007/BF00338261>
- Brandsdóttir, B., Hooft, E. E. E., Mjelde, R., & Murai, Y. (2015). Origin and evolution of the Kolbeinsey ridge and Iceland Plateau, N-Atlantic. *Geochemistry, Geophysics, Geosystems*, 16(3), 612–634. <https://doi.org/10.1002/2014GC005540>
- Brandsdóttir, B., & Menke, W. H. (2008). The seismic structure of Iceland. *Jökull Journal*, 58, 17–34.
- Breddam, K. (2002). Kistufell: Primitive melt from the Iceland mantle plume. *Journal of Petrology*, 43(2), 345–373. <https://doi.org/10.1093/ptrology/43.2.345>
- Breivik, A. J., Faleide, J. I., & Mjelde, R. (2008). Neogene magmatism northeast of the Aegir and Kolbeinsey ridges, NE Atlantic: Spreading ridge–mantle plume interaction? *Geochemistry, Geophysics, Geosystems*, 9, Q02004. <https://doi.org/10.1029/2007GC001750>
- Breivik, A. J., & Mjelde, R. (2003). *Modeling of profile 8 across the Jan Mayen Ridge*. Rep. Institute of Solid Earth Physics, University of Bergen.
- Breivik, A. J., Mjelde, R., Faleide, J. I., & Murai, Y. (2012). The eastern Jan Mayen microcontinent volcanic margin. *Geophysical Journal International*, 188(3), 798–818. <https://doi.org/10.1111/j.1365-246X.2011.05307.x>
- Brooks, C. K. (2011). The East Greenland rifted volcanic margin. *Geological Survey of Denmark and Greenland Bulletin*, 24, 96. <https://doi.org/10.34194/geusb.v24.4732>
- Butt, E. A., Elverhøi, A., Forsberg, C. F., & Solheim, A. (2001). Evolution of the Scoresby Sund Fan, central East Greenland—Evidence from ODP site 987. *Norwegian Journal of Geology*, 81, 3–15.
- Campsie, J., Rasmussen, M. H., Kovacs, L. C., Dittmer, F., Bailey, J. C., Hansen, N. O., et al. (1990). Chronology and evolution of the northern Iceland Plateau. *Polar Research*, 8(2), 237–243. <https://doi.org/10.1111/j.1751-8369.1990.tb00386.x>
- Channell, J. E. T., Amigo, A. E., Fronval, T., Rack, F., & Lehman, B. (1999). Magnetic stratigraphy at Sites 907 and 985 in the Norwegian-Greenland Sea and a revision of the Site 907 composite section. *Proceedings of the Ocean Drilling Program, Scientific Results*, 162, 131–148. <https://doi.org/10.2973/odp.proc.sr.162.036.1999>
- Channell, J. E. T., Smelror, M., Jansen, E., Higgins, S. M., Lehman, B., Eidvin, T., & Solheim, A. (1999). Age models for glacial fan deposits off East Greenland and Svalbard (sites 986 and 987). *Proceedings of the Ocean Drilling Program, Scientific Results*, 162, 149–166. <https://doi.org/10.2973/odp.proc.sr.162.008.1999>
- Chauvel, C., & Hémond, C. (2000). Melting of a complete section of recycled oceanic crust: Trace element and Pb isotopic evidence from Iceland. *Geochemistry, Geophysics, Geosystems*, 1(2), 31. <https://doi.org/10.1029/1999GC000002>
- Childs, J. R., & Cooper, A. K. (1978). *Collection, reduction and interpretation of marine seismic sonobuoy data* (pp. 78–442). U.S. Geological Survey, Department of interior. technical report.
- Cohen, K. M., Finney, S. C., Gibbard, P. L., & Fan, J.-X. (2013). The ICS international chronostratigraphic chart. *Episodes*, 36, 199–204. <https://doi.org/10.18814/epiiugs/2013/v36i3/002>
- Dauteuil, O., & Brun, J.-P. (1993). Oblique rifting in a slow-spreading ridge. *Nature*, 361, 145–148. <https://doi.org/10.1038/361145a0>
- Davis, L. L., & McIntosh, W. C. (1996). The petrology and (super 40) Ar/(super 39) Ar age of tholeiitic basalt recovered from Hole 907A, Iceland Plateau. *Proceedings of the Ocean Drilling Program, Scientific Results*, 151, 351–365. <https://doi.org/10.2973/odp.proc.sr.151.124.1996>
- Debaille, V., Trønnes, R. G., Brandon, A. D., Waight, T. E., Graham, D. W., & Lee, C.-T. A. (2009). Primitive off-rift basalts from Iceland and Jan Mayen: Os-isotopic evidence for a mantle source containing enriched subcontinental lithosphere. *Geochimica et Cosmochimica Acta*, 73(11), 3423–3449. <https://doi.org/10.1016/J.GCA.2009.03.002>

- Devey, C. W., Garbe-Schönberg, C. D., Stoffers, P., Chauvel, C., & Mertz, D. F. (1994). Geochemical effects of dynamic melting beneath ridges: Reconciling major and trace element variations in Kolbeinsey (and global) mid-ocean ridge basalt. *Journal of Geophysical Research*, 99, 9077–9095.
- Diebold, J. B., & Stoffa, P. L. (1981). The traveltimes equation, tau-p mapping, and inversion of common midpoint data. *Geophysics*, 46(3), 238–254. <https://doi.org/10.1190/1.1441196>
- Doré, A. G., Lundin, E. R., Jensen, L. N., Birkeland, O., Eliassen, P. E., & Fichler, C. (1999). Principal tectonic events in the evolution of the northwest European Atlantic margin. In A. J. Fleet & S. A. R. Boldy (eds.), *Petroleum Geology Conference series* (Vol. 5, pp. 41–61). Geological Society of London. <https://doi.org/10.1144/0050041>
- Dobrovine, P. V., Steinberger, B., & Torsvik, T. H. (2012). Absolute plate motions in a reference frame defined by moving hot spots in the Pacific, Atlantic, and Indian oceans. *Journal of Geophysical Research*, 117(B9). <https://doi.org/10.1029/2011JB009072>
- Dupuy, P. Y., & Sogorb, G. (2017). *Survey report—NARVAL 2016 hydrographic and oceanographic cruise onboard R/V Beautemps-Beaupré*. Groupe hydrographique et océanographique de l'Atlantique, N° 113 SHOM/GHOA/NP.
- Eggen, S. S. (1984). *Jan Mayen-ryggens geologi* (Vol. 20, p. 29). Norwegian Petroleum Directorate contribution.
- Eide, C. H., Schofield, N., Howells, J., & Dougal, A. J. (2021). Transport of mafic magma through the crust and sedimentary basins: Jameson Land, East Greenland. *Journal of the Geological Society*, jgs2021-043. <https://doi.org/10.1144/jgs2021-043>
- Einarsson, P. (2008). Plate boundaries, rifts and transforms in Iceland. *Jökull Journal*, 58, 35–58.
- Einarsson, P., Hjartardóttir, Á. R., Hreinsdóttir, S., & Imsland, P. (2020). The structure of seismogenic strike-slip faults in the eastern part of the Reykjanes Peninsula Oblique Rift, SW Iceland. *Journal of Volcanology and Geothermal Research*, 391, 106372. <https://doi.org/10.1016/j.jvolgeores.2018.04.029>
- Einarsson, P., & Sæmundsson, K. (1987). Earthquake epicenters 1982–1985 and volcanic systems in Iceland, map. In T. Sigfússon (Ed.), *Í hlutarskrifum edli. Festschrift for Thorbjörn Sigurgeirsson, Menningarsjóður, Iceland*.
- Eldholm, O., & Grue, K. (1994). North Atlantic volcanic margins: Dimensions and production rates. *Journal of Geophysical Research*, 99(B2), 2955–2968. <https://doi.org/10.1029/93JB02879>
- Eldholm, O., Karasik Deceased, A. M., & Reksnes, P. A. (1990). The North American plate boundary. In A. Grantz, L. Johnson, & J. F. Sweeney (Eds.), *The Arctic Ocean region* (Vol. L, pp. 171–184). Geological Society of America. <https://doi.org/10.1130/DNAG-GNA-L.171>
- Eldholm, O., Thiede, J., & Taylor, E. (1987a). Evolution of the Norwegian continental margin: Background and objectives. In O. Eldholm, J. Thiede, E. Taylor, et al. (Eds.), *Proceedings of the Ocean Drilling Program Initial Reports* (Vol. 104, pp. 5–25). Ocean Drilling Program. <https://doi.org/10.2973/odp.proc.ir.104.101.1987>
- Eldholm, O., Thiede, J., & Taylor, E. (1987b). Shipboard scientific party, 1987. Site 642: Norwegian Sea. In O. Eldholm, J. Thiede, E. Taylor, et al. (Eds.), *Proceedings of the Ocean Drilling Program Initial Reports* (Vol. 104, pp. 53–453). Ocean Drilling Program. <https://doi.org/10.2973/odp.proc.ir.104.104.1987>
- Eldholm, O., & Windisch, C. C. (1974). Sediment distribution in the Norwegian–Greenland Sea. *The Geological Society of America Bulletin*, 85, 1661–1676. [https://doi.org/10.1130/0016-7606\(1974\)85<1661:sditms>2.0.co;2](https://doi.org/10.1130/0016-7606(1974)85<1661:sditms>2.0.co;2)
- Ellis, D., & Stoker, M. S. (2014). The Faroe–Shetland Basin: A regional perspective from the Paleocene to the present day and its relationship to the opening of the north Atlantic Ocean. In S. J. C. Cannon, & D. Ellis (Eds.), *Hydrocarbon exploration to exploitation west of Shetlands*. Geological Society, London, Special Publications. <https://doi.org/10.1144/SP397.1397>
- Erlendsson, Ö. (2010). *Seismic investigation of the Jan Mayen Ridge—With a Close Study of Sill Intrusions*. MSc. Thesis (Vol. 111). Aarhus University.
- Erlendsson, Ö., & Blischke, A. (2013). *Haffréttarmál: Hljóðendurvarps- og bylgjubrotsmælingar: Skýrsla um stöðu mála á úrvinnslu og túlkun gagna (Law of the sea: Seismic reflection and refraction database and interpretation status report)*. Iceland GeoSurvey. Report ÍSOR-2013/067.
- Faleide, J. I., Bjørlykke, K., & Gabrielsen, R. H. (2010). Geology of the Norwegian continental shelf. In K. Bjørlykke (Ed.), *Petroleum geoscience: From sedimentary environments to rock physics* (pp. 467–499). Springer. https://doi.org/10.1007/978-3-642-02332-3_22
- Fitch, F. J. (1964). The development of the Beerenberg volcano, Jan Mayen. *Proceedings of the Geologists' Association*, 75, 133–IN9. [https://doi.org/10.1016/S0016-7878\(64\)80002-X](https://doi.org/10.1016/S0016-7878(64)80002-X)
- Fitton, J. G., Saunders, A. D., Norry, M. J., Hardarson, B. S., & Taylor, R. N. (1997). Thermal and chemical structure of the Iceland plume. *Earth and Planetary Science Letters*, 153(3–4), 197–208. [https://doi.org/10.1016/S0012-821X\(97\)00170-2](https://doi.org/10.1016/S0012-821X(97)00170-2)
- Foulger, G. R., Doré, T., Emelous, C. H., Franke, D., Geoffroy, L., Gernigon, L., et al. (2020). The Iceland microcontinent and a continental Greenland–Iceland–Faroe Ridge. *Earth-Science Reviews*, 206, 102926. <https://doi.org/10.1016/j.earscirev.2019.102926>
- Foulger, G. R., Gernigon, L., & Geoffroy, L. (2021). Icelandia. In G. R. Foulger, L. C. Hamilton, D. M. Jurdy, C. A. Stein, K. A. Howard, & S. Stein (Eds.), *In the footsteps of Warren B. Hamilton: New ideas in Earth science* (Vol. 553, pp. 1–12). Geological Society of America Special Paper. [https://doi.org/10.1130/2021.2553\(04](https://doi.org/10.1130/2021.2553(04)
- Franke, D., Klitzke, P., Barckhausen, U., Berglar, K., Berndt, C., Damm, V., et al. (2019). Polyphase magmatism during the formation of the northern East Greenland continental margin. *Tectonics*, 38, 2961–2982. <https://doi.org/10.1029/2019TC005552>
- Funck, T., Erlendsson, Ö., Geissler, W. H., Gradmann, S., Kimbell, G. S., McDermott, K., & Petersen, U. K. (2017). A review of the NE Atlantic conjugate margins based on seismic refraction data. *Geological Society, London, Special Publications*, 447(1), 171–205. <https://doi.org/10.1144/SP447.9>
- Funck, T., Geissler, W. H., Kimbell, G. S., Gradmann, S., Erlendsson, Ö., McDermott, K., & Petersen, U. K. (2017). Moho and basement depth in the NE Atlantic Ocean based on seismic refraction data and receiver functions. *Geological Society, London, Special Publications*, 447(1), 207–231. <https://doi.org/10.1144/SP447.1>
- Funck, T., Hopper, J. R., Fattah, R. A., Blischke, A., Ebbing, J., Erlendsson, Ö., et al. (2014). Crustal structure. In J. R. Hopper, T. Funck, M. S. Stoker, U. Ártung, G. Peron-Pinvidic, H. Doornenbal, & C. Gaina (Eds.), *Tectonostratigraphic Atlas of the north-east Atlantic region. The geological survey of Denmark and Greenland (GEUS)* (1st ed.).
- Gaina, C. (2014). Plate reconstructions and regional kinematics. In J. R. Hopper, T. Funck, M. Stoker, U. Ártung, G. Peron-Pinvidic, H. Doornenbal, & C. Gaina (Eds.), *Tectonostratigraphic Atlas of the north-east Atlantic region* (1st ed., p. 340). The Geological Survey of Denmark and Greenland. (GEUS).
- Gaina, C., Blischke, A., Geissler, W. H., Kimbell, G. S., & Erlendsson, Ö. (2017). Seamounts and oceanic igneous features in the NE Atlantic: A link between plate motions and mantle dynamics. *Geological Society, London, Special Publications*, 447(1), 419–442. <https://doi.org/10.1144/SP447.6>
- Gaina, C., Gernigon, L., & Ball, P. (2009). Palaeocene—Recent plate boundaries in the NE Atlantic and the formation of the Jan Mayen microcontinent. *Journal of the Geological Society*, 166, 1–16. <https://doi.org/10.1144/0016-76492008-112>
- Gaina, C., Müller, R. D., Brown, B. J., & Ishihara, T. (2003). *Microcontinent formation around Australia* (p. 372). Geological Society of America. <https://doi.org/10.1130/0-8137-2372-8.405>

- Gaina, C., Nasuti, A., Kimbell, G. S., & Blischke, A. (2017). Break-up and seafloor spreading domains in the NE Atlantic. *Geological Society, London, Special Publications*, 447(1), SP447–417. <https://doi.org/10.1144/SP447.12>
- Gaina, C., & Whittaker, J. (2020). Microcontinents. In H. Gupta (Ed.), *Encyclopedia of Solid Earth geophysics. Encyclopedia of Earth Sciences series* (pp. 1–5). Springer. https://doi.org/10.1007/978-3-030-10475-7_240-1
- Gairaud, H., Jacquart, G., Aubertin, F., & Beuzart, P. (1978). Jan Mayen Ridge synthesis of geological knowledge and new data. *Oceanologica Acta*, 1(3), 335–358.
- Ganerød, M., Wilkinson, C. M., & Hendriks, B. (2014). Geochronology. In J. R. Hopper, T. Funck, M. Stoker, U. Ártung, G. Peron-Pinvidic, H. Doornenbal, & C. Gaina (Eds.), *Tectonostratigraphic Atlas of the north-east Atlantic region, the geological survey of Denmark and Greenland (GEUS)* (1st ed.).
- Geissler, W. H., Gaina, C., Hopper, J. R., Funck, T., Blischke, A., Arting, U., et al. (2017). Seismic volcanostratigraphy of the NE Greenland continental margin. *Geological Society, London, Special Publications*, 447(1), 149–170. <https://doi.org/10.1144/SP447.11>
- Geodekyan, A. A., Verkhovskaya, Z. I., Sudin, A. V., & Trotsiuk, V. Y. (1980). Gases in seawater and bottom sediments. In C. B. Udintsev (Ed.), *Iceland and mid-oceanic ridge—Structure of the ocean-floor* (pp. 19–36). Academy of Sciences of the USSR Soviet Geophysical Committee.
- Gernigon, L., Blischke, A., Nasuti, A., & Sand, M. (2015). Conjugate volcanic rifted margins, seafloor spreading, and microcontinent: Insights from new high-resolution aeromagnetic surveys in the Norway Basin. *Tectonics*, 34(5), 907–933. <https://doi.org/10.1002/2014TC003717>
- Gernigon, L., Franke, D., Geoffroy, L., Schiffer, C., Foulger, G. R., & Stoker, M. (2019). Crustal fragmentation, magmatism, and the diachronous opening of the Norwegian-Greenland Sea. *Earth-Science Reviews*. <https://doi.org/10.1016/j.earscirev.2019.04.011>
- Gernigon, L., Gaina, C., Olesen, O., Ball, P. J., Péron-Pinvidic, G., & Yamasaki, T. (2012). The Norway Basin revisited: From continental breakup to spreading ridge extinction. *Marine and Petroleum Geology*, 35(1), 1–19. <https://doi.org/10.1016/j.marpetgeo.2012.02.015>
- Gernigon, L., Zastrozhnov, D., Planke, S., Manton, B., Abdelmalak, M. M., Olesen, O., et al. (2021). A digital compilation of structural and magmatic elements of the mid-Norwegian continental margin (Version 1.0). *Norsk Geologisk Tidsskrift*, 101(1), 202112. <https://doi.org/10.17850/njg101-3-2>
- Govindaraju, K., & Mevelle, G. (1987). Fully automated dissolution and separation methods for inductively coupled plasma atomic emission spectrometry rock analysis. Application to the determination of rare Earth elements. Plenary lecture. *Journal of Analytical Atomic Spectrometry*, 2(6), 615–621. <https://doi.org/10.1039/JA9870200615>
- Gradstein, F. M., Ogg, J. G., Schmitz, M. D., & Ogg, G. M. (2012). *The geologic time scale* (1st ed.). Elsevier. <https://doi.org/10.1016/C2011-1-08249-8>
- Grønlie, G., Chapman, M., & Talwani, M. (1979). Jan Mayen Ridge and Iceland plateau: Origin and evolution. *Norsk Polarinstitutt Skrifter*, 170, 25–47.
- Grönvold, K., & Mäkipää, H. (1978). *Chemical composition of Krafla lavas 1975-1977*. Nordic volcanological institute, University of Iceland. Report 7816.
- Guarnieri, P. (2015). Pre-break-up palaeostress state along the East Greenland margin. *Journal of the Geological Society*, 172, 727–739. <https://doi.org/10.1144/jgs2015-053>
- Guarnieri, P., Brethes, A., Rasmussen, T. M., Blischke, A., Erlendsson, Ö., & Bauer, T. (2016). *CRUSMID-3D crustal structure and Mineral deposit systems: 3D-modelling of base metal mineralization in Jameson Land (East Greenland)* (p. 182). Nordisk Ministerråd. <https://doi.org/10.6027/TN2016-562>
- Gudlaugsson, S. T., Gunnarsson, K., Sand, M., & Skogseid, J. (1988). Tectonic and volcanic events at the Jan Mayen Ridge microcontinent. In A. C. Morton, & L. M. Parson (Eds.), *Early tertiary volcanism and the opening of the NE Atlantic* (Vol. 39, pp. 85–93). Geological Society of London. <https://doi.org/10.1144/gsl.sp.1988.039.01.09>
- Gunnarsson, K., Sand, M., & Gudlaugsson, S. T. (1989). *Geology and hydrocarbon potential of the Jan Mayen Ridge*. Report OS-98014, 143, 5 appendices incl. 9 maps Reykjavik.
- Haase, C., & Ebbing, J. (2014). Gravity data. In J. R. Hopper, T. Funck, M. S. Stoker, U. Ártung, G. Peron-Pinvidic, H. Doornenbal, & C. Gaina (Eds.), *Tectonostratigraphic Atlas of the north-east Atlantic region. The geological survey of Denmark and Greenland (GEUS)* (1st ed.).
- Haase, C., Ebbing, J., & Funck, T. (2017). A 3D regional crustal model of the NE Atlantic based on seismic and gravity data. *Geological Society, London, Special Publications*, 447(1), 233–247. <https://doi.org/10.1144/SP447.8>
- Haase, K. M., Devey, C. W., Mertz, D. F., Stoffers, P., & Garbe-Schonberg, D. (1996). Geochemistry of lavas from Mohns ridge, Norwegian-Greenland Sea: Implications for melting conditions and magma sources near Jan Mayen. *Contributions to Mineralogy and Petrology*, 123(3), 223–237. <https://doi.org/10.1007/s004100050152>
- Hald, N., & Tegner, C. (2000). Composition and age of tertiary sills and dykes, Jameson land basin, east Greenland: Relation to regional flood volcanism. *Lithos*, 54(3–4), 207–233. [https://doi.org/10.1016/S0024-4937\(00\)00032-3](https://doi.org/10.1016/S0024-4937(00)00032-3)
- Halldórsson, S. A., Oskarsson, N., Grönvold, K., Sigurdsson, G., Sverrisdóttir, G., & Steinthorsson, S. (2008). Isotopic-heterogeneity of the Thjorsa lava—Implications for mantle sources and crustal processes within the Eastern Rift Zone, Iceland. *Chemical Geology*, 255(3–4), 305–316. <https://doi.org/10.1016/j.chemgeo.2008.06.050>
- Hanan, B. B., Blichert-Toft, J., Kingsley, R., & Schilling, J. G. (2000). Depleted Iceland mantle plume geochemical signature: Artifact of multi-component mixing? *Geochemistry, Geophysics, Geosystems*, 1(4), 19. <https://doi.org/10.1029/1999GC000009>
- Hanan, B. B., & Schilling, J.-G. (1997). The dynamic evolution of the Iceland mantle plume: The lead isotope perspective. *Earth and Planetary Science Letters*, 151(1–2), 43–60. [https://doi.org/10.1016/S0012-821X\(97\)00105-2](https://doi.org/10.1016/S0012-821X(97)00105-2)
- Harðardóttir, S., Halldórsson, S. A., & Hilton, D. R. (2018). Spatial distribution of helium isotopes in Icelandic geothermal fluids and volcanic materials with implications for location, upwelling and evolution of the Icelandic mantle plume. *Chemical Geology*, 480, 12–27. <https://doi.org/10.1016/j.chemgeo.2017.05.012>
- Harðarson, B. S., Fitton, J. G., Ellam, R. M., & Pringle, M. S. (1997). Rift relocation—A geochemical and geochronological investigation of a palaeo-rift in northwest Iceland. *Earth and Planetary Science Letters*, 153(3), 181–196. [https://doi.org/10.1016/S0012-821X\(97\)00145-3](https://doi.org/10.1016/S0012-821X(97)00145-3)
- Harðarson, B. S., Fitton, J. G., & Hjartarson, A. (2008). Tertiary volcanism in Iceland. *Jökull Journal*, 58, 161–178.
- Hart, S. R., Schilling, J. G., & Powell, J. L. (1973). Basalts from Iceland and along the Reykjanes ridge: Sr isotope geochemistry. *Nature; Physical Science*, 246, 104–107. <https://doi.org/10.1038/physci246104a0>
- Helgadóttir, G. (2008). Preliminary results from the 2008 Marine Research Institute multibeam survey in the Dreki area, with some examples of potential use. In *Iceland exploration conference 2008*.
- Helgadóttir, G., & Reynisson, P. (2010). Setkjarnataka, fjölgeisla- og lágtíðniðýptarmælingar á Drekasvæði og Jan Mayen hryggárs. Árna Friðrikssyni RE 200 haustið 2010. Prepared for Orkustofnun and Norsku Olüstofnunina, Hafrannsóknastofnunin, Leiðangurskýrsla A201011, hluti 1 og 2.
- Henriksen, N. (2008). *Geological History of Greenland - Four billion years of earth evolution*. Geological Survey of Denmark and Greenland (GEUS).

- Higgins, A. K., & Leslie, A. G. (2008). Architecture and evolution of the east Greenland Caledonides—An introduction. In A. K. Higgins, J. A. Gilotti, & M. P. Smith (Eds.), *The Greenland Caledonides: Evolution of the Northeast Margin of Laurentia* (Vol. 202, pp. 29–53). GSA Memoirs. [https://doi.org/10.1130/2008.1202\(02\)](https://doi.org/10.1130/2008.1202(02))
- Hinz, K. (1981). An hypothesis on terrestrial catastrophes wedges of very thick oceanward dipping layers beneath passive continental margins; their origin and palaeoenvironmental significance. *Geologisches Jahrbuch, E2*, 3–28.
- Hinz, K., & Schlüter, H. U. (1978). The North Atlantic - Results of geophysical investigations by the Federal Institute for Geosciences and natural Resources on north Atlantic continental margins. *Erdoel-Erdgas-Zeitschrift*, 94, 271–280.
- Hjartarson, Á., Erlendsson, Ö., & Blischke, A. (2017). The Greenland–Iceland–Faroe Ridge complex. *Geological Society, London, Special Publications*, 447(14), 127–148. <https://doi.org/10.1144/SP447.14>
- Hjelstuen, B. O., Eldholm, O., & Skogseid, J. (1997). Vøring Plateau diapir fields and their structural and depositional settings. *Marine Geology*, 144(1–3), 33–57. [https://doi.org/10.1016/s0025-3227\(97\)00085-6](https://doi.org/10.1016/s0025-3227(97)00085-6)
- Hjelstuen, B. O., Eldholm, O., & Skogseid, J. (1999). Cenozoic evolution of the northern Vøring margin. *GSA Bulletin*, 111(12), 1792–1807. [https://doi.org/10.1130/0016-7606\(1999\)111<1792:ceotnv>2.3.co;2](https://doi.org/10.1130/0016-7606(1999)111<1792:ceotnv>2.3.co;2)
- Holbrook, W. S., Larsen, H. C., Korenaga, J., Dahl-Jensen, T., Reid, I. D., Kelemen, P. B., et al. (2001). Mantle thermal structure and active upwelling during continental breakup in the North Atlantic. *Earth and Planetary Science Letters*, 190(3–4), 251–266. [https://doi.org/10.1016/s0012-821x\(01\)00392-2](https://doi.org/10.1016/s0012-821x(01)00392-2)
- Hopper, J. R., Dahl-Jensen, T., Holbrook, W. S., Larsen, H. C., Lizarralde, D., Korenaga, J., et al. (2003). Structure of the SE Greenland margin from seismic reflection and refraction data: Implications for nascent spreading center subsidence and asymmetric crustal accretion during North Atlantic opening. *Journal of Geophysical Research*, 108(B5), 2269. <https://doi.org/10.1029/2002JB001996>
- Hopper, J. R., Funck, T., Stoker, M. S., Ártung, U., Peron-Pinvidic, G., Doornenbal, H., & Gaina, C. (2014). *Tectonostratigraphic Atlas of the North-East Atlantic region* (1st ed.). Geological Survey of Denmark-Greenland (GEUS).
- Horn, J. Á., Hopper, J. R., Blischke, A., Geissler, W., Judge, M., McDermott, K., et al. (2017). Regional distribution of volcanism within the north Atlantic igneous province. *Geological Society, London, Special Publications*, 447(18), 105–125. <https://doi.org/10.1144/SP447.18>
- Hreinsdóttir, S., Einarsson, P., & Sigmundsson, F. (2001). Crustal deformation at the oblique spreading Reykjanes Peninsula, SW Iceland: GPS measurements from 1993 to 1998. *Journal of Geophysical Research*, 106(B7), 13803–13816. <https://doi.org/10.1029/2001JB000428>
- Jakobsson, M., Mayer, L. A., Coakley, B., Dowdeswell, J. A., Forbes-Fridman, S. B., Hodnesdal, H., et al. (2012). The international bathymetric chart of the Arctic Ocean (IBCAO) version 3.0. *Geophysical Research Letters*, 39. <https://doi.org/10.1029/2012GL052219>
- Jansen, E., Raymo, M. E., Blum, P., Andersen, E. S., Austin, W. E. N., Baumann, K.-H., et al. (1996). *Initial reports, 162, Proceedings of the ocean drilling program*. Ocean Drilling Program. <https://doi.org/10.2973/odp.proc.ir.162.1996>
- Japsen, P., Green, P. F., Bonow, J. M., Bjerager, M., & Hopper, J. R. (2021). Episodic burial and exhumation in North-East Greenland before and after opening of the North-East Atlantic. *GEUS Bulletin*, 45(2), 154–5299. <https://doi.org/10.34194/geusb.v45.5299>
- Japsen, P., Green, P. F., Bonowa, J. M., Nielsen, T. F. D., & Chalmers, J. A. (2014). From volcanic plains to glaciated peaks: Burial, uplift and exhumation history of southern East Greenland after opening of the NE Atlantic. *Global and Planetary Change*, 116, 91–114. <https://doi.org/10.1016/j.gloplacha.2014.01.012>
- Johansen, B., Eldholm, O., Talwani, M., Stoffá, P. L., & Buhl, P. (1988). Expanding spread profile at the northern Jan Mayen Ridge. *Polar Research*, 6, 95–104. <https://doi.org/10.1111/j.1751-8369.1988.tb00584.x>
- Johnson, G. L., & Heezen, B. C. (1967). The morphology and evolution of the Norwegian-Greenland Sea. *Deep Sea Research and Oceanographic Abstracts*, 14, 755–771. [https://doi.org/10.1016/s0011-7471\(67\)80012-3](https://doi.org/10.1016/s0011-7471(67)80012-3)
- Johnson, G. L., & Tanner, B. (1971). Geophysical observations on the Iceland-Faeroe ridge. *Jökull Journal*, 21, 45–52.
- Kandilarov, A., Mjelde, R., Pedersen, R. B., Hellevang, B., Papenberg, C., Petersen, C. J., et al. (2012). The northern boundary of the Jan Mayen microcontinent, North Atlantic determined from ocean bottom seismic, multichannel seismic, and gravity data. *Marine Geophysical Research*, 33, 55–76. <https://doi.org/10.1007/s11001-012-9146-4>
- Karson, J. A., Brandsdóttir, B., Einarsson, P., Semundsson, K., Farrell, J., & Horst, A. (2019). Evolution of migrating transform faults in anisotropic oceanic crust: Examples from Iceland. *Canadian Journal of Earth Sciences*, 56(12), 1297–1308. <https://doi.org/10.1139/cjes-2018-0260>
- Karson, J. A., Farrell, J. A., Chutas, L. A., Nanfita, A. F., Proett, J. A., & Runnals, K. T. (2018). Rift-parallel strike-slip faulting near the Iceland plate boundary zone: Implications for propagating rifts. *Tectonics*, 37, 4567–4594. <https://doi.org/10.1029/2018TC005206>
- Kempton, P. D., Fitton, J. G., Saunders, A. D., Nowell, G. M., Taylor, R. N., Hardarson, B. S., & Pearson, G. (2000). The Iceland plume in space and time: A Sr–Nd–Pb–Hf study of the north Atlantic rifted margin. *Earth and Planetary Science Letters*, 177(3–4), 255–271. [https://doi.org/10.1016/S0012-821X\(00\)00047-9](https://doi.org/10.1016/S0012-821X(00)00047-9)
- Kharin, G. N., Udintsev, G. B., Bogatkov, O. A., Dmitriev, J. I., Raschka, H., Kreuzer, H., et al. (1976). K/AR ages of the basalts of the Norwegian-Greenland Sea DSDP Leg 38. In *Deep Sea drilling project, Part III: Shore-based Studies*. <https://doi.org/10.2973/dsdp.proc.38.116.1976>
- Kodaira, S., Mjelde, R., Gunnarsson, K., Shiobara, H., & Shimamura, H. (1998b). Evolution of oceanic crust on the Kolbeinsey Ridge, north of Iceland, over the past 22 Myr. *Terra Nova*, 10, 27–31. <https://doi.org/10.1046/j.1365-1321.1998.00166.x>
- Kodaira, S., Mjelde, R., Gunnarsson, K., Shiobara, H., & Shimamura, H. (1998a). Structure of the Jan Mayen microcontinent and implications for its evolution. *Geophysical Journal International*, 132, 383–400. <https://doi.org/10.1046/j.1365-246x.1998.00444.x>
- Kokfelt, T. F., & Ártung, U. (2014). Geochemistry. In J. R. Hopper, T. Funck, M. S. Stoker, U. Ártung, G. Peron-Pinvidic, H. Doornenbal, & C. Gaina (Eds.), *Tectonostratigraphic Atlas of the north-east Atlantic region*. Geological Survey of Denmark and Greenland (GEUS).
- Kokfelt, T. F., Hoernle, K., Hauff, F., Fiebig, J., Werner, R., & Garbe-SchÅunberg, D. (2006). Combined trace element and Pb–Nd–Sr–O isotope evidence for recycled oceanic crust (upper and lower) in the Iceland mantle plume. *Journal of Petrology*, 47(9), 1705–1749. <https://doi.org/10.1093/petrology/egl025>
- Kuvaas, B., & Kodaira, S. (1997). The formation of the Jan Mayen microcontinent: The missing piece in the continental puzzle between the Møre-Vøring basins and east Greenland. *First Break*, 15(7), 239–247. <https://doi.org/10.3997/1365-2397.1997008>
- Larsen, H. C., Blischke, A., Brandsdóttir, B., Leshner, C. E., Conrad, C. P., Brown, E. L., et al. (2021). Rift propagation north of Iceland: A case of asymmetric plume dynamics? In *Geoscience Society of Iceland, spring meeting 2021*.
- Larsen, H. C., Blischke, A., Halldórsson, S. A., Brandsdóttir, B., Leshner, C. E., Conrad, C. P., et al. (2021). Rift propagation north of Iceland: A case of asymmetric plume dynamics? *International Ocean drilling program (IODP) proposal—North Iceland rift propagation* (p. 140).
- Larsen, H. C., & Jakobsdóttir, S. (1988). Distribution, crustal properties and significance of seawards-dipping sub-basement reflectors off East Greenland. In A. C. Morton & L. M. Parson (Eds.), *Early tertiary volcanism and the opening of the Northeast Atlantic* (Vol. 39, pp. 95–114). Geol. Soc. London Spec. Publ. <https://doi.org/10.1144/GSL.SP.1988.039.01.10>
- Larsen, L. M., Pedersen, A. K., Sørensen, E. V., Watt, W. S., & Duncan, R. A. (2013). Stratigraphy and age of the Eocene Igertivå formation basalts, alkaline pebbles and sediments of the Kap Dalton Group in the graben at Kap Dalton, East Greenland. *Bulletin of the Geological Society of Denmark*, 61, 1–18. <https://doi.org/10.37570/bgsd-2013-61-01>

- Larsen, L. M., Pedersen, A. K., Tegner, T., & Duncan, R. A. (2014). Eocene to Miocene igneous activity in NE Greenland: Northward younging of magmatism along the east Greenland margin. *Journal of the Geological Society*, 171(4), 539–553. <https://doi.org/10.1144/jgs2013-118>
- Larsen, L. M., Waagstein, R., Pedersen, A. K., & Storey, M. (1999). Trans-atlantic correlation of the Palaeogene volcanic successions in the Faeroe islands and east Greenland. *Journal of the Geophysical Society*, 156(6), 1081–1095. <https://doi.org/10.1144/gsjgs.156.6.1081>
- Larsen, L. M., Watt, S. W., & Watt, M. (1989). Geology and petrology of the Lower Tertiary plateau basalts of the Scoresby Sund region, east Greenland. *Bulletin (Grønlands geologiske undersøgelse)*, 157, 164. <https://doi.org/10.34194/bullggu.v157.6699>
- Larsen, L. M., & Watt, W. S. (1985). Episodic volcanism during break-up of the north Atlantic: Evidence from the east Greenland plateau basalts. *Earth and Planetary Science Letters*, 73(1), 105–116. [https://doi.org/10.1016/0012-821X\(85\)90038-X](https://doi.org/10.1016/0012-821X(85)90038-X)
- Larsen, M., Heilmann-Clausen, C., Piasecki, S., & Stemmerik, L. (2005). At the edge of a new ocean: Post-volcanic evolution of the Palaeogene Kap Dalton Group, east Greenland. In A. G. Doré & B. A. Vining (Eds.), *Petroleum geology: North-west Europe and global perspectives, proceedings of the 6th Petroleum geology conference* (pp. 923–932). Geological Society of London. <https://doi.org/10.1144/0060923>
- Larsen, M., Piasecki, S., & Stemmerik, L. (2002). The post-basaltic Palaeogene and Neogene sediments at Kap Dalton and Savoia Halvø, east Greenland. *Geology of Greenland Survey Bulletin*, 191, 103–110. <https://doi.org/10.34194/ggub.v191.5136>
- Le Bas, M. J., Le Maitre, R. W., Streckeisen, A., & Zanettini, B. (1989). IUGS sub-commission on the systematics of igneous rocks. A chemical classification of volcanic rocks based on the total alkali-silica diagram. *Journal of Petrology*, 27(3), 745–750. <https://doi.org/10.1093/ptrology/27.3.745>
- Le Breton, E., Brune, S., Ustaszewski, K., Zahirovic, S., Seton, M., & Müller, R. D. (2021). Kinematics and extent of the Piemont-Liguria Basin—Implications for subduction processes in the Alps. *Solid Earth*, 12, 885–913. <https://doi.org/10.5194/se-12-885-2021>
- Lofgren, G. E. (1974). An experimental study of plagioclase crystal morphology: Isothermal crystallization. *American Journal of Science*, 274, 243–273. <https://doi.org/10.2475/ajs.274.3.243>
- Lofgren, G. E. (1983). Effect of heterogeneous nucleation on basaltic textures: A dynamic crystallization study. *Journal of Petrology*, 24(3), 229–255. <https://doi.org/10.1093/ptrology/24.3.229>
- Lundin, E., & Doré, A. G. (2002). Mid-Cenozoic post-breakup deformation in the ‘passive’ margins bordering the Norwegian-Greenland Sea. *Marine and Petroleum Geology*, 19, 79–93. [https://doi.org/10.1016/s0264-8172\(01\)00046-0](https://doi.org/10.1016/s0264-8172(01)00046-0)
- Lundin, E. R., & Doré, A. G. (2005). NE Atlantic breakup: A re-examination of the Iceland mantle plume model and the Atlantic-Arctic linkage. In A. G. Doré, & B. A. Vining (Eds.), *Petroleum geology: North-west Europe and global perspectives. Proceedings of the 6th Petroleum geology conference* (pp. 739–754). <https://doi.org/10.1144/0060739>
- Manum, S. B., Raschka, H., & Eckhardt, F. J. (1976). Site 350. In M. Talwani & G. Udintsev (Eds.), *Initial reports of the Deep Sea Drilling Project* (Vol. 38, pp. 1–655). U.S. Government Printing Office.
- Manum, S. B., Raschka, H., Eckhardt, F. J., Schrader, H., Talwani, M., & Udintsev, G. (1976). Site 337. In M. Talwani, G. Udintsev, et al. (Eds.), *Initial reports of the Deep Sea Drilling Project*. (Vol. 38, pp. Wash 117–150). U.S. Government Printing Office.
- Manum, S. B., & Schrader, H. J. (1976). Sites 346, 347, and 349. In M. Talwani, & G. Udintsev (Eds.), *Initial reports of the Deep Sea Drilling Project* (Vol. 38, pp. 521–594). U.S. Government Printing Office.
- Martos, Y. M., Jordan, T. A., Catalán, M., Jordan, T. M., Bamber, J. L., & Vaughan, D. G. (2018). Geothermal heat flux reveals the Iceland hotspot track underneath Greenland. *Geophysical Research Letters*, 45, 8214–8222. <https://doi.org/10.1029/2018GL078289>
- Mathiesen, A., Bidstrup, T., & Christensen, F. G. (2000). Denudation and uplift history of the Jameson Land Basin, East Greenland—constrained from maturity and apatite fission track data. *Global and Planetary Change*, 24, 275–301. [https://doi.org/10.1016/s0921-8181\(00\)00013-8](https://doi.org/10.1016/s0921-8181(00)00013-8)
- Menke, W., West, M., Brandsdóttir, B., & Sparks, D. (1998). Compressional and shear velocity structure of the lithosphere in northern Iceland. *Bulletin of the Seismological Society of America*, 88(6), 1561–1571.
- Mertz, D. F., Devey, C. W., Todt, W., Stoffers, P., & Hofmann, A. W. (1991). Sr-Nd-Pb isotope evidence against plume-asthenosphere mixing north of Iceland. *Earth and Planetary Science Letters*, 107(2), 243–255. [https://doi.org/10.1016/0012-821X\(91\)90074-R](https://doi.org/10.1016/0012-821X(91)90074-R)
- Mertz, D. F., & Haase, K. M. (1997). The radiogenic isotope composition of the high-latitude North Atlantic mantle. *Geology*, 25(5), 411–414. [https://doi.org/10.1130/0091-7613\(1997\)025<0411:tricot>2.3.co;2](https://doi.org/10.1130/0091-7613(1997)025<0411:tricot>2.3.co;2)
- Mertz, D. F., Sharp, W. D., & Haase, K. M. (2004). Volcanism on the Eggvin Bank (central Norwegian-Greenland Sea, latitude approximately 71 degrees N); age, source, and relation-ship to the Iceland and putative Jan Mayen Plumes. *Journal of Geodynamics*, 38(1–1), 57–84. <https://doi.org/10.1016/j.jog.2004.03.003>
- Meyer, O., Voppel, D., Fleischer, U., Gloss, H., & Gerke, K. (1972). Results of bathymetric, magnetic and gravimetric measurements between Iceland and 70°N. *Deutsche Hydrographische Zeitschrift*, 25, 193–201. <https://doi.org/10.1007/bf02299456>
- Meyer, R., Hertogen, J., Pedersen, R. B., Viereck-Götte, L., & Abratis, M. (2009). Interaction of mantle derived melts with crust during the emplacement of the Vøring Plateau, N.E. Atlantic. *Marine Geology*, 261(1–4), 3–16. <https://doi.org/10.1016/j.margeo.2009.02.007>
- Mjelde, R., Aurvåg, R., Kodaira, S., Shimamura, H., Gunnarsson, K., Nakanishi, A., & Shiobara, H. (2002). Vp/Vs-ratios from the central Kolbeinsey ridge to the Jan Mayen Basin, North Atlantic; implications for lithology, porosity and present-day stress field. *Marine Geophysical Researches*, 23, 123–145. <https://doi.org/10.1023/a:1022439707307>
- Mjelde, R., Eckhoff, I., Solbakken, S., Kodaira, S., Shimamura, H., Gunnarsson, K., et al. (2007). Gravity and S-wave modelling across the Jan Mayen Ridge, North Atlantic; implications for crustal lithology. *Marine Geophysical Researches*, 28, 27–41. <https://doi.org/10.1007/s11001-006-9012-3>
- Mjelde, R., Kvarven, T., Faleide, J. I., & Thybo, H. (2016). Lower crustal high-velocity bodies along North Atlantic passive margins, and their link to Caledonian suture zone eclogites and Early Cenozoic magmatism. *Tectonophysics*, 670, 16–29. <https://doi.org/10.1016/j.tecto.2015.11.021>
- Mjelde, R., Raum, T., Breivik, A. J., & Faleide, J. I. (2008). Crustal transect across the north Atlantic. *Marine Geophysical Researches*, 29, 73–87. <https://doi.org/10.1007/s11001-008-9046-9>
- Mohr, M. (1976). Additional petrographic studies of basalts, DSDP, leg 38. In *Initial reports DSDP* (Vol. 38, pp. 717–718). U.S. Government Printing Office. <https://doi.org/10.2973/dsdp.proc.38.111.1976>
- Mordret, A. (2018). Uncovering the Iceland hot spot track beneath Greenland. *Journal of Geophysical Research: Solid Earth*, 123, 4922–4941. <https://doi.org/10.1029/2017JB015104>
- Mudge, D. C. (2015). Regional controls on lower tertiary sandstone distribution in the North Sea and NE Atlantic margin basins. In T. McKie, P. T. S. Rose, A. J. Hartley, D. W. Jones, & T. L. Armstrong (Eds.), *Tertiary deep-marine reservoirs of the North Sea region* (Vol. 403, pp. 17–42). Geological Society, London, Special Publications. <https://doi.org/10.1144/SP403.5>
- Müller, R. D., Gaina, G., Roest, W. R., & Hansen, D. L. (2001). A recipe for microcontinent formation. *Geology*, 29, 203–206.
- Murton, B. J., & Parson, L. M. (1993). Segmentation, volcanism and deformation of oblique spreading centres: A quantitative study of the Reykjanes ridge. *Tectonophysics*, 222, 237–257. [https://doi.org/10.1016/0040-1951\(93\)90051-K](https://doi.org/10.1016/0040-1951(93)90051-K)
- Mutter, J. C., Talwani, M., & Stoffa, P. L. (1982). Origin of seaward-dipping reflectors in oceanic crust off the Norwegian margin by “subaerial sea-floor spreading”. *Geology*, 10, 3–12. [https://doi.org/10.1130/0091-7613\(1982\)10<353:ooorio>2.0.co;2](https://doi.org/10.1130/0091-7613(1982)10<353:ooorio>2.0.co;2)

- Myhre, A. M., Eldholm, O., & Sundvor, E. (1984). The Jan Mayen Ridge; present status. *Polar Research*, 2(1), 47–59. <https://doi.org/10.3402/polar.v2i1.6961>
- Nasuti, A., & Olesen, O. (2014). Magnetic data. In J. R. Hopper, T. Funck, M. S. Stoker, U. Ártung, G. Peron-Pinvidic, H. Doornenbal, & C. Gaina (Eds.), *Tectonostratigraphic Atlas of the north-east Atlantic region. The geological survey of Denmark and Greenland (GEUS)* (1st ed.). Nemčok, M., Sinha, S., Dore, A. G., Lundin, E., & Rybár, S. (2016). *Mechanisms of microcontinent release associated with wrenching-involved continental break-up; a review* (Vol. 431). Geological Society London Special Publications. <https://doi.org/10.1144/SP431.14359>
- Nilsen, T. H., D. R. Kerr, M. Talwani, & G. E. A. Udintsev (Eds.). (1978). Turbidites, redbeds, sedimentary structures, and trace fossils observed DSDP Leg 38 cores and the sedimentary history of the Norwegian-Greenland Sea. In *Initial reports of the Deep Sea drilling project* (Vol. 38, pp. 259–288). U.S. Government Printing Office.
- Norcliffe, J., Paton, D., Mortimer, E., McCaig, A., & Rodriguez, K. (2019). Asymmetric emplacement of seaward dipping reflectors during rifting: Where; when; how and why? In *Proceedings of EGU2019* (Vol. 21, pp. EGU2019–10085).
- Olafsson, I., & Gunnarsson, K. (1989). The Jan Mayen Ridge: Velocity structure from analysis of sonobuoy data. *Orkustofnun, Reykjavik, OS-89030/JHD-04* (pp. 1–62).
- Ólafsdóttir, J., Stoker, M. S., Boldreel, L. O., Andersen, M. S., & Eidesgaard, Ó. R. (2019). Seismic-stratigraphic constraints on the age of the Faroe Islands basalt Group, Faroe–Shetland region, northeast Atlantic Ocean. *Basin Research*, 31(5), 841–865. <https://doi.org/10.1111/bre.12348>
- Parkin, C. J., & White, R. S. (2008). Influence of the Iceland mantle plume on oceanic crust generation in the North Atlantic. *Geophysical Journal International*, 173(1), 168–188. <https://doi.org/10.1111/j.1365-246X.2007.03689.x>
- Parnell-Turner, R., White, N., Henstock, T., MurtonMurton, B. B., MacLennan, J., & Jones, S. M. (2014). A continuous 55-million-year record of transient mantle plume activity beneath Iceland. *Nature Geoscience*, 7, 914–919. <https://doi.org/10.1038/ngeo2281>
- Parson, L., Viereck, L., Love, D., Gibson, I., Morton, A., & Hertogen, J. (1989). The petrology of the lower series volcanics, ODP Site 642. In O. Eldholm, J. Thiede, E. Taylor, et al. (Eds.), *Proceedings of the Ocean Drilling Program, Scientific Results* (Vol. 104, pp. 419–428). Ocean Drilling Program. <https://doi.org/10.2973/odp.proc.sr.104.134.1989>
- Parsons, A. J., Whitham, A. G., Kelly, S. R. A., Vautravers, B. P. H., Dalton, T. J. S., Andrews, S. D., et al. (2017). Structural evolution and Basin architecture of the Traill Ø region, NE Greenland: A record of polyphase rifting of the east Greenland continental margin. *Geosphere*, 13(3), 1–38. <https://doi.org/10.1130/GES01382.1>
- Passéy, S. R. (2009). Recognition of a faulted basalt lava flow sequence through the correlation of stratigraphic marker units, Skopunarfjörður, Faroe Islands. In T. Varming, & H. Ziska (Eds.), *Faroe Islands exploration conference: Proceedings of the 2nd conference* (pp. 174–204). Annales Societatis Scientiarum Faeroensis.
- Passéy, S. R., & Hitchen, K. (2011). Cenozoic (igneous). In J. D. Ritchie, H. Ziska, H. Johnson, & D. Evans (Eds.), *Geology of the Faroe-Shetland Basin and adjacent areas. BGS research report, RR/11/01, Jarðfeingi research report* (pp. 209–228). RR/11/01.
- Passéy, S. R., & Jolley, D. W. (2009). A revised lithostratigraphic nomenclature for the Palaeogene Faroe Islands basalt Group, NE Atlantic Ocean. *Earth and Environmental Science Transactions of the Royal Society of Edinburgh*, 99, 127–158.
- Pedersen, A. K., Watt, M., Watt, W. S., & Larsen, L. M. (1997). Structure and stratigraphy of the early tertiary basalts of the Blossville Kyst, east Greenland. *Journal of the Geological Society*, 154, 565–570. <https://doi.org/10.1144/gsjgs.154.3.0565>
- Peron-Pinvidic, G., Gernigon, L., Gaina, C., & Ball, P. (2012a). Insights from the Jan Mayen system in the Norwegian-Greenland Sea—I: Mapping of a microcontinent. *Geophysical Journal International*, 191, 385–412. <https://doi.org/10.1111/j.1365-246X.2012.05639.x>
- Peron-Pinvidic, G., Gernigon, L., Gaina, C., & Ball, P. (2012b). Insights from the Jan Mayen system in the Norwegian-Greenland Sea—II: Architecture of a microcontinent. *Geophysical Journal International*, 191, 413–435. <https://doi.org/10.1111/j.1365-246X.2012.05623.x>
- Pitman, W. C. I., & Talwani, M. (1972). Sea-floor spreading in the north Atlantic. *The Geological Society of America Bulletin*, 83, 619–646. [https://doi.org/10.1130/0016-7606\(1972\)83\[619:ssitna\]2.0.co;2](https://doi.org/10.1130/0016-7606(1972)83[619:ssitna]2.0.co;2)
- Planke, S., & Cambray, H. (1998). Seismic properties of flood basalts from Hole 917A downhole data, southeast Greenland volcanic margin. *Proceedings of the Ocean Drilling Program*, 152.
- Planke, S., & Eldholm, O. (1994). Seismic response and construction of seaward dipping wedges of flood basalts: Voring volcanic margin. *Journal of Geophysical Research*, 99(B5), 9263–9278. <https://doi.org/10.1029/94JB00468>
- Planke, S., Svensen, H., Myklebust, R., Bannister, S., Manton, B., & Lorenz, L. (2015). Geophysics and remote sensing. In C. Breitkreuz & S. Rocchi (Eds.), *Physical geology of shallow magmatic systems. Advances in volcanology (an official book series of the international association of volcanology and Chemistry of the Earth's interior)* (pp. 131–146). Springer. https://doi.org/10.1007/11157_2014_6
- Planke, S., Symonds, P. A., Alvestad, E., & Skogseid, J. (2000). Seismic volcanostratigraphy of large-volume basaltic extrusive complexes on rifted margins. *Journal of Geophysical Research*, 105(B8), 19335–19351. <https://doi.org/10.1029/1999jb900005>
- Polteau, S., Mazzini, A., Hansen, G., Planke, S., Jerram, D. A., Millett, J., et al. (2018). The pre-breakup stratigraphy and petroleum system of the Southern Jan Mayen Ridge revealed by seafloor sampling. *Tectonophysics*, 760, 152–164. <https://doi.org/10.1016/j.tecto.2018.04.016>
- Polteau, S., Mazzini, A., Trulsvik, M., & Planke, S. (2012). *JMRS11—Jan Mayen Ridge sampling survey 2011. VBPR-TGS, commercial report, February 2012*.
- Polteau, S., Planke, S., Zastrozhnov, D., Abdelmalak, M. M., Lebedeva-Ivanova, N., Eckhoff Planke, E., et al. (2020). Upper Cretaceous-Paleogene stratigraphy and development of the Mimir high, Vøring transform margin, Norwegian Sea. *Marine and Petroleum Geology*, 122, 104717. <https://doi.org/10.1016/j.marpetgeo.2020.104717>
- Raschka, H., Eckhardt, F. J., & Manum, S. B. (1976). Site 348. In M. Talwani & G. Udintsev (Eds.), *Initial reports of the Deep Sea drilling project* (Vol. 38, pp. 595–654). U.S. Government Printing Office.
- Reiche, S., Reid, I., & Thybo, H. (2011). *Crustal structure of the Greenland-Iceland Ridge inferred from wide-angle seismic data EGU General Assembly 2011*. Geophysical Research Abstracts.
- Rey, S. S., Eldholm, O., & Planke, S. (2003). Formation of the Jan Mayen microcontinent, the Norwegian Sea. *EOS Transactions AGU*, 84, Abstract T31D-0872.
- Richardson, K. R., Smallwood, J. R., White, R. S., Snyder, D. B., & Maguire, P. K. H. (1998). Crustal structure beneath the Faroe Islands and the Faroe-Iceland ridge. *Tectonophysics*, 300(1–4), 159–180. [https://doi.org/10.1016/s0040-1951\(98\)00239-x](https://doi.org/10.1016/s0040-1951(98)00239-x)
- Ridley, W. I., Perfit, M. R., & Adams, M. L. (1976). Petrology of basalts from deep sea drilling project. Leg 38. *Initial reports DSDP*, 38, 731–739. <https://doi.org/10.2973/dsdp.proc.38.113.1976>
- Ritchie, D. K., Ziska, H., Johnson, H., & Evans, D. (2011). Geology of the Faroe-Shetland Basin and adjacent areas. In *Rep. British geological survey research report, RR/11/01, Jarðfeingi research report, RR/11/01* (p. 317).
- Ritchie, J. D., Johnson, H., Quinn, M. F., & Gatliff, R. W. (2008). The effects of Cenozoic compression within the Faroe-Shetland Basin and adjacent areas. In H. Johnson, A. G. Doré, R. W. Gatliff, R. W. Holdsworth, E. R. Lundin, & J. D. Ritchie (Eds.), *The nature and origin of compression in passive margins* (Vol. 306, pp. 121–136). Geological Society of London, Special Publication. <https://doi.org/10.1144/sp306.5>

- Sæmundsson, K. (1979). Outline of the geology of Iceland. *Jökull Journal*, 29, 7–28.
- Sandstå, N. R., Pedersen, R. B., Williams, R. D., Bering, D., Magnus, C., Sand, M., & Brekke, H. (2012). *Submarine fieldwork on the Jan Mayen Ridge; integrated seismic and ROV-sampling*. Norwegian Petroleum Directorate. Retrieved from <http://www.npd.no/>
- Sandstå, N. R., Sand, M., & Brekke, H. (2013). *Ressursrapporter 2013, Jan Mayen*. Project web publication Norwegian Petroleum Directorate.
- Saunders, A.D., Fitton, J.G., Kerr, A.C., Norry, M.J., & Kent, R.W. (2013). *The North Atlantic Igneous Province* (pp. 45–93). <https://doi.org/10.1029/GM100p0045>
- Schilling, J. G., Kingsley, R., Fontignie, D., Poreda, R., & Xue, S. (1999). Dispersion of the Jan Mayen and Iceland mantle plumes in the Arctic: A He-Pb-Nd-Sr isotope tracer study of basalts from the Kolbeinsey, Mohns, and Knipovich ridges. *Journal of Geophysical Research*, 104(B5), 10543–10569. <https://doi.org/10.1029/1999jb900057>
- Scott, R. A., Ramsey, L. A., Jones, S. M., Sinclair, S., & Pickles, C. S. (2005). Development of the Jan Mayen microcontinent by linked propagation and retreat of spreading ridges. In B. T. G. Wandås, J. P. Nystuen, E. Eide, & F. Gradstein (Eds.), *Onshore–offshore relationships on the north Atlantic margin* (pp. 69–82). Norwegian Petroleum Society. [https://doi.org/10.1016/s0928-8937\(05\)80044-x](https://doi.org/10.1016/s0928-8937(05)80044-x)
- Skogseid, J., & Eldholm, O. (1987). Early Cenozoic crust in the Norwegian continental margin and the conjugate Jan Mayen Ridge. *Journal of Geophysical Research*, 92(1), 11471–11491. <https://doi.org/10.1029/JB092iB11p11471>
- Skogseid, J., Planke, S., Faleide, J. I., Pedersen, T., Eldholm, O., & Neverdal, F. (2000). NE Atlantic continental rifting and volcanic margin formation. *Geological Society, London, Special Publications*, 167(1), 295–326. <https://doi.org/10.1144/GSL.SP.2000.167.01.12>
- Skovgaard, A. C., Storey, M., Baker, J., Blusztajn, J., & Hart, S. R. (2001). Osmium-oxygen isotopic evidence for a recycled and strongly depleted component in the Iceland mantle plume. *Earth and Planetary Science Letters*, 194(1), 259–275. [https://doi.org/10.1016/S0012-821X\(01\)00549-0](https://doi.org/10.1016/S0012-821X(01)00549-0)
- Smallwood, J. R., Staples, R. K., Richardson, K. R., White, R. S., & the FIRE Working Group. (1999). Crust generated above the Iceland mantle plume: From continental rift to oceanic spreading center. *Journal of Geophysical Research*, 104(B10), 22885–22902. <https://doi.org/10.1029/1999JB900176>
- Srivastava, S. P., & Tapscott, C. R. (1986). Plate kinematics of the north Atlantic. *The Geology of North America, Vol. M, the Western North Atlantic Region* (Vol. 379–404). Geol. Soc. of Am.
- Staples, R. K., White, R. S., Brandsdóttir, B., Menke, W., Maguire, P. K. H., & McBride, J. H. (1997). Faroe-Iceland ridge experiment 1. Crustal structure of northeastern Iceland. *Journal of Geophysical Research*, 102(B4), 7849–7866. <https://doi.org/10.1029/96JB03911>
- Stärz, M., Jokat, W., Knorr, G., & Lohmann, G. (2017). Threshold in North Atlantic-Arctic Ocean circulation controlled by the subsidence of the Greenland-Scotland ridge. *Nature Communications*, 8, 15681.
- Storey, M., Duncan, R., & Tegner, C. (2007). Timing and duration of volcanism in the north Atlantic igneous province: Implications for geodynamics and links to the Iceland hotspot. *Chemical Geology*, 241(3–4), 264–281. <https://doi.org/10.1016/j.chemgeo.2007.01.016>
- Stracke, A., Zindler, A., Salters, V. J. M., McKenzie, D., Blichert-Toft, J., Albarède, F., & Grönvold, K. (2003). Theistareykir revisited. *Geochemistry, Geophysics, Geosystems*, 4(2). <https://doi.org/10.1029/2001GC002001>
- Sun, S. S., Tatsumoto, M., & Schilling, J. G. (1975). Mantle plume mixing along the Reykjanes ridge axis—Lead isotope evidence. *Science*, 190(4210), 143–147. <https://doi.org/10.1126/science.190.4210.143>
- Svellingen, W., & Pedersen, R. (2003). Jan Mayen: A result of ridge-transform-micro-continent interaction. *Geophysical Research Abstracts*, 5, 12993.
- Sylvester, A. G. (1975). History and surveillance of volcanic activity on Jan Mayen island. *Bulletin of Volcanology*, 39, 313–335. <https://doi.org/10.1007/bf02597834>
- Sylvester, A. G. (1978). Petrography of volcanic ashes in deep-sea cores near Jan-Mayen island: Sites 338 dsdp leg 38. *Initial reports of the Deep Sea drilling project* (Vol. 38, pp. 345–350). U.S. Government Printing Office.
- Symonds, P. A., Planke, S., Frey, Ø., & Skogseid, J. (1998). Volcanic evolution of the western Australian continental margin and its implications for basin development. In R. R. Purcell (Ed.), *The sedimentary basins of western Australia* (pp. 33–54).
- Talwani, M., & Eldholm, O. (1977). Evolution of the Norwegian-Greenland Sea. *The Geological Society of America Bulletin*, 88, 969–999. [https://doi.org/10.1130/0016-7606\(1977\)88<969:eotns>2.0.co;2](https://doi.org/10.1130/0016-7606(1977)88<969:eotns>2.0.co;2)
- Talwani, M., Mutter, J., & Eldholm, O. (1981). The initiation of opening of the Norwegian Sea. *Oceanologica Acta SP*, 23–30.
- Talwani, M., & Udintsev, G. (1976). Tectonic synthesis. *Initial reports Deep Sea Drill. Project* (Vol. 38, pp. 1214–1232). U.S. Government Printing Office. <https://doi.org/10.2973/dsdp.proc.38.134.1976>
- Talwani, M., Udintsev, G., Mirlin, E., Beresnev, A. F., Kanayev, V. F., Chapman, M., et al. (1978). *Survey at sites 346, 347, 348, 349, and 350, the area of the Jan-Mayen Ridge and the Icelandic plateau*. <https://doi.org/10.2973/dsdp.proc.38.394041s.127.1978>
- Talwani, M., Udintsev, G., & Shirshov, P. R. (1976). Tectonic synthesis. In M. Talwani & G. Udintsev (Eds.), *Initial reports of the Deep Sea drilling project* (Vol. 38, pp. 1213–1242). U.S. Government Printing Office. <https://doi.org/10.2973/dsdp.proc.38.134.1976>
- Talwani, M., Udintsev, G., & White, S. M. (1976). Introduction and explanatory notes, leg 38, Deep Sea drilling project. In M. Talwani, & G. Udintsev (Eds.), *Initial reports of the Deep Sea drilling project* (Vol. 38, pp. 3–19). U.S. Government Printing Office. <https://doi.org/10.2973/dsdp.proc.38.101.1976>
- Talwani, M., Udintsev, G. B., Bjoerklund, K., Caston, V. N. D., Faas, R. W., van Hinte, J. E., et al. (1976a). *Initial Reports of the Deep Sea Drilling Project* (Vol. 38, pp. 655–682). Texas A & M University, Ocean Drilling Program. 0080-8334 CODEN: IDSDA6. <https://doi.org/10.2973/dsdp.proc.38.109.1976>
- Talwani, M., Udintsev, G. B., Bjoerklund, K., Caston, V. N. D., Faas, R. W., van Hinte, J. E., et al. (1976b). Site 350. In *Initial reports of the Deep Sea drilling project* (Vol. 38, pp. 655–682). Texas A & M University, Ocean Drilling Program. 0080-8334 CODEN: IDSDA6. <https://doi.org/10.2973/dsdp.proc.38.109.1976>
- Talwani, M., Udintsev, G. B., Bjoerklund, K., Caston, V. N. D., Faas, R. W., van Hinte, J. E., et al. (1976c). Site 348. In *Initial reports of the Deep Sea drilling project* (Vol. 38, pp. 595–654). Texas A & M University, Ocean Drilling Program. 0080-8334 CODEN: IDSDA6. <https://doi.org/10.2973/dsdp.proc.38.108.1976>
- Talwani, M., Udintsev, G. B., Bjoerklund, K., Caston, V. N. D., Faas, R. W., van Hinte, J. E., et al. (1976d). Site 345. In *Initial reports of the Deep Sea drilling project* (Vol. 38, pp. 595–654). Texas A & M University, Ocean Drilling Program. 0080-8334 CODEN: IDSDA6. <https://doi.org/10.2973/dsdp.proc.38.106.1976>
- Talwani, M., Udintsev, G. B., Bjoerklund, K., Caston, V. N. D., Faas, R. W., van Hinte, J. E., et al. (1976e). Sites 346, 347, and 349. *Initial reports of the Deep Sea drilling project* (Vol. 38, pp. 521–594). Texas A & M University, Ocean Drilling Program. ISSN: 0080-8334 CODEN: IDSDA6. <https://doi.org/10.2973/dsdp.proc.38.107.1976>
- Talwani, M., Udintsev, G. B., Bjoerklund, K., Caston, V. N. D., Faas, R. W., van Hinte, J. E., et al. (1976f). Sites 338-343. In *Initial reports of the Deep Sea drilling project* (Vol. 38, pp. 595–654). Texas A & M University, Ocean Drilling Program. 0080-8334 CODEN: IDSDA6. <https://doi.org/10.2973/dsdp.proc.38.104.1976>

- Talwani, M., Udintsev, G. B., Bjoerklund, K., Caston, V. N. D., Faas, R. W., van Hinte, J. E., et al. (1976g). Site 337. In *Initial reports of the Deep Sea drilling project* (Vol. 38, pp. 595–654). Texas A & M University, Ocean Drilling Program. 0080-8334 CODEN: IDSDA6. <https://doi.org/10.2973/dsdp.proc.38.103.1976>
- Talwani, M., Udintsev, G. B., Bjoerklund, K., Caston, V. N. D., Faas, R. W., van Hinte, J. E., et al. (1976h). Sites 336 and 352. In *Initial reports of the Deep Sea drilling project* (Vol. 38, pp. 595–654). Texas A & M University, Ocean Drilling Program. 0080-8334 CODEN: IDSDA6. <https://doi.org/10.2973/dsdp.proc.38.102.1976>
- Tan, P., Breivik, A. J., Trønnes, R. G., Mjeldre, R., Azuma, R., & Eide, S. (2017). Crustal structure and origin of the Eggvin Bank west of Jan Mayen, NE Atlantic. *Journal of Geophysical Research: Solid Earth*, *122*, 43–62. <https://doi.org/10.1002/2016JB013495>
- Tan, P., Sippel, J., Breivik, A. J., Meeßen, C., & Scheck-Wenderoth, M. (2018). Lithospheric control on asthenospheric flow from the Iceland plume: 3-D density modeling of the Jan Mayen-east Greenland region, NE Atlantic. *Journal of Geophysical Research: Solid Earth*, *123*, 9223–9248. <https://doi.org/10.1029/2018JB015634>
- Taylor, B., Crook, K., & Sinton, J. (1994). Extensional transform zones and oblique spreading centers. *Journal of Geophysical Research*, *99*, 19707–19718. <https://doi.org/10.1029/94JB01662>
- Tegner, C., Andersen, T. B., Kjøl, H. J., Brown, E. L., Hagen-Peter, G., Corfu, F., et al. (2019). A mantle plume origin for the Scandinavian Dyke complex: A “piercing point” for 615 Ma plate reconstruction of Baltica? *Geochemistry, Geophysics, Geosystems*, *20*, 1075–1094. <https://doi.org/10.1029/2018GC007941>
- Tegner, C., Brooks, C. K., Duncan, R. A., Heister, L. E., & Bernstein, S. (2008). 40Ar–39Ar ages of intrusions in East Greenland: Rift-to-drift transition over the Iceland hotspot. *Lithos*, *101*, 480–500. <https://doi.org/10.1016/j.lithos.2007.09.001>
- Tegner, C., Leshar, C. E., Larsen, L. M., & Watt, W. S. (1998). Evidence from the rareearth-element record of mantle melting for cooling of the Tertiary Iceland plume. *Nature*, *395*(6702), 591–594. <https://doi.org/10.1038/26956>
- Theissen-Krah, S., Zastrozhnov, D., Abdelmalak, M. M., Schmid, D. W., Faleide, J. I., & Gernigone, L. (2017). Tectonic evolution and extension at the Møre Margin—Offshore mid-Norway. *Tectonophysics*, *721*, 227–238. <https://doi.org/10.1016/j.tecto.2017.09.009>
- Thiede, J., Firth, J. V., et al. (Eds.). (1995). Site 907. In *Proceedings of the Ocean drilling Program* (pp. 57–111). Ocean Drilling Program. Initial Reports, 151. http://www-odp.tamu.edu/publications/151_IR/VOLUME/CHAPTERS/ir151_05.pdf
- Thiede, J., Myhre, A. M., & Firth, J. V. (1995). Cenozoic northern hemisphere polar and subpolar ocean paleoenvironments. *Proceedings of the Ocean Drilling Program*, *151*, 397–420. Initial Reports. <http://www-odp.tamu.edu/publications/citations/cite151.html>
- Thirlwall, M. F., Gee, M. A. M., Taylor, R. N., & Murton, B. J. (2004). Mantle components in Iceland and adjacent ridges investigated using double-spike Pb isotope ratios. *Geochimica et Cosmochimica Acta*, *68*(2), 361–386. [https://doi.org/10.1016/S0016-7037\(03\)00424-1](https://doi.org/10.1016/S0016-7037(03)00424-1)
- Torsvik, T. H., Amundsen, H. E. F., Trønnes, R. G., Doubrovine, P. V., Gaina, C., Kuznir, N. J., et al. (2015). Continental crust beneath southeast Iceland. *Proceedings of the National Academy of Sciences of the United States of America*, *112*(15), E1818–E1827. <https://doi.org/10.1073/pnas.1423099112>
- Toyokuni, G., Matsuno, T., & Zhao, D. (2020a). P wave tomography beneath Greenland and surrounding regions: 1. Crust and upper mantle. *Journal of Geophysical Research: Solid Earth*, *125*, e2020JB019837. <https://doi.org/10.1029/2020JB019837>
- Toyokuni, G., Matsuno, T., & Zhao, D. (2020b). P wave tomography beneath Greenland and surrounding regions: 2. Lower mantle. *Journal of Geophysical Research: Solid Earth*, *125*, e2020JB019839. <https://doi.org/10.1029/2020JB019839>
- Trønnes, R. G., Planke, S., Sundvoll, B., & Imsland, P. (1999). Recent volcanic rocks from Jan Mayen: Low-degree melt fractions of enriched northeast Atlantic mantle. *Journal of Geophysical Research*, *104*(B4), 7153–7168.
- Vogt, P. R. (1986). Magnetic anomalies of the north Atlantic Ocean. In P. R. Vogt, & B. E. Tucholke (Eds.), *The western North Atlantic region*. Geological Society of America.
- Vogt, P. R., Anderson, C. N., Bracey, D. R., & Schneider, E. M. (1970). North Atlantic magnetic smooth zones. *Journal of Geophysical Research*, *75*, 3955–3968. <https://doi.org/10.1029/jb075i020p03955>
- Vogt, P. R., & Avery, O. E. (1974). Detailed magnetic surveys in the northeast Atlantic and Labrador Sea. *Journal of Geophysical Research*, *79*, 363–389. <https://doi.org/10.1029/jb079i002p00363>
- Vogt, P. R., Johnson, G. L., & Kristjansson, L. (1980). Morphology and magnetic anomalies north of Iceland. *Journal of Geophysical Research*, *85*, 67–80.
- Weigel, W., Flüh, E., Miller, H., Butzke, A., Deghani, A., Gebhardt, V., et al. (1995). Investigations of the East Greenland continental margin between 70° and 72°N by deep seismic sounding and gravity studies. *Marine Geophysical Research*, *17*(2), 167–199. <https://doi.org/10.1007/bf01203425>
- White, R. S., Bown, J. W., & Smallwood, J. R. (1995). The temperature of the Iceland plume and origin of outward-propagating V-shaped ridges. *Journal of the Geological Society*, *152*, 1039–1045. <https://doi.org/10.1144/GSL.JGS.1995.152.01.26>
- White, W. M., & Schilling, J.-G. (1978). The nature and origin of geochemical variation in Mid-Atlantic Ridge basalts from the Central North Atlantic. *Geochimica et Cosmochimica Acta*, *42*(10), 1501–1516. [https://doi.org/10.1016/0016-7037\(78\)90021-2](https://doi.org/10.1016/0016-7037(78)90021-2)
- Wolfe, C. J., Bjarnason, I. T., VanDecar, J. C., & Solomon, S. C. (1997). Seismic structure of the Iceland mantle plume. *Nature*, *385*, 245–247. <https://doi.org/10.1038/385245a0>
- Zastrozhnov, D., Gernigone, L., Gogin, I., Abdelmalak, M. M., Planke, S., Faleide, J. I., et al. (2018). Cretaceous-paleocene evolution and crustal structure of the northern Vøring margin (offshore mid-Norway): Results from integrated geological and geophysical study. *Tectonics*, *37*, 497–528. <https://doi.org/10.1002/2017TC004655>
- Zhang, T., Gordon, R. G., & Wang, C. (2018). Oblique seafloor spreading across intermediate and superfast spreading centers. *Earth and Planetary Science Letters*, *495*, 146–156. <https://doi.org/10.1016/j.epsl.2018.05.001>

Reference From the Supporting Information

- Helgadóttir, H. M. (2006). *Formation of palagonite. Petrographic analysis of hyaloclastite tuffs from the western volcanic zone in Iceland*. B.Sc. Thesis (p. 40). Department of Geology and Geography, University of Iceland.